Liquid water flow and discolouration of wood during kiln drying

by

G.C. Scheepers

Dissertation presented for the degree of Doctor of Forestry (Wood Science) at the University of Stellenbosch.

Promotor: Prof. Tim Rypstra

April 2006

Declaration

I, the undersigned, hereby declare that the work contained in this dissertation is my own original work and that I have not previously in its entirety or in part submitted it at any university for a degree.

Signature: .....

Date: …….....

Opsomming

Die verkleuring van Suid-Afrikaanse naaldhout gedurende kamerdroging kan die waarde van meubelgraad gesaagde hout verlaag. Termiese verkleuring van hout, soos wat plaasvind tydens behandelings by verhoogde temperature, lei tot 'n homogeen bruiner kleur as die gewone kleur van hout. Hierdie soort verkleuring word toegeskryf aan reaksies van die makro-molekulêre komponente van hout en kan plaasvind in beide loof- en naaldhoutsoorte. Geel- en bruinverkleuring kan die kleur in die buitenste paar millimeter van 'n plank beduidend verander, en word toegeskryf aan die neerslagreaksie van wateroplosbare suikers en stikstofhoudende verbindings aanwesig in die houtsap by die houtoppervlak as gevolg van vrye water of kapillêre vogbeweging gedurende droging.

'n Bespreking van die meganisme van geel- en bruinverkleuring sou onvolledig wees sonder 'n goeie begrip van vrye water vloei gedurende droging bo veselversadigingspunt. Hierdie proefskrif plaas die twee begrippe van vrye water vloei en verkleuring bymekaar, en bestaan uit vier hoofstukke:

- 'n inleiding wat die doel van die ondersoek motiveer (Hoofstuk 1);
- 'n literatuurstudie van die faktore wat verkleuring en vrye water vloei tydens droging sou kon beïnvloed (Hoofstuk 2);
- oorsponklike manuskripte wat die verkleuring van Suid-Afrikaanse naaldhout en vrye water vloei in loof- en naaldhout beskryf (Hoofstuk 3); en
- 'n finale gevolgtrekking wat die bevindings van die onderskeie ondersoeke saamvat en in verband plaas (Hoofstuk 4).

Die resultate toon dat die omvang van geel- en bruinverkleuring hoofsaaklik beïnvloed word deur geografiese oorsprong (en/of klimaat), boomspesie, skaafdiepte van gedroogde hout, en drogingskeduleparameters soos temperatuur en tyd. Die kenmerkende verkleuringspatroon van geel- en bruinverkleuring het gewys dat hierdie soort verkleuring verwant is aan die natlynverskynsel wat aangetref word tydens die kapillêre vloeifase van droging van nat hout. In kontras hiermee, het termiese verkleuring homogeen regdeur die volume van die hout voorgekom, en is daarom nie verwant aan vrye water vloei nie, maar aan chemiese reaksies van die makro-molekules in hout.

Resultate van die vrye water vloei ondersoeke ondersteun die infiltrasie perkolasie teorie van droging, naamlik dat, tydens droging van 'n vloeistofgevulde kapillêre netwerk, die grootste meniskus sal intrek tot dit nie meer die grootste meniskus is nie. Fluktuasies in die tempo van vogverlies vanuit die kerne van houtstukke bo veselversadigingspunt is ook gevind. Die patroon van fluktuasie het aansienlik verskil tussen *Betula verrucosa* en *Pinus radiata*. In beide gevalle het die begin van die laaste fase in tempo van vogverlies van die kern tipies saamgeval met 'n verkleining van die dwarssnitoppervlak van die drogende houtstuk. Hierdie gedrag word verklaar deur die hipotese dat onderskeibare kapillêre grootte-klasse leeggemaak word van vrye water in volgorde van groot na klein. Soos kleiner kapillêre leeggemaak word, word die kapillêre kragte groter, tot die punt waar die kragte groot genoeg is om permanente of tydelike vervorming van die oorblywende, watergevulde kapillêre te veroorsaak.

Klassifikasie- en regressieboomanalise was 'n nuttige statistiese tegniek om 'n groot kleurdatastel met baie veranderlikes te analiseer. Die belangrikheid van temperatuur en skaafdiepte om geel- en bruinverkleuring te beheer word goed uitgewys deur dié tegniek, wat kan help om die beheer vir kleurkwaliteit tydens industriële prosessering van hout te vereenvoudig.

Summary

The discolouration of South African softwood during kiln drying can reduce the value of furniture grade lumber. Thermal discolouration of wood, as found due to heat treatment, produces a homogeneously browner colour in wood than is normally expected. This type of discolouration is attributed to reactions of the macromolecules present in wood and is found in both hard- and softwoods. Yellow stain and kiln brown stain can severely alter the colour of the outer few millimeters of a wooden board and is attributed to the reaction of water-soluble sugars and nitrogenous compounds, present in the wood sap, after deposition at the wood surface due to liquid or capillary water flow during drying.

A discussion of the mechanism of discolouration due to yellow stain and kiln brown stain would be incomplete without a good understanding of the liquid flow of water during drying above fibre saturation point. This thesis brings the two concepts of liquid water flow and discolouration in context and is presented in four chapters:

- an introduction motivating the aims of the investigation (Chapter 1);
- a literature review of factors which may influence discolouration and liquid water flow during drying (Chapter 2);
- original manuscripts describing the discolouration of South African softwood and liquid water flow in hard- and softwood (Chapter 3); and
- a final conclusion that links up the results from the investigations (Chapter 4).

The investigations into the occurrence of yellow stain and kiln brown stain showed that the intensity of these types of discolouration was influenced by geographical origin (and/or climate), tree species, planing depth of dried lumber, and kiln schedule parameters like dry- and wet bulb temperature and time. The characteristic discolouration pattern of yellow stain and kiln brown stain indicated that this stain type was related to the wetline phenomenon that is found during the liquid water flow phase of drying wet wood. Thermal discolouration, on the other hand, occurred homogeneously throughout the volume of lumber and is, therefore, not related to free water flow, but to chemical changes of the macromolecules in wood.

The results of the liquid water flow investigations support the invasion percolation theory of drying that states that the largest meniscus will retract into a drying liquid-filled capillary network until it is not the largest meniscus anymore. Fluctuations in the rate of moisture loss from the cores of wood pieces above fibre saturation point were also found. The pattern of fluctuation differed appreciably between *Betula verrucosa* and *Pinus radiata*. In both cases, the start of the last phase in rate of moisture loss from the core coincided with a reduction in the cross-sectional area of the drying wood piece. This behaviour is explained by the hypothesis that distinct capillary size classes are emptied of free water, in order, from large to small. As smaller capillaries are emptied, the capillary forces become greater, to the point where the forces are great enough to cause permanent or temporary deformation of the remaining water-filled capillaries.

Classification and regression tree analysis was a useful statistical technique to analyse a large multivariate dataset. The importance of kiln schedule temperatures and planing depth to control yellow stain and kiln brown stain was clearly pointed out by the technique, which can help to simplify the control of colour quality during the industrial processing of wood.

Table of Contents

Chapter 1: General Introduction and Purpose

By the turn of the previous century, the exchange rate of the South African Rand against foreign currencies was extremely favourable for exporters in South Africa. South African exports of lumber, especially furniture-grade, soared (Figure 1). Some importers of South African furniture quality lumber complained about the colour of the wood. Yellow and brown stains at the lumber surface negatively affected its appearance. The same type of stains have been encountered in lumber from New Zealand, and was called yellow stain (YS) and kiln brown stain (KBS). Soon the problem became prominent enough for the South African Lumber Millers' Association to initiate a study at the Department of Forestry and Wood Science at the University of Stellenbosch.

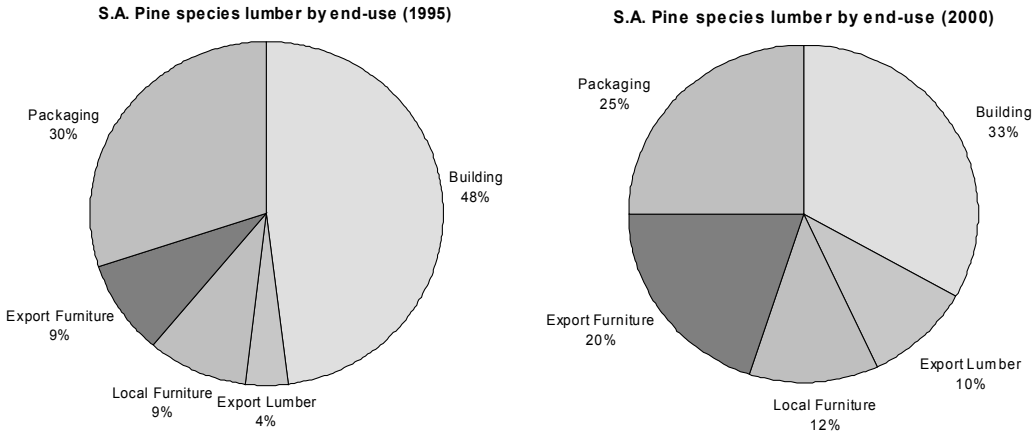

Figure 1: The change in end-use of S.A. pine species lumber (SALMA 2001).

The chemical reactions responsible for YS and KBS in softwood are well-known in the food industry and detailed information on browning reactions has been available since the 1950's (Danehy and Pigman 1951, Ellis 1959). The first studies on the occurrence of YS and KBS in kiln-dried softwood were conducted in the 1990's. From the start, it was clear that liquid water flow through the capillaries in wood was carrying discolouration precursors to a wetline, or the border of a zone still above fibre saturation point, at wood surfaces during kiln drying (Terziev *et al.* 1993, Kreber *et al.* 1998).

These discolourations reduced the value of furniture-grade lumber and seemed to have a real impact on the lumber industry in New Zealand. A number of studies were conducted to find possible control methods (Kreber *et al.* 1999). At of the writing of this thesis, the only known industrially employed control method, is the use of low temperature, high air velocity kilns.

Ironically, the characteristic stain patterns helped to verify wood scientists' theories on the existence of a wetline and capillary water transport during drying. Direct evidence of the existence of a wetline was only presented by Wiberg and Morén (1999) when wood pieces were dried while taking periodic x-ray computed

tomography scans. Evidently, the occurrence of YS and KBS was closely intertwined with the capillary water movement of free water during the first phase of drying. Mathematical models of wood drying have also shown that the existence of a wetline and development of a thin dry shell at the board surface support the invasion percolation theory of drying (Prat 2002, Salin 2003).

Hence, this thesis presents:

1. a review of information relevant to liquid water flow and discolouration during kiln drying (Chapter 2);

2. results of investigations into the occurrence of YS and KBS in South African *Pinus spp.* and liquid water flow during kiln drying of both hardwood and softwood (Chapter 3), *i.e.*:

    - "Yellow and kiln brown stain in South Africa" was intended to get an industrial perspective on the occurrence and importance of yellow stain and kiln brown stain in South Africa.

    - "Factors influencing the development of yellow stain and kiln brown stain in South African grown *Pinus spp."* looks at the effect of specie, board type and kiln schedule on discolouration.

    - "Digital image analysis and colorimetric measurement of yellow and brown stained *Pinus elliottii*" was a preliminary study conducted to characterise yellow stain and kiln brown stain, and to compare two colour measurement methods.

    - "The occurrence of discolouration due to kiln drying in South African grown *Pinus elliottii*" gives a detailed characterisation of yellow stain and kiln brown stain occurrence with the help of bag plots.

    - "The effect of surface tension on liquid water flow and discolouration in softwood" directly links liquid water flow phenomena to discolouration.

    - "An investigation of liquid water movement in Birch during drying through variation of wood sap surface tension and initial average moisture content" investigates the mechanism of liquid water flow in hardwood during drying.

    - "Liquid flow during drying in *Pinus radiata*" investigates the mechanism of liquid water flow in softwood during drying while also providing a hypothesis on the effect of anatomical differences through comparison with the similar previous study on Birch.

    - "Classification and regression tree analysis as a tool for predicting wood colour" investigates the use of this statistical technique as a decision-making tool to control the dried and planed surface colour of lumber in industrial processing.

3. a conclusion that links up the information presented in the preceding chapters (Chapter 4).

1.1.1 References

Danehy, J.P. and W.W. Pigman. 1951. Reactions between sugars and nitrogenous compounds and their relationship to certain food problems. Advances in Food Research 3, 241-290.

Ellis, G.P. 1959. The Maillard reaction. Advances in Carbohydrate Chemistry. 14, 63-134.

Kreber, B., M. Fernandez and A.G. McDonald. 1998. Migration of kiln brown stain precursors during the drying of radiata pine sapwood. Holzforschung 52, 441-446.

Kreber, B., A.N. Haslett and A.G. McDonald. 1999. Kiln brown stain in radiata pine: a short review on cause and methods for prevention. Forest Products Journal 49 (4), 66-70.

Prat, M. 2002. Recent advances in pore-scale models for drying of porous media. Chemical Engineering Journal 86, 153-164.

Salin, J.-G. 2003. External heat and mass transfer – some remarks. Proceedings of the 8th International IUFRO Wood Drying Conference, Brasov, Romania. p. 343-348.

SALMA (South African Lumber Millers' Association). 2001. Lumber Industry Trade Report.

Terziev, N., J.B. Boutelje and O. Söderström. 1993. The influence of drying schedules on the redistribution of low-molecular sugars in *Pinus sylvestris* L. Holzforschung 47, 3-8.

Wiberg, P. and T.J. Morén. 1999. Moisture flux determination in wood during drying above fibre saturation point using CT-scanning and digital image processing. Holz als Roh- und Werkstoff 57, 137-144.

Chapter 2: Theoretical and Literature Review

2.1 Wood structure and its effect on drying processes

Softwoods are members of the Gymnospermae and hardwoods are members of the Angiospermae. Although the terms softwood and hardwood were originally intended to indicate the relative hardness of the timbers, it is not an appropriate distinction. A wood anatomical difference is more descriptive. Softwoods and hardwoods have different cellular structures when viewed with a hand lens and microscope. To provide support and conducting pathways, the softwoods have radial and longitudinal tracheids and the hardwoods have respectively longitudinal fibres and longitudinal vessels (Siau 1995). In both softwoods and hardwoods parenchyma cells serve a storage function and can occur both longitudinally or radially. Groups of radial parenchyma cells form rays.

2.1.1 Softwood structure

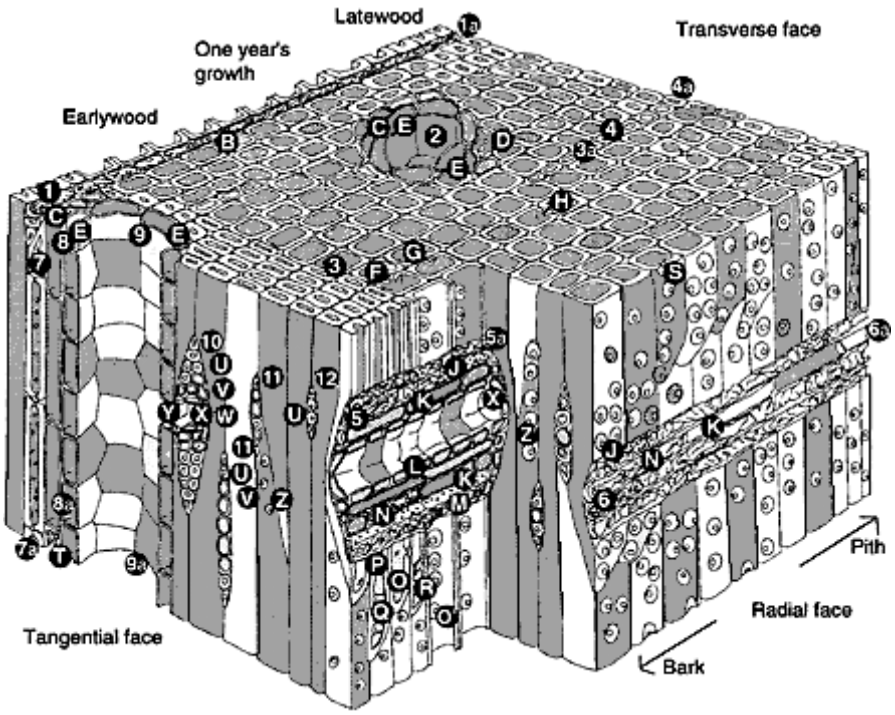

Figure 2: Anatomical structure of *Pinus palustris* (Koch 1972).

Figure 2 shows the different cell types and other structural features that are generally found in softwoods. The transverse surface in Figure 2 shows: 1-1a, ray; B, dentate ray tracheid; 2, resin canal; C, thin-walled longitudinal parenchyma; D, thick-walled longitudinal parenchyma; E, epithelial cells; 3-3a, earlywood longitudinal tracheids; F, radial bordered pit pair cut through torus and pit apertures; G, pit pair cut below pit apertures; H, tangential pit pair; 4-4a, latewood longitudinal tracheids.

The radial surface in Figure 2 shows: 5-5a, sectioned fusiform ray; J, dentate ray tracheid; K, thin-walled parechyma; L, epithelial cells; M, unsectioned ray tracheid; N, thick-walled parenchyma; O, latewood radial pit; O1, earlywood radial pit; P, tangential bordered pit; Q, callitroid-like thickenings; R, spiral thickening; S, radial bordered pits; 6-6a, sectioned uniseriate heterogenous ray.

The tangential surface in Figure 2 shows: 7-7a, strand tracheids; 8-8a, longitudinal parenchyma (thin-walled); T, thick-walled parenchyma; 9-9a, longitudinal resin canal; 10, fusiform ray; U, ray tracheids; V, ray parenchyma; W, horizontal epithelial cells; X, horizontal resin canal; Y, opening between horizontal and vertical resin canals; 11, uniseriate heterogenous rays; 12, uniseriate homogenous ray; Z, small tangential pits in latewood; Z1, large tangential pits in earlywood.

2.1.2 Hardwood structure

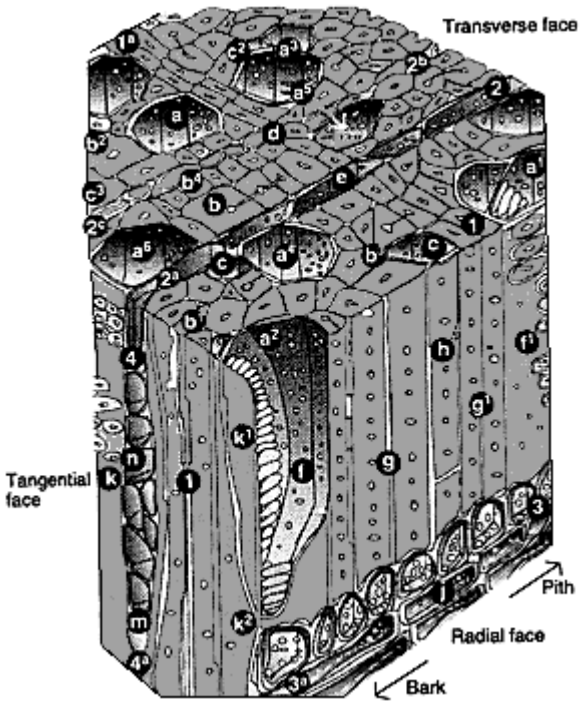

Figure 3: Anatomical structure of American Sweetgum, *Liquidambar styraciflua* (Koch 1985).

Figure 3 shows the different cell types and other structural features that are generally found in hardwoods. The transverse surface in Figure 3 shows: 1-1a, boundary between two annual rings (growth proceeding from right to left); 2-2a, wood ray consisting of procumbent cells; 2b2c, wood ray consisting of upright cells; a-a6 inclusive, pores (vessels in transverse section); b-b4 inclusive, fiber tracheids; c-c3 inclusive, cells of longitudinal parenchyma; e, procumbent ray cell.

The radial surface in Figure 3 shows: f, f1, portions of vessel elements; g1, portions of fiber tracheids in lateral surface aspect; 3-3a, upper portion of a heterocellular wood ray in lateral sectional aspect; i, a marginal row of upright ray cells; j, two rows of procumbent ray cells.

The tangential surface in Figure 3 shows: k, portion of a vessel element in tangential surface aspect; k1, k2, overlapping vessel elements in tangential surface aspect; 1, fibre tracheids in tangential surface aspect; 4-4a, portion of a wood ray in tangential sectional view; m, an upright cell in the lower margin; n, procumbent cells in the body of the ray.

When vessels are predominantly grouped in the earlywood, the pattern is described as ring porous. When they are distributed throughout the growth ring, it is described as diffuse porous.

2.1.3 Cell structure

Cellulose fibrils form a skeleton that is surrounded by other substances functioning as matrix (hemicelluloses) and encrusting (lignin) materials. The length of a native cellulose molecule is at least 5000 nm corresponding to a chain with about 10000 glucose units. The smallest building element of the cellulose skeleton is considered to be an elementary fibril. This is a bundle of 36 parallel cellulose molecules which are held together by hydrogen bonds. The bonding between cellulose molecules varies intermittently between crystalline structures and amorphous regions along the length of the fibril (Tsoumis 1991). The length of the crystallites can be 100-250 nm and the cross section, probably rectangular, is on an average 3 nm × 10 nm. Elementary fibrils are arranged into microfibrils that combine to larger fibrils and lamellae. Disordered cellulose molecules as well as hemicelluloses and lignin are located in the spaces between the microfibrils. The hemicelluloses are considered to be amorphous although they apparently are oriented in the same direction as the cellulose microfibrils. Lignin is both amorphous and isotropic (Sjöström 1993).

Figure 4 shows a typical cell wall structure. The cell wall is built up by several layers, namely the middle lamella (ML), primary wall (P), outer layer of the secondary wall (S_1), middle layer of the secondary wall (S_2), inner layer of the secondary wall (S_3) and warty layer (W). These layers differ from one another with respect to their structure as well as their chemical composition. The middle lamella is located between the cells and serves the function of binding the cells together (Tsoumis 1991).

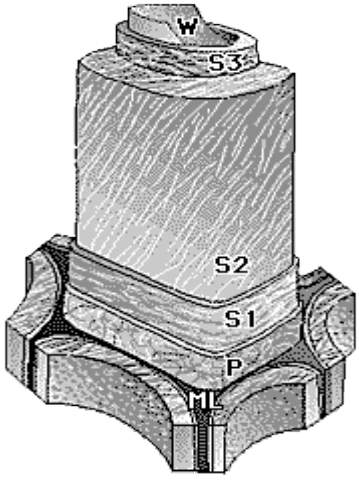

Figure 4: Cell wall structure (Côté 1967).

The primary wall is a thin layer, 0.1-0.2 μm thick, consisting of cellulose, hemicelluloses, pectin and protein, embedded in lignin. The microfibrils form an irregular network in the outer portion of the primary wall; in the interior they are oriented nearly perpendicularly to the cell axis. The middle lamella together with the primary walls on both sides, is often referred to as the compound middle lamella. Its relative lignin concentration is high, but because the layer is thin, only 20-25% of the total lignin in wood is located in this layer (Sjöström 1993).

The secondary wall consists of three layers, thin outer (S_1) and inner (S_3) layers and a thick middle (S_2) layer. These layers are built up by lamellae formed by almost parallel running microfibrils between which lignin and hemicelluloses are located (Butterfield and Meylan 1980). The outer layer is 0.2-0.3 μm thick and contains 3-4 lamellae where the microfibrils form a helix. The angle of orientation of the microfibril network varies between 50 and 70° with respect to the fibre axis. The middle layer forms the main portion of the cell wall. The inner layer is a thin layer of about 0.1 μm consisting of several lamellae, which contain microfibrils in helices with a 50-90° angle (Sjöström 1993). The warty layer (W) is a thin amorphous membrane located in the inner surface of the cell wall in all conifers and in some hardwoods, containing warty deposits of an unknown composition (Butterfield and Meylan 1980).

2.1.4 Water flow during wood drying

Since rays and resin canals form a small fraction of the volume of softwood, their contributions to the overall flow of water may be of secondary importance (Siau 1971). Water conduction between cells is made possible by pits, which are recesses in the secondary wall between adjacent cells. Two complementary pits normally occur in neighbouring cells thus forming a pit pair (Wilson and White 1986). The number of pits per tracheid varies from 50 to 300 in earlywood, with fewer and smaller pits in latewood (Siau 1971). Figure 5 shows the different types of pit pairs. Radially oriented microfibril bundles form a net-like membrane permeable to liquids (margo) in the pit (Siau 1995). Latewood margo microfibril bundles are much coarser than that of earlywood (Koch 1972). The openings in the margo have effective radii between 10 nm and 4 μm (Siau 1971). The central thickened portion of the pit membrane (torus) is rich in pectic material and in pine and spruce also contains cellulose. Bordered pit pairs are typical of softwood tracheids and hardwood fibres and vessels (Siau 1995). In softwood, especially earlywood, the pits can become aspirated during drying when the torus becomes pressed against the side of the pit border (Comstock and Côté 1968). Due to the rigidity in structure of the latewood cells, they were less prone to pit aspiration. Pit aspiration during drying increases greatly as fibre saturation point is approached (Erickson 1970). Comstock and Côté (1968) also showed that Eastern hemlock (*Tsuga canadensis*) dried at higher temperatures were less permeable, *i.e.* more aspirated. There was no significant difference in the permeability of fast and slow dried wood at the same dry bulb temperature. Hot water insoluble, lignin-like substances can also reduce permeability by encrusting the margo (Siau 1971, Thomas and Nicholas 1969).

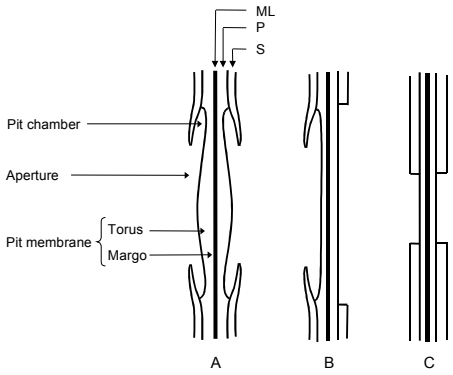

Figure 5: Types of pit pairs. A, bordered; B, half bordered; C, simple. ML, middle lamella; P, primary wall; S, secondary wall (Sjöström 1993).

In green wood, the majority of the water is held in the cell cavities as free water. Free water is found in wood with moisture contents above *ca.* 30%. This is known as the fibre saturation point (FSP). Moisture content at FSP varies between and within different timber species. Below FSP, water is held in the cell walls as bound water (Culpepper 1990).

In highly permeable woods heated almost to the boiling point of water, water and air within the cell cavities thermally expand and free water may move rapidly to the lumber surface, where it evaporates. At conventional drying temperatures, however, the pressure from inside the wood will probably be less than atmospheric pressure. In this case, little moisture is removed from the interior until surface moisture is evaporated and menisci form in the pits at the wood surface (Koch 1972). In high-temperature kilns (kilns that operate above 100°C) water literally boils out at first. High air velocity is required to remove this moisture from the surface. After the thermal expansion stage, free water continues to move to the surface by capillary action. Most high temperature kilns pass the fibre saturation point two-thirds of the way through the kiln schedule (Culpepper 1990).

The wetline borders the free water zone and below FSP zone in drying wood (Wiberg and Morén 1999). The wetline, or fibre saturation line, is also the evaporative front and, at the start of drying, lies approximately 0.5 mm below the surface, creating a thin dry shell at the surface. The dry shell is formed because large menisci move into the capillary network while smaller menisci remain stationary because of greater capillary forces. Machining of wet lumber results in damaged cells at lumber surfaces, thus creating a region with large apertures in the cellular structure of the wood. As a consequence, the large menisci of free water in this region quickly retracts into the wood to a point where the original anatomical structure of the wood is still intact. This would happen shortly after machining, creating the 0.5 mm thick dry shell at the surface (Salin 2003). As soon as the dry shell has been formed and the meniscii have found stable positions at the edge of the intact wood structure, free water is drawn towards the wood surface by capillary forces and then evaporates at the wetline on the border of the intact wood zone. The liquid tension due to capillary forces may be sufficient to cause temporary or permanent cell deformation. While water

evaporates, the largest meniscii in the interconnected capillary network start retracting into the wood piece through the largest cavities. This process continues until liquid continuity ceases due to the development of isolated regions of free water. From this point onwards, the wetline will recede into the lumber. The mechanism of drying where the largest meniscus penetrates a liquid-filled porous medium is called invasion percolation and has been modelled by Prat (2002). This model also predicts the existence of a wetline that recedes into lumber towards the later stages of the drying process. As drying continues the largest meniscus in the capillary network will become progressively smaller, thus increasing the liquid tension in the capillary network. Spolek and Plumb (1981) have also shown that the capillary forces in wood become progressively greater as the moisture content decreases. If the wood is not permeable, the wetline will recede from the start (Keey *et al.* 1999).

Below FSP, water is bound within the cell walls and is more difficult to remove. Its movement is by the slow diffusion of water from high (lumber core) to low (lumber surface) moisture content areas. Wood starts to shrink as water is removed below FSP (Culpepper 1990).

2.2 Chemical composition of wood

As mentioned, the thermal discolouration of wood as well as YS and KBS are the results of chemical reactions in wood during drying. Wood is a chemically complex material, which makes a variety of chemical reactions possible. Thus, even though the mentioned discolouration types can be attributed to the reactions of mostly certain specified precursors, it is possible that other compounds present in wood can also become chemically bonded to the final products. From this perspective it is important to be aware of the different types of compounds present in wood.

2.2.1 Basic composition of wood

The composition of wood is illustrated in Figure 6. The wood structure consists of the polysaccharides cellulose and hemicelluloses, and the polyphenolic lignin, which make up the cell walls. The rest of the material in wood is made up of low molecular weight extractives and ash. The relative contributions of these materials is given in Table 1. Protoplasm (everything except cell walls, intercellular structures and spaces) consists of more than 75% water and less than 25% materials that represent the dry weight. The dry matter is roughly 90% organic (proteins, fats, carbohydrates) and 10% inorganic. Proteins, lipids and water represent the main constituents of protoplasm (Sharp 1943).

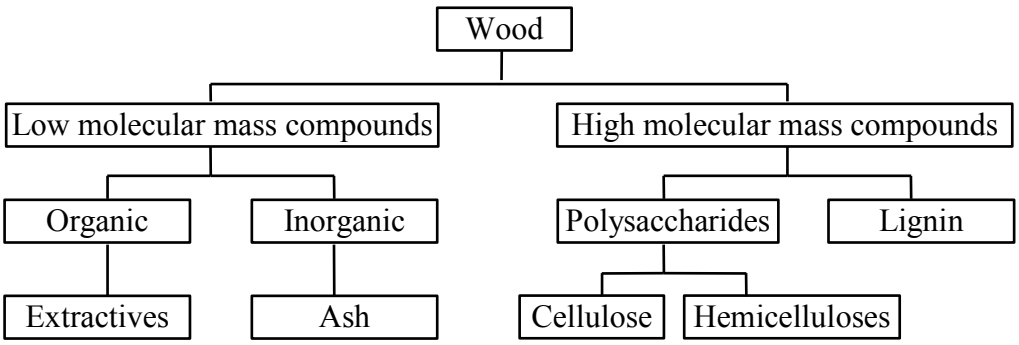

Figure 6: The composition of oven-dry wood (Fengel and Wegener 1989).

Table 1: Typical chemical composition of softwoods and hardwoods (Walker 1993)

Constituent	*Softwood (%)*	*Hardwood (%)*
Cellulose	42 ± 2	45 ± 2
Hemicelluloses	27 ± 2	30 ± 5
Lignin	28 ± 3	20 ± 4
Extractives	3 ± 2	5 ± 3

2.2.2 Carbohydrates

Carbohydrates are a group of organic compounds that includes low molecular weight sugars and large polymers like cellulose and hemicelluloses. Sugars or monosaccharides are carbohydrates with between 3 and 7 carbon atoms having many hydroxyl groups and either a ketone group or an aldehyde group (Chesworth *et al.* 1998). The sugars usually function as a source of energy in plants. On dissolution of a sugar in water, five and six carbon sugars can exist as several ring form isomers and an open chain form (Sjöström 1993). Figure 7 shows the open chain structures of several monosaccharides.

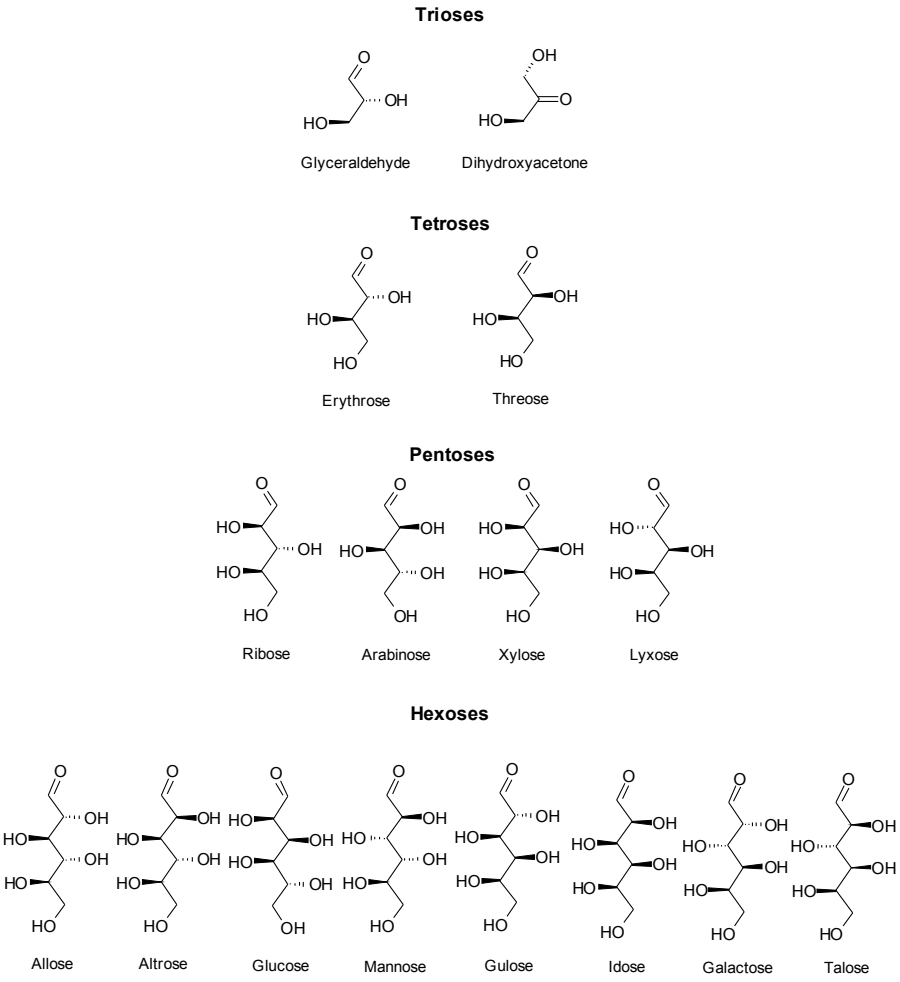

Figure 7: The structures of several aldoses. The pentoses and hexoses are able to form ring structures (Sjöström 1993).

Glucose and fructose (Figure 8) are the most abundant monosaccharides and sucrose (Figure 9) is the most abundant disaccharide occurring in plants (Sjöström 1993, McDonald *et al.* 2000). Sucrose consists of one glucose and one fructose unit. The glucose and fructose units are joined at their reducing ends, thus neither of the rings of sucrose can open to the straight chain form and, therefore, it is a non-reducing sugar (Chesworth *et al.* 1998).

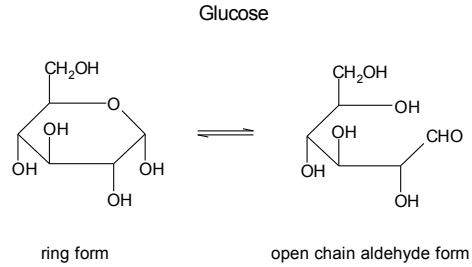

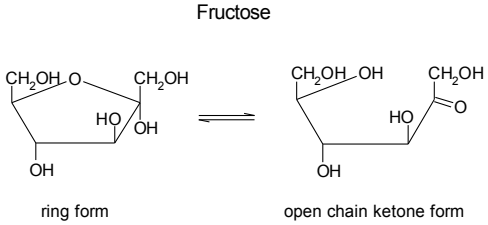

Figure 8: The structure of D-glucose and D-fructose (Chesworth et al. 1998). The open chain aldehyde and ketone forms are needed for sugar-amine condensation.

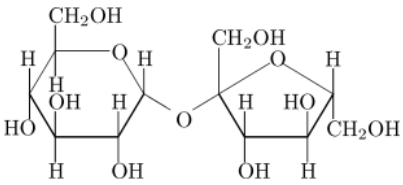

Figure 9: Sucrose, the most abundant disaccharide occurring in plants. It consists of a glucose and fructose unit (Chesworth et al. 1998).

The most abundant saccharide in wood is cellulose, a polysaccharide consisting of ß-D-glucopyranose as the repeating unit (Figure 10). About 40-45% of the dry substance in most wood species is cellulose, which fulfils a structural role in cell walls (Sjöström 1993). Other polysaccharide types that serve as supporting material in cell walls are polyoses or hemicelluloses (Figure 11). They are largely made up of glucose, mannose, arabinose, galactose and xylose. Reserve food in plants is stored in the form of starch, which is a polysaccharide that consists of glucose units (Sjöström 1993).

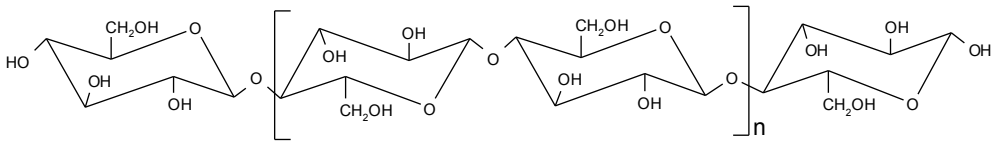

Figure 10: The structure of cellulose. ß-D-glucopyranose is the repeating unit (Sjöström 1993).

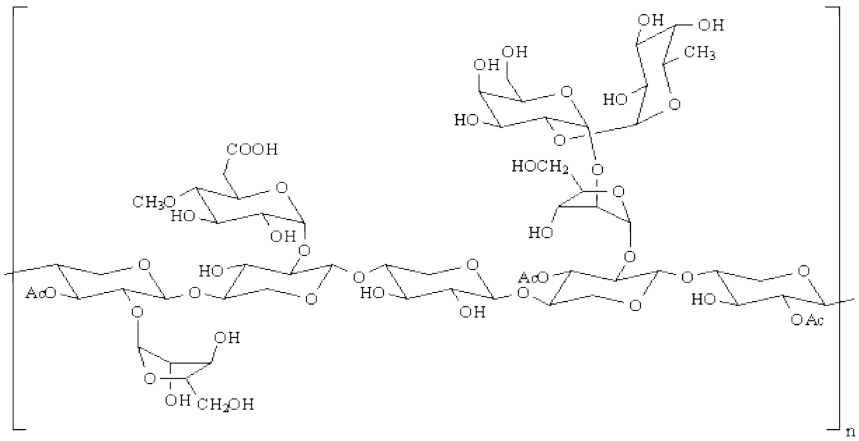

Figure 11: A hypothetical repeating unit of a wood hemicellulose unit (Fengel and Wegener 1989).

2.2.3 Lignin

Lignin is a polyphenol that is composed of three phenylpropane units, p-coumaryl- or p-hydroxyphenyl alcohol, coniferyl or guaiacyl alcohol, and sinapyl or syringyl alcohol (Figure 12). Gymnosperm lignin contains relatively fewer sinapyl alcohol units than angiosperms. The phenylpropanoid units that make up lignin are not linked in a simple repeating way (Figure 13). This makes these lignin molecules very complex and difficult to characterise. Lignin plays a structural role and is found in cell walls in a matrix together with cellulose and hemicelluloses (Fengel and Wegener 1989).

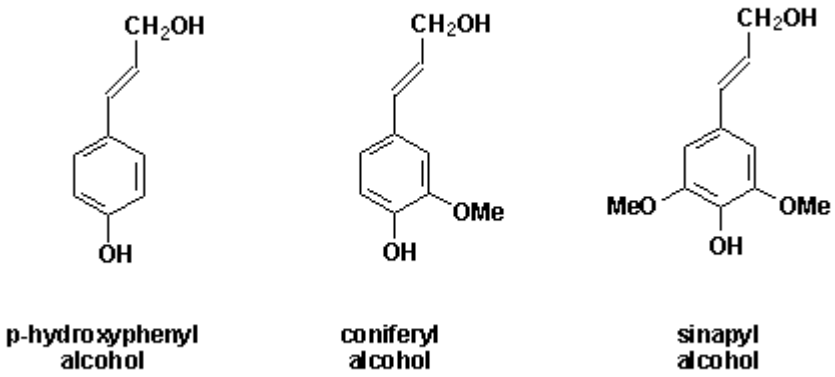

Figure 12: The building blocks of lignin (Fengel and Wegener 1989).

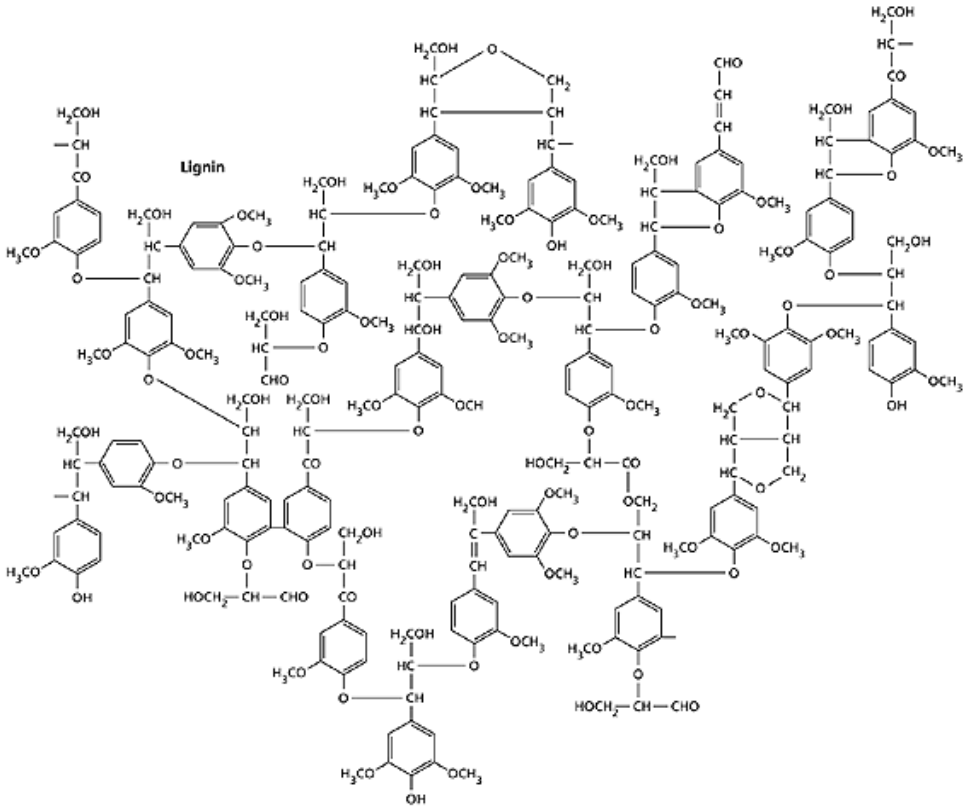

Figure 13: Partial structure of a hypothetical lignin molecule from European beech, *Fagus sylvatica* (Nimz 1974). The lignin of beech contains units derived from coniferyl alcohol, sinapyl alcohol, and *para*-coumaryl alcohol in the approximate ratio 100:70:7 and is typical of angiosperm lignin.

2.2.4 Extractives

A large number of wood components, although usually representing a minor mass fraction, are soluble in neutral organic solvents or water. They are called extractives. Extractives can be regarded as non-structural wood constituents, almost exclusively composed of low molecular mass, organic compounds (Jane 1970). Extractives comprise an extraordinarily large number of individual compounds of both lipophilic and hydrophilic types. Extractives occupy certain morphological sites in the wood structure. Lipids are concentrated in ray parenchyma cells while phenolic extractives are present mainly in heartwood and in bark.

Different types of extractives are necessary to maintain the diversified biological functions of the tree. Fats constitute the energy source of the wood cells, whereas lower terpenoids, resin acids, and phenolic substances protect the wood against microbiological damage or insect attacks. The term “resin” is used as a collective name for the lipophilic extractives (with the exception of phenolic substances) soluble in non-polar organic solvents but insoluble in water (Sjöström 1993).

On average, extractives make up only 2-8% of the oven-dry mass of hardwoods and 1-5% of softwoods (Table 1).

2.2.4.1 Terpenes and terpenoides

The terpene and terpenoid fractions of extractives are built up from a building block called an isoprene unit. The number of isoprene units present is used to classify the terpenes. Figure 14 shows the basic structures of terpenes. To date no mention has been made of the presence of resin acids, which are diterpenes, in hardwoods. It is, however, an abundant substance in softwoods (Biermann 1993).

Name	Number of 5C-units	Structure
Isoprene (basic unit)	1 × 5C	
Monoterpenes	2 × 5C	
Sesquiterpenes	3 × 5C	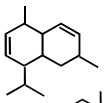
Diterpenes	4 × 5C	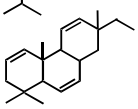

Figure 14: Basic structures of terpenes (Fengel and Wegener 1989).

2.2.4.2 Fats, waxes and their components.

A fat is an ester of glycerol and one or more fatty acids. A wax is an ester of a long chain fatty alcohol and fatty acids, thus its molecular mass is much higher than that of a fat. Examples of fats, waxes and their components are given in Figure 15. The fats are glycerol esters of fatty acids and occur in wood predominantly as triglycerides. More than thirty different fatty acids, both saturated and unsaturated, have been identified in softwoods and hardwoods (Fengel and Wegener 1989). Examples of the most common fatty acids are shown in Table 2.

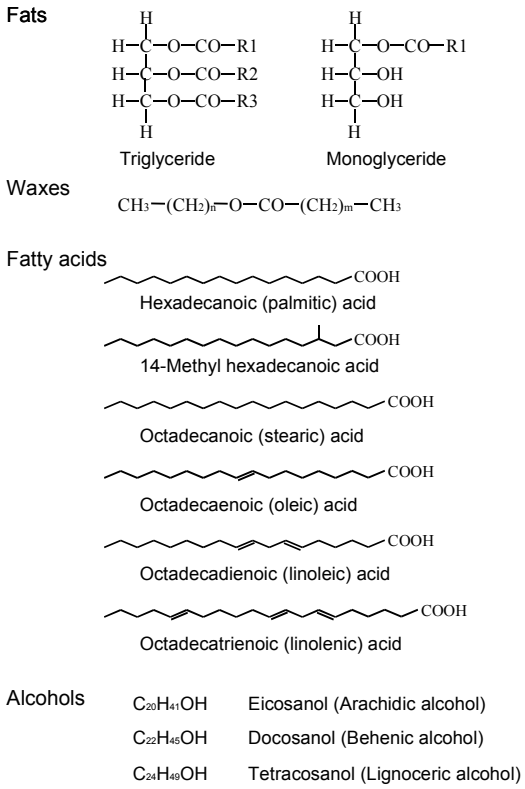

Figure 15: Fats, waxes and their components (Fengel and Wegener 1989).

Table 2: Abundant fatty acid components of fats and waxes (Sjöström 1993)

Trivial name	*Systematic name*	*Chain length*
Saturated		
Palmitic	Hexadecanoic	C_{16}
Stearic	Octadecanoic	C_{18}
Arachidic	Eicosanoic	C_{20}
Behenic	Docosanoic	C_{22}
Lignoceric	Tetracosanoic	C_{24}
Unsaturated		
Oleic	*cis*-9-Octadecanoic	C_{18}
Linoleic	*cis*,*cis*-9,12-Octadecadienoic	C_{18}
Linolenic	*cis*,*cis*,*cis*-9,12,15-Octadesatrienoic	C_{18}
Pinolenic	*cis*,*cis*,*cis*-5,9,12-Octadesatrienoic	C_{18}
Eicosatrienoic	*cis*,*cis*,*cis*-5,11,14-Eicosatrienoic	C_{20}

2.2.4.3 Phenolic substances

Extractives contain a large number of phenolic substances of simple and more complex structure. Those of more complex structure are the lignans and quinones. Some examples of the simple structure and complex phenols are displayed in Figure 16, Figure 17 and Figure 18. Phenolics give wood its resistance against microbial decay (Walker 1993).

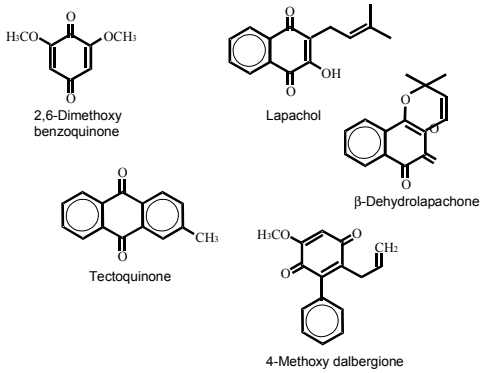

Figure 16: Kinones of hardwoods (Fengel and Wegener 1989).

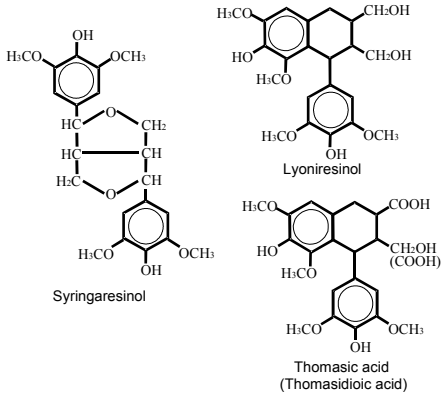

Figure 17: Well-known lignans of hardwoods (Fengel and Wegener 1989).

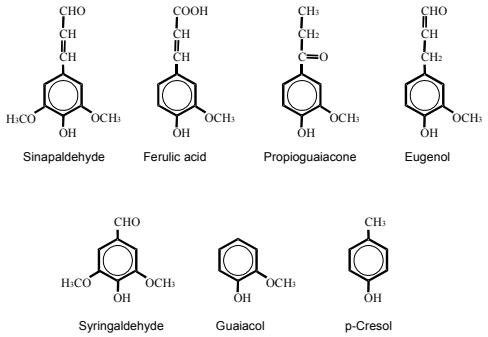

Figure 18: Some simple phenols (Fengel and Wegener 1989).

2.2.4.4 Tannins

Two types, hydrolisable and condensed tannins, exist. Among the condensed tannins are flavonoids, a substance of widespread occurrence in the plant kingdom. Hydrolisable tannins can be viewed as polyesters of gallic acid and its dimers (Figure 19). Examples of the hydrolisable tannins and flavonoids are displayed in Figure 20 and Figure 21, respectively (Fengel and Wegener 1989).

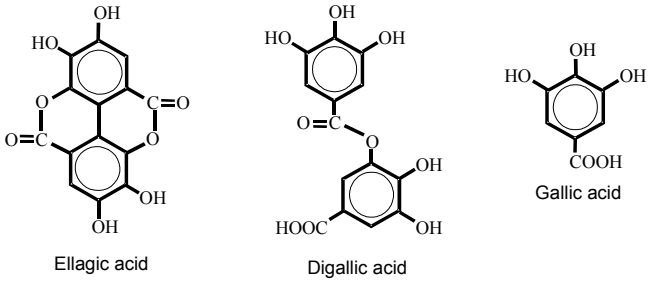

Figure 19: Gallic acid and its dimers (Fengel and Wegener 1989).

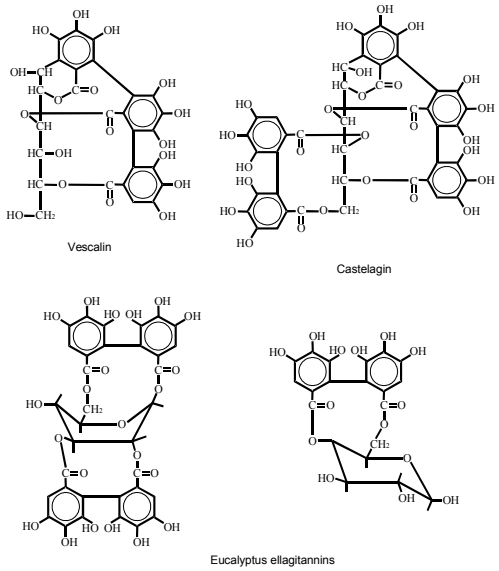

Figure 20: Some hydrolisable tannins (Fengel and Wegener 1989).

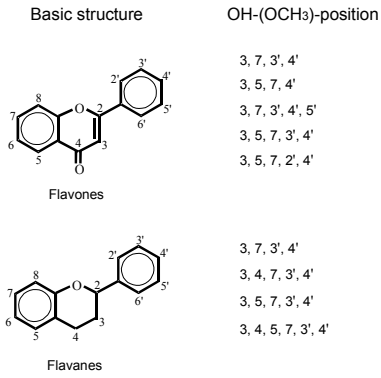

Figure 21: Some flavonoids (Fengel and Wegener 1989).

2.2.4.5 Proteins

Saturated hydrocarbons (Fengel and Wegener 1989) and free or bonded amino acids (Hägglund 1951) are also found in wood. The saturated hydrocarbons occur in a homologous range from C11 to C33 and in addition to the amino acids, there are also other nitrogen containing substances. Proteins and peptides are amino acid polymers. Proteins function as enzymes and structural components of the cell and have a function in molecular recognition within the cell. Although amino acids occur most commonly as components of proteins, some free amino acids are also found in cells. The concentrations of these are normally relatively low but when plants are subjected to water or salt stress, protein synthesis is slowed down and some free amino acids, especially proline, may accumulate and reach quite high concentrations. In addition to the amino acids that are found in proteins, there are also a number of other non-protein amino acids which exist in the free form in plants (Chesworth *et al.* 1998).

All free amino acids have the basic structure shown in Figure 22 and exist in the zwitterion form when in solution (Chesworth *et al.* 1998). There are approximately 20 different amino acids that occur in proteins (Figure 23).

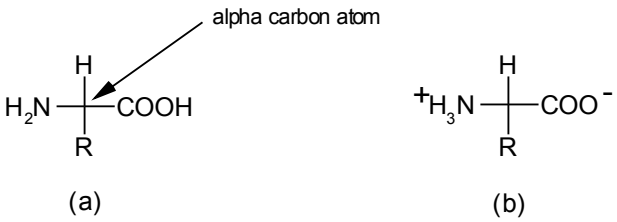

Figure 22: The basic structure of an amino acid in (a) the unionised form and (b) the zwitterion form (Chesworth et al. 1998).

Peptides are short polymers containing two to approximately twenty amino acid residues. Polypeptides combine to form proteins. Proteins normally consist of 100 to 3000 amino acid residues. Molecular masses vary from a few thousand Dalton to several hundred thousand Dalton. Proteins may act as enzymes, a means of storing nitrogen in a biologically accessible form, structural components of cells, antibodies, etc. (Chesworth *et al.* 1998).

The primary structure of a protein or peptide illustrating the repeating unit is shown in Figure 24. At one end of the chain there is a free amino group at the other there is a carboxyl group. A long chain protein has a stable folded structure due to the formation of intramolecular hydrogen bonds between amino acid residues (Chesworth *et al.* 1998).

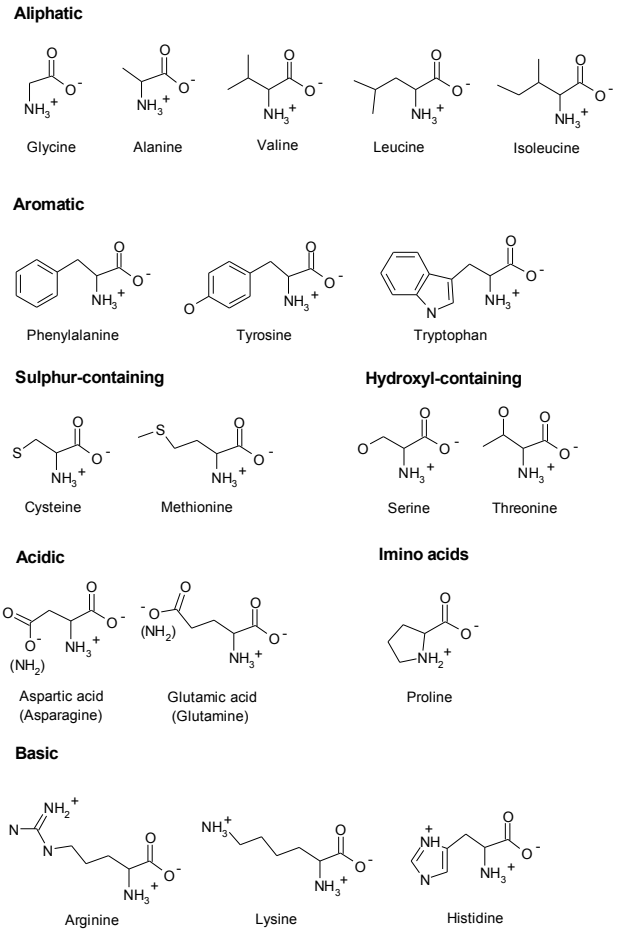

Figure 23: The structures of the amino acids commonly found in proteins (Chesworth et al. 1998).

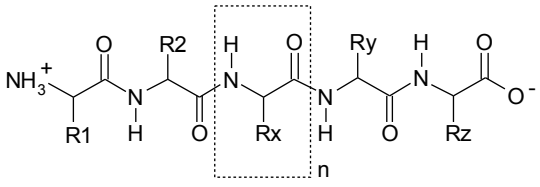

Figure 24: The primary structure of a protein. The chain normally contains 100 or more amino acids (Chesworth et al. 1998).

2.3 Discolouration reactions during kiln drying

There are a number of ways in which wood can discolour during processing. One is brown stain due to fungal growth (Fritz 1952), *i.e.* a microbial process. Another brown stain is a product of the reaction of polyphenols, which could be enzymatic or non-enzymatic and occurs in many fruits and vegetables (Martinez and Whitaker 1995). This stain occurs in both hardwoods (Charrier *et al.* 1992) and softwoods (Ellis and Avramidis 1993, Laver and Musbah 1997). Another type of brown stain is due to Maillard reactions. It is non-enzymatic and occurs between sugars (sugars and sugar derivatives containing aldehydes and ketones) and amino acids, peptides or proteins. Maillard reactions are believed to be the predominant cause of kiln brown stain (KBS) and yellow stain (YS) in softwoods (McDonald *et al.* 2000, Terziev *et al.* 1993, Terziev 1995). These reactions are possible in any substrate containing the necessary sugars and amino compounds and are commonplace in food processing and influence both colour and taste of foodstuffs. Despite a thorough literature search no incidence of KBS has been found to occur in hardwoods during conventional kiln drying. However, Maillard reactions have also been shown to occur in the hardwood *Quercus petraea* when toasted over a fire (Cutzach *et al.* 1999). Maillard reactions are not to be confused with sugar caramelization, which only occur at temperatures exceeding 120°C (Reyes *et al.* 1982, Walstra and Jenness 1984). Yet another type of discolouration is a homogeneous browning throughout the thickness of lumber that occurs at more elevated temperatures than the above mentioned discolouration types. It will be referred to as thermal discolouration in this thesis since it is especially prevalent in heat treatment, but can also occur to a lesser degree in conventional drying. This discolouration is associated with chemical changes of the macromolecules of wood (Sundqvist 2004).

In this section, and for the purpose of this study, discolouration due to Maillard reactions, *i.e.* YS and KBS, as well as thermal discolouration will be discussed since both types of discolouration can occur simultaneously. The focus is, however, on the type of reactions that result in YS and KBS since this type of discolouration is influenced by the capillary flow phase of drying.

2.3.1 Yellow stain and kiln brown stain

Maillard reactions start with the condensation reaction between carbohydrates and amino group containing compounds such as amino acids, peptides and proteins (Hodge 1953). The types of these substances present (and their concentration) in solution determine, to a large extent, the reactivity of a solution containing them (Adrian 1974).

The most frequently occurring browning reaction in food is the carbonyl-amino reaction which takes place between aldehydes, ketones or reducing sugars and amines, amino acids, peptides or proteins (Holtermand 1966). Maillard reaction intermediates may produce a yellow colour (Hodge 1953) that is probably responsible for YS. But extensive cross-linking of these and other intermediates produces the water-insoluble, brown products (melanoidins) (Danehy and Pigman 1951, Ellis 1959, Hodge 1953, Ledl and Schleicher 1990) that are observed as KBS.

Maillard reactions have nutritional consequences for food processed at high temperatures. Consequently, Maillard reactions have been studied extensively. Due to the chemical complexity of food these studies have focused on model systems and the effects that different parameters have on the extent of Maillard reaction product formation.

2.3.1.1 Maillard reaction mechanism example

Maillard reactions ultimately lead to the formation of cross-linked, water-insoluble browned proteins, which many times give rise to a brown discolouration of kiln-dried softwood. Many compounds present in wood, like lignin fragments and tannins, may take part in KBS and YS formation (McDonald *et al.* 2000). These compounds introduce many possible reaction pathways and ultimately produce an extremely complicated reaction scheme that would vary in structure with each parameter change. However, McDonald *et al.* (2000) maintained that Maillard reactions make a significant contribution to KBS formation. Consequently it is best to review the reaction mechanism of a model Maillard reaction system, where there are no contaminating substances present, to understand the discolouration mechanisms of KBS and YS.

The reaction pathway of glucose and a protein (lysozyme from egg white) as determined by Hayase *et al.* (1996) is shown in Figure 25. The figure shows that advanced glycation end products (AGE), which are precursors of melanoidins, can be formed via both oxidative and non-oxidative pathways. Browning significantly increased under anaerobic conditions compared to aerobic at pH 7.4.

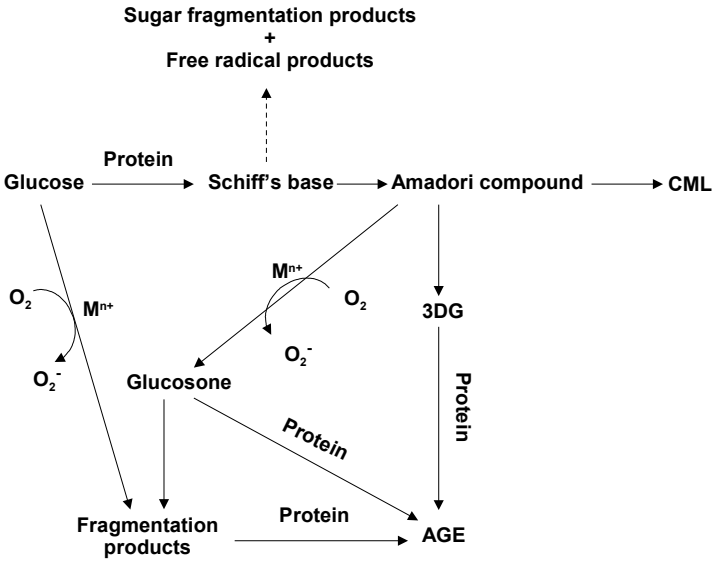

Figure 25: Reaction pathway for advanced glycation end products (AGE) formed by the protein-glucose reaction system (Hayase et al. 1996). Solid line, experimentally proved pathway; dotted line, speculated pathway. Key: CML, carboxymethyllysine; 3DG, 3-deoxyglucosone.

Sugar-amine condensation requires opening of the ring form of the sugar, addition of the amine to the carbonyl group, and subsequent elimination of a molecule of water to form the *N*-substituted glycosylamine

(Figure 26). The glycosylamine may then rearrange (Amadori rearrangement) to produce the 1-amino-1-deoxy-2-ketose derivative (Amadori compound/aminoketose) indicated in Figure 25 and Figure 26 (Ellis 1959). The Amadori rearrangement is a key reaction for browning in aldose-amine, and ketose-amine systems. Diglycosylamines may also be formed from reducing sugars and ammonia in aqueous solutions (Hodge 1953). Although reducing sugars and free amino groups of proteins combine initially in a 1 to 1 ratio, the ratio increases and approaches 1.5 to 1 during the latter stages of the reaction (Hodge 1953, Lea and Hannan 1950). Colour formation in aqueous reducing sugar-amino acid mixtures is directly proportional to the percentage of the reducing sugar in the aldehyde form (Hodge 1953).

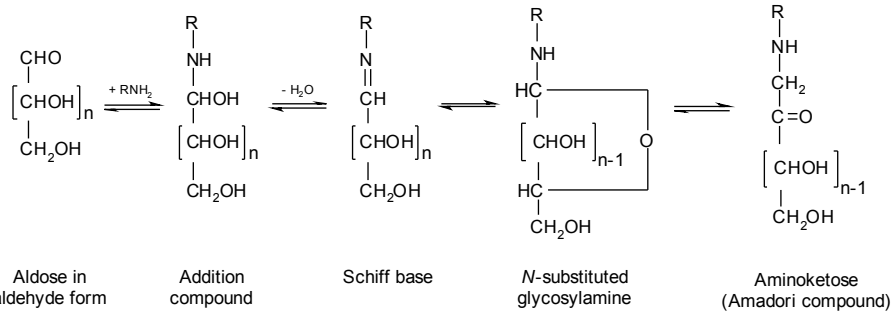

Figure 26: Reaction of an aldose (monosaccharide with an aldehyde group) with an amine compound (Hodge 1953, Ledl and Schleicher 1990).

Deoxydiketoses and deoxyaldoketoses like 3-deoxyglucosone (3DG in Figure 27) are formed as degradation products of the Amadori compounds in pH range 4-7 (Ledl and Schleicher 1990). Hayase *et al.* (1996) have proposed 3DG to be the major cross-linking molecule responsible for polymerisation of proteins in the Maillard reaction. The pH of wood is ideal for the formation of 3DG as it is usually in the 4-6 range (Fengel and Wegener 1989, Rayner and Boddy 1988). Amadori compounds lead to more browning pigments in the absence of oxygen than in its presence, but without formation of carboxymethyllysine (Ledl and Schleicher 1990).

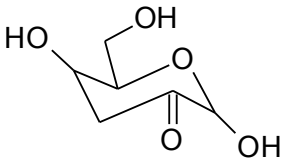

Figure 27: Structure of 3-deoxyglucosone.

Glyoxal (Figure 28) is reported to be a major product of glucose degradation under oxidative conditions (Schwarzenbolz *et al.* 1997). It is also recognised as a potent cross-linking agent that reacts readily with lysine and arginine residues in proteins (Wells-Knecht *et al.* 1995).

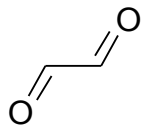

Figure 28: Structure of glyoxal.

In the final stage of browning, the Maillard reaction product (MRP) intermediates polymerise and unsaturated, fluorescent, coloured polymers (water-insoluble melanoidins) are formed. The chief reactions involved are thought to be aldol condensation, aldehyde-amine polymerisation, and the formation of heterocyclic nitrogen compounds, such as pyrroles, imidazoles, pyridines, and pyrazines shown in Figure 29 (Hodge 1953). The pigment isolated during the initial stages of the reaction (possibly YS pigments), especially at low temperature, is water-soluble while the brown pigment that is formed later, or at higher temperature, is insoluble in water. Strong alkali dissolves the pigment to give a brown liquid, from which a brown mass could be precipitated by acid.

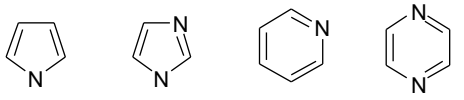

pyrrole imidazole pyridine pyrazine

Figure 29: Some heterocyclic nitrogen compounds formed during MRP polymerisation (Streitwieser et al. 1992).

2.3.1.2 Factors affecting Maillard reactions

The type of reducing sugar (sugar with an aldehyde or ketone group) determines the intensity of the Maillard reaction to a great extent. Sugar reactivity is related to the carbon chain length and partially to the stereochemical structure. The shorter the carbon chain of a sugar, the greater its reactivity. Pentoses are most active, followed by hexoses and then disaccharides.

In model compound research the following selected sugars can be placed in the following order of decreasing reactivity toward glycine: D-xylose, L-arabinose, hexoses (D-fructose, D-galactose, D-mannose and D-glucose) and disaccharides (maltose, lactose and sucrose). Sucrose can not produce any browning since it does not have any free aldehyde or ketone group. Melanoidins formed from free amino acids are more soluble than those yielded by proteins. D-xylose, L-arabinose and D-glucose are the most reactive sugars toward casein, followed by lactose, maltose and D-fructose (Ellis 1959).

In other studies, the order of reactivity of several sugars towards glycine correlated with the occurrence of the open-chain form of each sugar when in solution. The larger the proportion of the open-chain form of the sugar in solution, the higher its reactivity. This order of reactivity is as follows: methylglyoxal > 2-furaldehyde > D-ribose > D-lyxose > L-arabinose > D-xylose > D-galactose > D-mannose > D-fructose > D-glucose.

Due to the fact that amino acids exist primarily in protein form in plants, the reaction of proteins with sugars are of higher relevance to KBS than that of free amino acids with sugars. Maillard reactions do not occur with every amino acid in a protein; selection occurs, first of all with respect to the amino acid representing the N-terminal of the chain. Next to react are the basic amino acids, especially lysine, whose reactivity is often 5-15 times greater than the other amino acids. The sulphur-containing amino acids follow, and sometimes tryptophan. The protein type determines Maillard reaction intensity less than the sugar type. Proteins rich in lysine are more reactive (Adrian 1974).

Amino acid reactivity is in direct proportion to the distance between the α carbon and the amino group furthest from the α carbon (Adrian 1974). This is only true for amino acids with a four, or less, carbon chain length. Longer chain lengths can bend so that the amino group comes closer to the carboxyl group, which inhibits its reactivity. Browning also increases with increased basicity of the amino acid. L-lysine is the most chromogenic (colour generating) amino acid toward aldoses (Ellis 1959).

The following selected amino acids can be placed in this order of decreasing reactivity toward D-glucose: alanine, valine, glycine, glutamic acid, leucine, sarcosine and tyrosine. In another investigation, the following amino acids were placed in the following general order of decreasing reactivity toward several sugars: aspartic acid, glycine and DL-alanine (Ellis 1959).

A protein molecule may consist of one or more long backbone-polypeptide chains with short side chains branching from them. These chains are folded into each other in their natural environment to yield a complex structure, like the native state of glyceraldehyde-3-phosphate dehydrogenase illustrated in Figure 30. The folds of the polypeptide chain(s) are stabilised by intramolecular covalent disulphide bonds between cysteine residues, ionic bonds, hydrogen bonds, Van der Waals forces and electrostatic repulsive forces (Lee 1975). When the mentioned bonds are broken, the protein can unfold, resulting in a loss of functionality, increased solubility and reactivity. High temperatures, changes in pH, and denaturant chemicals, like sodium lauryl sulphate and urea, can cause the bonds between amino acid residues to be broken, which leads to unfolding or denaturation of the molecule (Privalov 1992). The covalent disulphide bonds are strong and require more energy to be broken. Hence, some researchers (Matsumura *et al.* 1989a 1989b) have been able to increase the thermal stability of proteins by substituting selected amino acid residues with cysteine residues to induce disulphide bond formation. They generated an increase in thermal stability from 3°C to as much as 23°C.

Proteins are typically stable in the 0-40°C temperature range (Richards 1992), so that heating to 40-80°C can cause denaturation and inactivation of the protein (Karplus and Shakhnovich 1992). The average midpoint temperature of denaturation of 1729 entries in the ProTherm protein thermodynamics database on the BioInfo Bank webpage (http://gibk26.bse.kyutech.ac.jp/jouhou/jouhoubank.html) is 58.4°C. DeMan (1979) states that meat proteins are denatured in the temperature range 57-75°C and plant leaf proteins at about 50°C. Some proteins also denature at low temperatures like 0-10°C. This is called cold denaturation (Richards 1992).

The denatured molecule would have a greater length than the native molecule, but frequently it would have a smaller volume. The native molecule has a more bulky structure, is less hydrated, and may thus fill a

greater space than the elongated denatured polypeptide. Denaturation or unfolding rarely reaches completion and the denatured molecule is typically two-thirds the length of the theoretically completely denatured molecule (Joly 1965). When comparing the structure of a denatured protein to its native form (see native form in Figure 30), it is apparent that more amino acid residues would be exposed to the environment in the case of the native protein. In the case of an *in vivo* solution, the environment includes water, carbohydrates, lipids, etc. Hypothetically, the increased number of exposed amino acid units would yield a greater potential for chemical interaction with the environment. A greater number of hydrogen bonds between the denatured protein and the solute should yield improved solubility. The newly exposed residues should also be available to form covalent bonds with, for instance, reducing sugars. Consequently, the chemical reaction rate of a denatured protein should be appreciably higher than that of the native folded molecule, also in the case of Maillard reactions. This hypothesis has been verified by Seidler and Yeargans (2001) who showed that the reaction of glyceraldehyde with denatured aspartate aminotransferase increased the absorbance of a solution at 365 nm approximately $2^2/_3$ times more than that of the native protein. The higher absorbance of the solution indicated a greater concentration of Amadori products and advanced glycation end products (AGE).

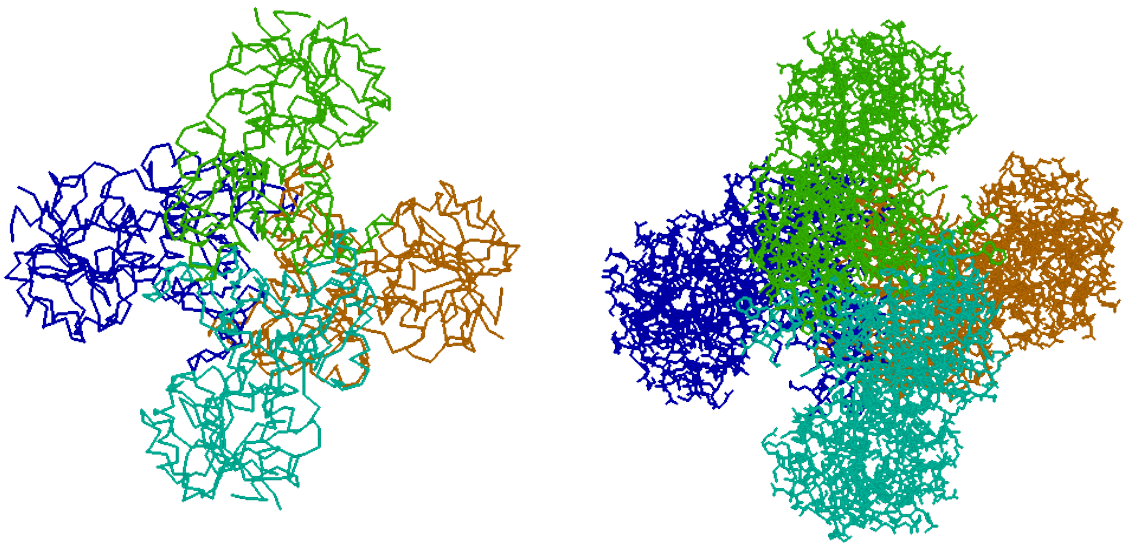

Figure 30: The molecular structure of the protein glyceraldehyde-3-phosphate dehydrogenase in its native form (http://gibk26.bse.kyutech.ac.jp/jouhou/jouhoubank.html). The molecule consists of four main chains, which are colour-coded in this representation. On the left, only the backbone of the polypeptide chains are illustrated. On the right, all carbon-to-carbon covalent bonds are illustrated.

The rate of browning increases with rising temperature. In model systems, the development increases 2 to 3 times for each 10°C rise in temperature. In natural systems, particularly those high in sugar content, the increase may be faster (Lee 1975). In the reaction between D-glucose and glycine the density of colour reached in 2 hours at 100°C requires 250 hours at 56.5°C, while the reaction between D-glucose and casein proceeds twenty times faster at 60°C than at 37°C (Ellis 1959). The reaction rate between sugars and proteins increase linearly from 0°C to 90°C (Ellis 1959) while browning of sugar-amino acid solutions

increases exponentially from 80°C to 125°C (Imming *et al.* 1996). The brown compounds are melanoidins that polymerise to molecular weights of about 7000 Da or even higher (Ledl and Schleicher 1990).

In model solutions of sugars and amino acids, a colour progression in the order light yellow, yellow, orange, brown and dark brown was observed (Ellis 1959; Hodge 1953). The more acid the medium the greater is the stability of amino acids. Amino acid degradation begins at neutrality and increases with alkalinity (Adrian 1974). Tryptophan is an exception; it is more reactive in acid than basic solutions. Since the basic amino group disappears in the Maillard reaction, the pH of an aqueous solution of the reactants will decrease as the reaction progress (Ellis 1959). Generally speaking, Maillard reactions increase approximately linearly with increasing alkalinity from values at pH 3 up to pH 9 (Adrian 1974).

No reaction takes place in the anhydrous state (mixture of sugar and amino compound in 0% relative humidity), the reaction is maximal for a relative humidity of 40-70%, decreases as aqueous dilution increases, and little reaction takes place in extremely diluted solutions. The reaction needs water to ensure the mobility of the initial reagents and is consequently favoured in poorly hydrated mediums. Water becomes an inhibitor of the dehydration reactions of further stages of the Maillard reactions (Adrian 1974). A D-glucose and glycine mixture at 65°C showed that maximum browning is reached when the water content is about 30%, based on the weight of the total mixture. When the water content was zero, or above 90%, no browning was observed (Ellis 1959).

As mentioned, AGE can be formed via both oxidative and non-oxidative pathways. There are conflicting reports on the effect of oxygen on discolouration of glucose/amino acid mixtures. According to Hayase *et al.* (1996) browning of glucose/protein significantly increased under anaerobic conditions compared to aerobic at pH 7.4. Some found that glucose and several amino acids brown in air at a reduced rate compared to anaerobic conditions, while others found that the presence of oxygen results in a more intense colouration and also affects the nature of the product (Ellis 1959). Intermediate and end products under aerobic and anaerobic conditions will certainly differ as illustrated in the reaction scheme in Figure 25.

The Maillard reaction is sensitive to metals. Copper and iron positively catalyse the browning of lactose solutions, while tin retards it. In a D-glucose/glycine system at 50°C, ferric ions accelerated the reaction four- or five-fold, but manganese ions (Mn^{2+}, 0.4 parts per million) reduced the intensity of colour by 17 to 24%. When 2 parts of manganese per million were present, colouration was reduced by 30 to 40%, as compared to controls (Ellis 1959).

Sulphur dioxide, formic acid, urea, thiourea, benzaldehyde, formaldehyde, hydroxylamine, hydrazine, semicarbazide, sodium bisulphite and sodium borohydride inhibit Maillard reactions by reacting with the precursors. Sulphur dioxide is a widely used inhibitor of browning in the food industry (Ellis 1959).

2.3.1.3 Postulated mechanism for the formation of KBS and YS

It is probable that Maillard reactions in wood predominantly occur between the common mono- and disaccharides and proteins. Free amino acids are not in abundance in plants, consequently mainly proteins would react with the saccharides present in the free water. Sucrose, a non-reducing disaccharide, could

hydrolyse to the reducing sugars fructose and glucose, which are also the most abundant monosaccharides in wood.

KBS and YS occur about 0.5-3 mm below the wood surface, excluding the areas underneath the stickers. A large portion of the water-soluble saccharides and proteins in a board would be carried to the wetline near the surface during the preliminary stage of drying. Because no evaporation of water takes place beneath the stickers, there is not such a large concentration of water-solubles. According to current knowledge on the ideal conditions for Maillard reactions, the precursors to stain formation would probably not significantly react with each other while they are in dilute solution in free water. However, Kreber *et al.* (1999) postulates that the initial reaction of the precursors likely occurs deeper in the wood. The products of these reactions are probably of low molecular weight and colourless. Upon deposition at the wetline ideal conditions (high concentrations and temperature) exist at FSP for the reactions to take place at an accelerated rate. It has also been proven that the melanoidin formation occurs at the wood surface.

Kreber *et al.* (1998) determined that the level of kiln brown stain did not further intensify beyond that occurring after the first 12 hours of drying at 90/60°C. Therefore, the critical period is the initial stage when the wetline lies just below the surface. The water-soluble substances from deeper within the board are drawn to the surface as water evaporates from the wetline. The reaction rate of these substances would be accelerated as their concentrations increase at the wetline. The pH at the wetline (FSP) may differ from the average pH of the board due to the deposition of these substances.

Kreber *et al.* (1999) mentioned that the intensity of KBS increased dramatically in *in vitro* trials as temperatures went above 80°C. Consequently, the higher temperatures drive Maillard reactions to a further extent and yields stains of higher intensity.

2.3.1.4 Control methods

Due to the fact that KBS and YS have the same chemical mechanism, methods of prevention of KBS would also suffice for the prevention of YS. To date, there are no commercially applicable prevention methods that eliminate YS or KBS satisfactorily.

Compression-rolling of fresh sawn lumber approximately halves KBS occurrence, but does not eliminate it. It causes disruption of water pathways in the wood by compressing the cells at the surface of a board. Consequently the wood is made more permeable at the surface and the wetline recedes through the damaged cells without drawing free water from the board core and thus concentrating water-solubles. Because of this treatment, drying times were increased by 15% in a 70/60°C drying schedule and by more than 25% in a 90/60°C schedule. Compression-rolling also caused increased thickness shrinkage from 4.9% to 6.0% (Kreber *et al.* 1999). Kreber *et al.* (1999) have done a cost analysis of compression-rolling by: drying with a 90/60°C or 70/60°C schedule, compression-rolling in conjunction with kiln drying with these schedules, and by drying with a 90/60°C schedule where oversized (4-5 mm) material was dried and KBS removed during planing. Among the five options, over-sawing, drying, and removal of stain during planing was the most cost-effective alternative for reducing loss in revenues due to the occurrence of KBS. This option was best even when log prices were double that of the market at that time, *i.e.* 1999.

A topical application of sodium dithionite has been shown to decrease KBS formation (Kreber *et al.* 1999). Sodium dithionite controls KBS by reacting with sugars to make them unavailable for Maillard reactions. As with other chemicals, the problem is to penetrate green lumber with the chemical solution (Kreber *et al.* 1999). Because precursors to KBS and YS may react a long way from the board surface, it is necessary that chemicals penetrate deeper than only the outer 5 mm of a board. Dipping is insufficient, thus sap-displacement by using pressure is needed to get the chemicals into the wood. Fumigation with methyl bromide and sulphuryl fluoride also slightly reduces the occurrence of KBS.

High temperatures significantly accelerate the rate of Maillard reactions. Kiln schedules utilising low dry bulb temperatures yield less KBS. The considerable increase in drying time is, however, unacceptable from a commercial standpoint. The use of higher air velocities in combination with lower temperatures does help to control discolouration. The use of stepped kiln schedules where the schedules start with a low temperature and progressively higher temperatures are used, do not significantly reduce stain formation. The reasoning behind this method was that the reaction would not take place at low temperatures. The wood was then dried to about 60% moisture content where pit aspiration and reduced mass flow of water starts, before the temperature was raised. However, the precursors would accumulate at the surface anyway, so the higher temperatures that follow later on, would yield KBS or YS.

Kreber and Haslett (1997) reported that low relative humidity kiln drying is linked to higher kiln brown stain intensity in *Pinus radiata*. They postulated that evaporation takes place just beneath the surface (0.5-2 mm) during drying at low relative humidity; because of reduced permeability at the surface as a result of pit aspiration induced by sawing. Vacuum drying at low temperatures reduces stain formation. However, vacuum drying while using high temperatures does not reduce stain formation satisfactorily.

Table 3 shows a North American kiln schedule that has been developed to control stain. This schedule would dry 40 mm thick *Pinus radiata* in five to seven days. Drying times for 40 mm thick *P. radiata* sapwood of 50 to 60 hours are attainable when using variations of the North American kiln schedule. The success of the schedule is attributed to maintaining a low wet bulb temperature until the lumber has dried to about 50 to 60% moisture content, thus minimising thermal degradation of the lumber during the initial stages of drying (Laytner 1995).

Table 3: A typical North American kiln schedule (air speed: 2 m/s) developed to minimise kiln brown stain. It proved to be effective in reducing KBS in *Pinus radiata* from New Zealand (Laytner 1995)

Moisture content (%)	Dry bulb temperature (°C)	Wet bulb temperature (°C)	EMC (%)
60+	43	35	9.8
60	49	38	8.0
50	54	40	6.7
40	54	37	5.6
35	54	35	5.0
30	60	41	5.2
25	65	46	5.2
20	71	52	5.2
15	71	43	3.4

2.3.2 Thermal discolouration

Nowadays, heat treatment is also used to protect wood against insects and fungi (Kamden *et al.* 1999). Thermal discolouration is usually associated with the heat treatment of wood when wood is heated to temperatures of 150°C or more, but it is also known to occur to a lesser extent at temperatures below 100°C. Birch in a steam atmosphere at 95°C for 144 hours discoloured to the same extent as when kept at 160°C for 2,5 hours and 200°C for 1 hour, respectively (Sundqvist 2002). The discolouration is homogeneously brown throughout the thickness of lumber and is, therefore, associated with depolymerisation of the macromolecules of wood. Of the three types of macromolecules in wood, hemicelluloses become hydrolysed at the lowest temperatures when heat is applied, followed by lignin and cellulose, respectively (Figure 31). Hence, heat treatment causes depolymerisation of the macromolecules in wood, producing water-soluble compounds (Fengel and Wegener 1989), which would be responsible for the observed discolouration. If oxygen is present during the heating of wood, low molecular weight phenolic products may not only be formed from the lignin, but also from the polysaccharides (Fengel and Wegener 1989). The degradation rate of hemicelluloses during thermal treatment in model systems was four times higher than that of cellulose (Stamm 1956).

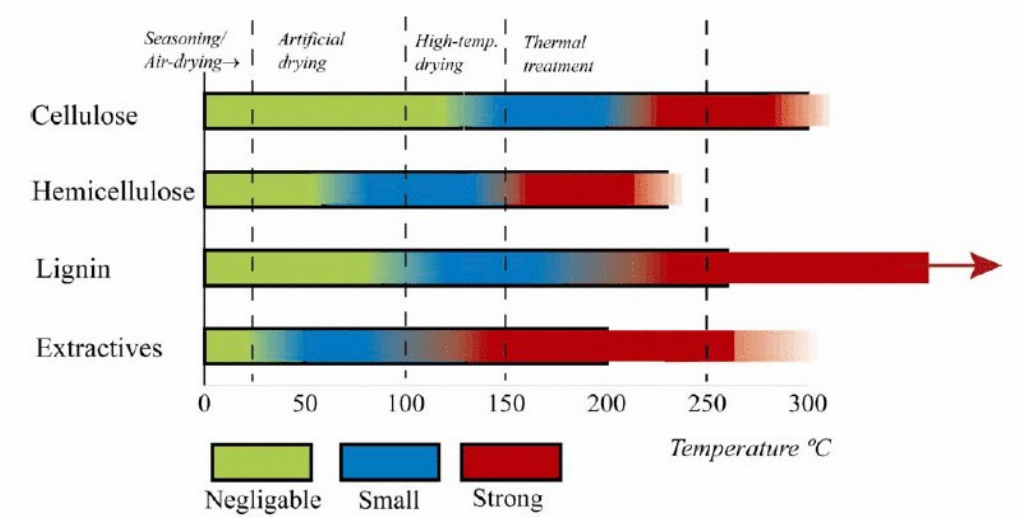

Figure 31: Chemical changes in wood components due to the application of heat (Sundqvist 2004).

After treatment at 100-150°C wood strength is diminished and water sorption ability is reduced (Schneider 1971 and 1973). The thermally treated wood is less hygroscopic (Stamm and Hansen 1937) and can have its equilibrium moisture content reduced by up to 40% (Viitaniemi and Jämsä 1996). Organic acids generated at elevated temperatures are thought to contribute to the degradation rate and discolouration of wood (Stamm 1956 and Sundqvist 2004). Harsher treatments or kiln schedules yield darker colours. The darkening is, therefore, correlated to the degree of degradation (Bourgois *et al.* 1991) and also the decline in mechanical strength (Bekhta and Niemz 2003).

2.4 References

Adrian, J. 1974. Nutritional and physiological consequences of the Maillard reaction. World Review of Nutrition and Dietetics 19, 71-122.

Bekhta, P. and P. Niemz. 2003. Effect of high temperature on the change in colour, dimensional stability and mechanical properties of spruce wood. Holzforschung 57, 539-546.

Biermann, C.J. 1993. Essentials of Pulping and Paper Making. Academic Press, San Diego.

Bourgois, P.J., G. Janin and R. Guyonnet. 1991. The colour measurement: A fast method to study and to optimise the chemical transformations undergone in the thermically treated wood. Holzforschung 45, 377-382.

Butterfield B.G., and B.A. Meylan. 1980. Three-Dimensional Structure of Wood: An Ultrastructural Approach. Chapman & Hall, London.

Charrier, B., J.P. Haluk and G. Janin. 1992. Prevention of brown discolouration in European oakwood occurring during kiln drying by a vacuum process. Holz als Roh- und Werkstoff 50, 433-437.

Chesworth, J.M., T. Stuchbury and J.R. Scaife. 1998. An Introduction to Agricultural Chemistry. Chapman & Hall, London.

Comstock, G.L. and W.A. Côté. 1968. Factors affecting permeability and pit aspiration in coniferous sapwood. Wood Science and Technology 2, 279-291.

Côté, W.L. 1967. Wood Ultrastructure. University of Washington Press, New York.

Culpepper, L.G. 1990. High Temperature Drying. Miller Freeman Publications Inc., Chicago.

Cutzach, I., P. Chatonnet, R. Henry and D. Dubourdieu. 1999. Identifying new volatile compounds in toasted oak. Journal of Agricultural and Food Chemistry 47, 1663-1667.

Danehy, J.P. and W.W. Pigman. 1951. Reactions between sugars and nitrogenous compounds and their relationship to certain food problems. Advances in Food Research 3, 241-290.

DeMan, J.M. 1979. Principles of Food Chemistry. The Avi Publishing Company, Inc., Westport, Connecticut.

Ellis, G.P. 1959. The Maillard reaction. Advances in Carbohydrate Chemistry. 14, 63-134.

Ellis, S. and S. Avramidis. 1993. Brown stain in pacific coast hemlock. IAWA Journal 14 (1), 23-28.

Erickson, H.D. 1970. Permeability of southern pine wood: A review. Wood Science 2 (3), 149-158.

Fengel, D. and G. Wegener. 1989. Wood: Chemistry, Ultrastructure, Reactions. Berlin, Walter de Gruyter.

Fritz, C.W. 1952. Brown stain in pine sapwood caused by *Cytospora sp*. Canadian Journal of Botany 30 (4), 349-359.

Hayase, F., T. Shibuya, J. Sato and M. Yamamoto. 1996. Effects of oxygen and transition metals on the advanced Maillard reaction of proteins with glucose. Bioscience, Biotechnology, and Biochemistry 60 (11), 1820-1825.

Hägglund, E. 1951. Chemistry of Wood. Academic Press Inc. New York.

Hodge, J.E. 1953. Dehydrated foods: Chemistry of browning reactions in model systems. Agricultural and Food Chemistry 1 (15), 928-943.

Holtermand, A. 1966. The browning reaction. Die Stärke 10, 319-328.

Imming, R., R. Buczys, A. Lehnberger and K.-M. Bliesener. 1996. A new appoach to the kinetics of colour formation in concentrated carbohydrate solutions. Stärke 48 (5), 163-166.

Jane, F.W. 1970. The structure of wood. 2nd ed. Adam and Charles Black, London.

Joly, M. 1965. A Physico-chemical Approach to the Denaturation of Proteins. Academic Press, London.

Kamden, D.P., A. Pizzi, R. Guyonnet and A. Jermannaud. 1999. Durability of heat-treated wood. Proceedings of the International Research Group on Wood Preservation conference, Rosenheim, Germany, p. 1-15.

Karplus, M. and E. Shakhnovich. 1992. In: Protein Folding. T.E. Creighton, ed. p. 137. W.H. Freeman and Company, New York.

Keey, R.B., T.A.G. Langrish and J.C.F. Walker. 1999. Kiln-Drying of Lumber. Springer-Verlag, Berlin.

Koch, P. 1972. Utilization of the Southern Pines. US Department of Agriculture Forest Service Handbook No. 420, Washington.

Koch, P. 1985. Utilization of Hardwoods Growing on Southern Pine Sites. USDA Forest Service Handbook No. 605, Washington.

Kreber, B. and A.N. Haslett. 1997. A study of some factors promoting kiln brown stain formation in radiata pine. Holz als Roh- und Werkstoff 55, 215-220.

Kreber, B., A.N. Haslett and A.G. McDonald. 1999. Kiln brown stain in radiata pine: a short review on cause and methods for prevention. Forest Products Journal 49 (4), 66-70.

Kreber, B., M. Fernandez and A.G. McDonald. 1998. Migration of kiln brown stain precursors during the drying of radiata pine sapwood. Holzforschung 52, 441-446.

Laver, M.L. and D.A.A. Musbah. 1997. Chemical brown staining of Douglas-fir wood: characterization of a wood enzyme extract. Forest Products Journal 47 (4), 93-98.

Laytner, F. 1995. Tackling problem stains. New Zealand Forest Industries 26 (5), 31-32.

Lea, C.H. and R.S. Hannan. 1950. Biochemical and nutritional significance of the reaction between proteins and reducing sugars. Nature 165, 438-439.

Lee, F.A. 1975. Basic Food Chemistry. The Avi Publishing Company, Inc. Westport, Connecticut.

Ledl, F. and E. Schleicher. 1990. New aspects of the Maillard reaction in foods and in the human body. Angewandte Chemie: International Edition in English 29 (6), 565-594.

Matsumura, M., W.J. Becktel, M. Levitt and B.W. Matthews. 1989a. Stabilization of phage T4 lysozyme by engineered disulfide Bonds. Proceedings of the National Academy of Sciences of the United States of America 86, 6562-6566.

Matsumura, M., G. Signor and B.W. Matthews. 1989b. Substantial increase in protein stability by multiple disulphide bonds. Nature 342, 291-293.

Martinez, M.V. and J.R. Whitaker. 1995. The biochemistry and control of enzymatic browning. Trends in Food Science & Technology 6 195-200.

McDonald, A.G., M. Fernandez, B. Kreber and F. Laytner. 2000. The chemical nature of kiln brown stain in radiata pine. Holzforschung 54, 12-22.

Nimz, H. 1974. Beech lignin - Proposal of a constitutional scheme. Angewandte Chemie International Edition 13, 313–321.

Prat, M. 2002. Recent advances in pore-scale models for drying of porous media. Chemical Engineering Journal 86, 153-164.

Privalov, P.L. 1992. In: Protein Folding. T.E. Creighton, ed. pp. 83-126. W.H. Freeman and Company, New York.

Rayner, A.D.M. and L. Boddy. 1988. Fungal Decomposition of Wood: Its Biology and Ecology. Chichester, West Sussex, John Wiley & Sons Ltd.

Reyes, F.G.R., B. Poocharoen and R.E. Worlstad. 1982. Maillard browning reaction of sugar-glycine model systems: changes in sugar concentration, colour and appearance. Journal of Food Science 47, 1376-1377.

Richards, F.M. 1992. In: Protein Folding. T.E. Creighton, ed. p. 15. W.H. Freeman and Company, New York.

Salin, J.-G. 2003. External heat and mass transfer – some remarks. Proceedings of the 8th International IUFRO Wood Drying Conference, Brasov, Romania. p. 343-348.

Schneider, A. 1971. Investigations on the influence of heat treatments within a range of temperature from 100°C to 200°C on the modulus of elasticity, maximum crushing strength, and impact work of Pine sapwood and Beechwood. Holzforschung 29, 431-440.

Schneider, A. 1973. Investigation on the convection drying of lumber at extremely high temperatures. Part II: Drying degrade, changes in sorption, colour and strength of pine sapwood and beech wood at drying temperatures form 110°C to 180°C. Holz als Roh- und Werkstoff 31, 95-99.

Schwarzenbolz, U., T. Henle, R. Haeßner and H. Klostermeyer. 1997. On the reaction of glyoxal with proteins. Zeitschrift fur Lebensmittel Untersuchung und Forschung 205, 121-124.

Seidler, N.W. and G.S. Yeargans. 2002. Effect of thermal denaturation on protein glycation. Life Sciences 70, 1789-1799.

Sharp, L.W. 1943. Fundamentals of cytology. McGraw-Hill Book Company, Inc. New York.

Siau, J.F. 1971. Flow in Wood. Syracuse University Press, Syracuse.

Siau, J.F. 1995. Wood: Influence of Moisture on Physical Properties. Department of Wood Science and Forest Products, Virginia Polytechnic Institute and State University, Virginia.

Sjöström, E. 1993. Wood Chemistry: Fundamentals and Applications. Academic Press, New York.

Spolek, G.A. and O.A. Plumb. 1981. Capillary Pressure in Softwoods. Wood Science and Technology 15, 189-199.

Stamm, A. 1956. Thermal degradation of wood and cellulose. Journal of Industrial and Engineering Chemistry 48, 413-417.

Stamm, A.J. and L.A. Hansen. 1937. Minimizing wood shrinkage and swelling: Effect of heating in various gases. Industrial and Engineering Chemistry 29, 831-833.

Streitwieser, A., C.H. Heathcock and E.M. Kosower. 1992. Introduction to Organic Chemistry. Macmillan Publishing Company, New York.

Sundqvist, B. 2002. Colour response of Scots Pine (*Pinus sylvestris*), Norway Spruce (*Picea abies*) and Birch (*Betula pubescens*) subjected to heat treatment in capillary phase. Holz als Roh- und Werkstoff 60 (2), 106-114.

Sundqvist, B. 2004. Colour Changes and Acid Formation in Wood During Heating. Doctoral thesis, Luleå University of Technology, Skellefteå, Sweden.

Terziev, N. 1995. Migration of low-molecular sugars and nitrogenous compounds in *Pinus sylvestris* L. during kiln and air drying. Holzforschung 49, 565-574.

Terziev, N., J.B. Boutelje and O. Söderström. 1993. The influence of drying schedules on the redistribution of low-molecular sugars in *Pinus sylvestris* L. Holzforschung 47, 3-8.

Thomas, R.J. and D.D. Nicholas. 1969. The ultrastructure of the ray tracheid bordered pit membranes in southern pine. Tappi Journal 52 (11), 2160-2163.

Tsoumis, G.T. 1991. Science and Technology of Wood: Structure, Properties, Utilisation. Van Nostrand Reinhold, New York.

Viitaniemi, P. and S. Jämsä. 1996. Modification of wood with heat treatment. Rep. no. 814, VTT Building Technology, Espoo, Finland.

Walker, J.C.F. 1993. Primary wood processing: Principles and practice. 1st ed., Chapman and Hall, London.

Walstra, P. and R. Jenness. 1984. Dairy Chemistry and Physics. Wiley-Interscience, New York.

Wells-Knecht, K.J., D.V. Zyzak, J.E. Litchfield, S.R. Thorpe and J.W. Baynes. 1995. Mechanism of autoxidative glycosylation: Identification of glyoxal and arabinose as intermediates in the autoxididative modification of proteins by glucose. Biochemistry 34, 3702-3709.

Wiberg, P. and T.J. Morén. 1999. Moisture flux determination in wood during drying above fibre saturation point using CT-scanning and digital image processing. Holz als Roh- und Werkstoff 57, 137-144.

Wilson, K. and D.J.B. White. 1986. The Anatomy of Wood: Its Diversity and Variability. Stobart & Son, London.

Chapter 3: Experimental Work and Results

Each section or manuscript in this chapter has been written to function as a standalone unit. The purpose of each section being:

3.1 "Yellow and kiln brown stain in South Africa" was intended to get an industrial perspective on the occurrence and importance of yellow stain and kiln brown stain in South Africa.

3.2 "Factors influencing the development of yellow stain and kiln brown stain in South African grown *Pinus spp."* looks at the effect of specie, board type and kiln schedule on discolouration.

3.3 "Digital image analysis and colorimetric measurement of yellow and brown stained *Pinus elliottii*" was a preliminary study conducted to characterise yellow stain and kiln brown stain, and to compare two colour measurement methods.

3.4 "The occurrence of discolouration due to kiln drying in South African grown *Pinus elliottii*" gives a detailed characterisation of yellow stain and kiln brown stain occurrence with the help of bag plots.

3.5 "The effect of surface tension on liquid water flow and discolouration in softwood" directly links liquid water flow phenomena to discolouration.

3.6 "Liquid water movement in Birch during drying" investigates the mechanism of liquid water flow in hardwood during drying.

3.7 "Liquid water flow during drying in *Pinus radiata*" investigates the mechanism of liquid water flow in softwood during drying while also providing a hypothesis on the effect of anatomical differences through comparison with a similar previous study on Birch.

3.8 "Classification and regression tree analysis as a tool for predicting wood colour" investigates the use of this statistical technique as a tool to control the dried and planed surface colour of lumber in industrial processing.

3.1 Yellow and kiln brown stain in South Africa

3.1.1 Abstract

The furniture and joinery market has grown in recent years and the demand for greater volumes of high quality wood has increased correspondingly. The incidence of yellow stain (YS) and kiln brown stain (KBS) adversely affects wood quality. Consequently, a survey was undertaken to determine the effect of the yellow and kiln brown stain phenomena on the South African sawmilling industry as well as local furniture and joinery manufacturers. The feedback from respondents indicated that wood species, geographic location and particularly drying schedule are the most important determinants of YS and KBS development. Wood from all regions of the country, except the Western Cape, appeared to be prone to discolour. In general, furniture and joinery manufacturers do not accept discoloured wood.

3.1.2 Introduction

The demand for export and furniture lumber has almost doubled from 22% of total lumber output in 1995 to 42% in 2000 (Figure 1).

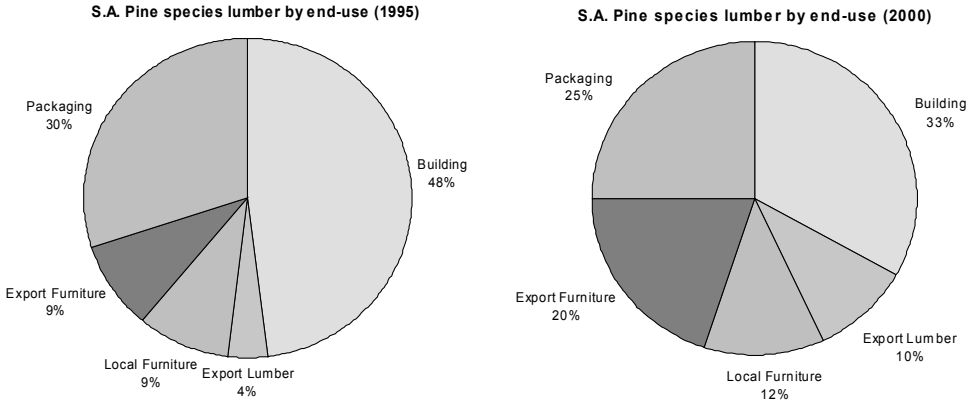

Figure 1: The change in end-use of S.A. pine species lumber (SALMA 2001).

This dramatic increase in demand for furniture and joinery products has given rise to a corresponding greater demand for defect-free or high quality lumber suitable for use in the decorative markets. Previously, as the bulk of lumber was destined for the building and packaging markets, little emphasis was placed on dry wood quality. Discoloured and surface checked wood was not considered to be unsuitable. However, lumber for furniture and joinery applications has to pass certain norms of visual acceptability. In South Africa, no formal standards for visual acceptability exist. As a consequence, furniture and joinery manufacturers have coined the term “furniture grade” when conveying and specifying their need for clear, defect-free lumber to suppliers.

The recent developments have highlighted common defects of lumber produced in the past. These defects are mostly related to kiln drying practices. Of these defects, YS and KBS, commonly occur in kiln-dried lumber, making it less suitable for use in furniture and joinery markets. As a result, the South African Lumber Millers' Association (SALMA) deemed it necessary to fund research into lumber discolouration associated with kiln drying. Hence, the first objective of this research was to gather information from the experiences and feedback of sawmillers as well as furniture and joinery manufacturers. The feedback given by the sawmillers would serve to indicate the parameters that influence yellow and kiln brown stain formation, while the survey conducted amongst the furniture and joinery manufacturers would give an idea of the importance of the discolouration phenomena to their industry. As the respondents would not intentionally have collected data on, or conducted scientific study of the discolouration prior to this investigation, it should be noted that this report could only reflect the subjective perceptions, experiences and opinions of several individuals.

3.1.3 Survey method

3.1.3.1 Sawmillers survey

The possible influence of variables such as drying schedule, wood species, geographical region, time of the year, zone of trunk and resin content on the occurrence of discolouration were investigated. Forty-two questionnaires were sent out to softwood sawmills throughout South Africa and Swaziland to determine the extent of discolouration problems as well as the effect of these variables on the severity of discolouration. Eighteen responded, providing valuable information and making it possible to observe patterns in the formation of YS and KBS.

3.1.3.2 Furniture and joinery manufacturers survey

Six furniture and joinery manufacturers who source dried lumber from many different suppliers, were personally interviewed to give an account of their experience with stained lumber. They were questioned on the impact that discoloured wood had on their business and on methods employed to limit the impact. In view of their close contact and interaction with the furniture and joinery market, they were also asked to comment on future trends of the market relating to colour quality standards.

3.1.4 Sawmill survey results and discussion

3.1.4.1 Influence of drying schedules used

Two of the eighteen respondents employed air-drying and experienced no stain problems. Of the sixteen remaining respondents that made use of kilns, two produced structural wood exclusively and never noticed or kept a look out for discolourations. The information of these two respondents was omitted. The remaining fourteen respondents employed 24 drying schedules in total. Since maximum dry bulb temperatures in drying schedules play a key role in the formation of stain, it was decided to evaluate the

received information according to maximum dry bulb temperatures employed. The schedules are listed in Table 1.

Table 1: The effect of dry bulb temperature on stain development during kiln drying of Southern African *Pinus spp.*

Schedule type	Number of schedules yielding:			
	no significant stain/never noticed	yellow stain only	kiln brown stain only	yellow and kiln brown stain
Uncontrolled/unknown temperature	1	0	0	0
Maximum dry bulb temperature < 80°C	2	5	0	0
Maximum dry bulb temperature >= 80°C	5	2	5	4
Totals	8	7	5	4

KBS was observed in all drying schedules that reached a maximum dry bulb temperature above 80°C. YS was found in both above and below 80°C schedules. Five of the seven schedules that yielded only YS had a maximum dry bulb temperature below 80°C. In one case, YS was observed in a progressive kiln that reached a maximum dry bulb temperature of 54°C.

3.1.4.2 Influence of wood species

In general the respondents indicated that stain problems occurred to the same degree in *Pinus elliottii*, *P. patula* and *P. taeda*. One respondent stated that *P. elliottii* gave a darker yellow stain than *P. taeda*. At drying temperatures of ±50°C, *P. elliottii* and *P. taeda* produced yellow stain, while *P. patula* did not. *P. canarienses* and *P. pinaster* from the Eastern Cape also developed yellow stain at 70°C while *P. radiata* became kiln brown stained at 90°C.

3.1.4.3 Geographical origin of wood

No stain problems were experienced with the *P. radiata* and *P. pinaster* grown in the Western Cape region even though schedules with maximum dry bulb temperatures exceeding 80°C were employed (Table 2). *P. pinaster* of the Eastern Cape developed yellow stain. Kreber *et. al* (1999) also reported frequent kiln brown stain in *P. radiata* grown in New Zealand. *P. radiata* from the Tsitsikamma region also developed yellow and kiln brown stain. Therefore, the area of cultivation did have an effect.

Table 2: The effect of geographical origin on stain development

Origin of wood	Number of schedules yielding:			
	no significant stain/never noticed	yellow stain only	kiln brown stain only	yellow and kiln brown stain
Western Cape	2	0	0	0
Tsitsikamma	0	0	1	0
Kwazulu/Natal and Eastern Cape	2	2	0	2
Northern Province, Mpumalanga and Swaziland	4	5	4	2
Totals	8	7	5	4

3.1.4.4 Time of year

Conflicting responses were received on which time of year the discolouration appeared to be more prevalent. One respondent reported that July to October were the most severe months, another selected May to August and one experienced the most severe stain from November to March. All of these respondents were from Mpumalanga. Three others mentioned that the staining was equally severe throughout the year. Two of these respondents were from Mpumalanga and one was from Swaziland.

3.1.4.5 Zone of trunk

Two respondents made an identical claim on the zones of the trunk most affected. Both experienced that the sapwood as well as the butt log produced the most stain. One respondent worked exclusively with *P. patula* and the other exclusively with *P. elliottii* from Mpumalanga. Another two respondents, one from Mpumalanga and one from Swaziland, stated that there was no noticeable difference. They worked with a mix of *P. taeda*, *P. patula* and *P. elliottii*.

3.1.4.6 Resin content

Several respondents could not recall whether the resin content of the lumber made a difference to the severity of stain development or not. Four respondents experienced the stain as more severe when more resinous lumber was dried while three others reported that it made no difference.

3.1.4.7 Effect on lumber sales

Yellow stain negatively affected the lumber sales of three respondents while “not significantly” affecting another. One of these three respondents reported that the total furniture lumber production was affected by yellow stain during the winter months. Another respondent only mentioned customer complaints but no real loss of sales although 600 m^3 of lumber was affected in total by yellow and kiln brown stain per month. Kiln brown stain affected 10% of the production volume of one respondent without affecting sales while 5% of the furniture lumber sales of one respondent were affected by kiln brown stain.

The sales of two respondents experiencing a combination of yellow stain and kiln brown stain were not affected at all, another two were not affected by yellow stain and two respondents were not affected by kiln brown stain at all.

3.1.5 Furniture manufacturers survey results and discussion

One joinery manufacturer, based in the Western Cape, procured wood from the Tsitsikamma and Western Cape. The green *P. elliottii* and *P. radiata* flitches they received from the Tsitsikamma developed kiln brown stain upon kiln drying under 90°C dry bulb and 60°C wet bulb conditions. The stain was not acceptable from a decorative point of view as the lumber was used for making doors. The flitches, supplied by a small sawmill in the Southern Cape, were 43 mm thick instead of the standard 38 mm to enable the joinery plant to plane off the stain after kiln drying. The lumber they received from the Western Cape did not discolour upon drying.

Several of the furniture and joinery manufacturers do not accept stained lumber and request “furniture grade” lumber from suppliers. One joinery manufacturer from Kwazulu/Natal regularly evaluates the boards supplied by 21 sawmills. The boards are checked for correct dimensions and moisture content as well as blue stain, yellow stain/kiln brown stain, knots, wane, bow, spring, cup, handling damage, twist and apparent resin content. Some loads have been sent back to suppliers for failing the mutually agreed upon quality specifications.

Twenty to thirty percent of the lumber received by another furniture manufacturer was discoloured, with yellow stained boards making up the bulk of the discoloured lumber. The manufacturer produced bed frames and got around the problem by using the stained lumber in places where it would not be visible to the end user. The manufacturer purchased wood from sawmills that produced smaller percentages of stained lumber. Another company concealed stained lumber when producing doors in such a manner that the stain was only visible as a thin line at glue joints. Nevertheless, some of company’s lumber was discarded for the intended purpose due to stain.

The furniture and joinery manufacturers were of opinion that clear and semi-transparent finishes enhanced stain colour and that discoloured wood will become less acceptable as international quality standards become stricter. Apparently, European consumers prefer lighter shaded lumber as European lumber tends to be whiter than South African lumber. As a result, the European market is more sensitive to darker coloured wood.

3.1.6 Conclusions

The information gathered from eighteen out of a possible forty-two respondents throughout South Africa and Swaziland proved to be of great value in determining the most important parameters in stain development. It also gave an idea of the extent of discolouration problems and the effect it had on lumber sales.

- The kiln dry bulb temperature seems to be the most important process variable for wood discolouration. Kiln brown stain developed exclusively in above 80°C schedules. Yellow stain developed predominantly at temperatures below 80°C and was also formed at temperatures as low as 54°C.

- KBS and YS seem to be chemically closely linked; with the brown discolouration being a product of polymerisation or the propagation of reactions that produce a yellow discolouration at first. The length of the drying time also determines the extent to which the discolouration reactions take place, *i.e.* longer drying times at the same temperature produced more KBS.

- Because of chemical variation between tree species, some species seemed to be more prone to yield stained lumber. Information gathered from the questionnaire suggests that *P. elliottii* may be the most likely species to develop stain during drying. It is also one of the more resinous *Pinus spp.* in South Africa.

- Stain problems were absent in the Western Cape region where mostly *P. radiata* and *P. pinaster* is found. *P. radiata* is well-known to develop kiln brown stain. Consequently, climate/soil type seemed to have an effect on the tendency of the wood to discolour.

- It is possible that certain zones of the trunk are more prone to discolour due to the variation in chemical composition within a tree. Two respondents stated that the sapwood as well as the butt log produced the most stain.

- No general conclusions could be drawn on the effect of resin content and time of year on stain development. On the topic of resin content there were conflicting reports. In the case of time of year it seemed that, though the respondents were geographically and climatically not far removed, there were differences in the effect that the time of year had on discolouration. In some cases, the respondents were adamant that time of year had an effect on stain development.

- The effect of discolouration on overall lumber sales and profit margins was generally not considered severe, though a few mills were seriously affected.

3.1.7 Acknowledgements

The authors wish to acknowledge the contributions of all respondents as well as the financial support of SALMA for this project.

3.1.8 References

Kreber, B., A.N. Haslett and A.G. McDonald. 1999. Kiln brown stain in radiata pine: a short review on cause and methods for prevention. Forest Products Journal 49 (4), 66-70.

SALMA (South African Lumber Millers' Association). 2001. Lumber Industry Trade Report.

3.2 Factors influencing the development of yellow stain and kiln brown stain in South African grown *Pinus spp.*

3.2.1 Abstract

Pinus elliottii, *P. patula* and *P. taeda* boards were dried using different drying schedules and stain development was assessed. Results indicated that kiln brown stain and yellow stain development is chemically linked, as suggested by other workers. The degree of discolouration is highly dependent on kiln schedule and species as well as the schedule/species interaction. In high temperature schedules, *P. elliottii* discoloured to a greater degree than *P. patula*, while the opposite was true at lower temperatures. Irrespective of schedule, *P. taeda* was always least prone to discolour. *P. taeda* core boards were significantly less inclined to discolour than side boards. In the other species the difference between core/side board discolouration was less distinct.

3.2.2 Introduction

Discolouration in general and irregular discolouration in particular, decreases the value of lumber destined for decorative markets such as furniture, flooring and wall cladding. Some softwood species may discolour when kiln or air drying causes low molecular weight carbohydrates and nitrogenous compounds in wood to accumulate and react with each other just beneath lumber surfaces (Boutelje 1990; Kreber *et al* 1999; Long 1978; Terziev *et al.* 1993; Theander *et al.* 1993). Brown or yellow stains are often not visible in the rough sawn condition and are only revealed upon planing. The chemical reactions responsible for discolouration are referred to as Maillard reactions and are well known in the food industry (Danehy and Pigman 1951). Maillard reactions are complex, various pathways exist and numerous reaction products are formed (Ledl and Schleicher 1990). In model solutions of sugars and amino acids, a colour progression from light yellow, yellow, orange, brown to dark brown has been observed (Ellis 1959; Hodge 1953). Consequently, as suggested in previous publications, the development of kiln brown stain and yellow stain could be chemically linked. Some of the variables that determine the reaction rate are temperature, water concentration (*i.e.* wood moisture content in the case of wood), pH, oxygen availability, carbohydrate and nitrogenous compound type and concentration (Ellis 1959).

The occurrence of yellow stain and kiln brown stain during kiln drying of South African grown *Pinus spp.* raised questions about the effect of wood species, kiln schedules and board type (core/side board) on stain development. In this investigation, three softwood species were dried under different conditions to answer these questions and elucidate the mechanism of stain formation.

3.2.3 Materials and methods

Five logs each of *Pinus elliottii*, *P. patula* and *P. taeda* were obtained in the Sabie district of Mpumalanga (log origins are indicated in Table 1) and two 38 mm thick boards, one core board and one side board, were

sawn from each log, giving 5 core and 5 side boards per species. Six samples of 0.7 m length were cut from each board, giving 60 samples per species and 180 samples in total. Each sample was marked with a code indicating its log number, species, core/side board and position in the board. For example, the code 1ES1 would indicate that the sample came from the *first* log in the *P. elliotti* batch, was a *sideboard*, and was the *first* sample cut from the board.

Table 1: Origin of the log samples

Wood species	Compartment code	Supplier
Pinus elliottii	Q11	Mondi Forests
Pinus patula	F17 Hendriksdal	Mondi Forests
Pinus taeda	802 Bergvliet	SAFCOL

The six samples from each board were dried with six different schedules (in six different industrial kilns) representing a range of different drying conditions, as illustrated in Table 2. The samples were placed into the sides of the kiln charges so as not to interrupt mill production flow. The samples in kilns 1-4 were dried to a final moisture content of 10%. The samples in kilns 5 and 6 were dried with charges of smaller thickness (25 mm and 19 mm respectively) to determine the effect of a higher final moisture content (20+ %) on stain characteristics.

Table 2: Kiln conditions. All charges were dried to a final moisture content of 10%

Schedule number	Kiln type	Maximum T_d/T_w (°C/°C)	Drying time (h)	Charge thickness (mm)
1	Compartment	90/60	38	38
2	Progressive	60/50	144	38
3	Compartment	100/80	32	38
4	Compartment	88/62	50	38
5	Compartment	90/65	41	25
6	Compartment	75/58	45	19

After drying, the samples were planed on one face to a depth of approximately 1 mm to reveal any stain present under the surface of the board. The planed surfaces were then visually classified as having no stain (0), mild yellow stain (Y1), severe yellow stain (Y2), mild brown stain (B1) or severe brown stain (B2).

3.2.4 Results and discussion

The visual evaluation results are listed in Table 3. The table gives an indication of how sections of the same board underwent different reactions under the various kiln-drying conditions. Nine samples were lost in production. Because the sample thickness (38 mm) was greater than the charge thickness for schedules 5 (25 mm) and 6 (19 mm), the sample moisture content was still above 20% at termination of the drying schedule. Despite the higher moisture content of these samples, the samples in these two schedules still underwent significant stain development (Table 3). Evidently, precursor deposition and stain development took place while the lumber was still quite wet.

An analysis of variance was done to examine the effects of the factors that could have an impact on the discolouration outcome of the samples. The factors considered were schedule, species and board type. It

was considered ideal to generate discolouration means for easy interpretation of the effects of different factors. Consequently, the stain classes 0, Y1, Y2, B1 and B2 were converted to the integer code 1, 2, 3, 4 and 5 to facilitate this kind of analysis. Thus, it was assumed that there were equal differences with respect to the severity of discolouration between these stain classes. This assumption was tested by using various transformations that distorted the stain classification scale, creating unequal distances between successive stain classes, while keeping the minimum and maximum values at 1 and 5 respectively. The idea was to determine whether substantially different conclusions would be made with the transformed data. The transformations considered were Box-Cox (λ=2, 1, 0, -1) and the ordinates of Beta (p=q=2, 3) distributions. These not too extreme distortions did not change any of the conclusions about the significance of the factors. Consequently, the assumption that the stain classifications could be treated as linear measurements was reasonable.

Table 3: Stain occurrence by board and schedule

Specie	Board code	Schedule					
		1	2	3	4	5	6
P. elliottii	1EC	B2	Y1	B1	B1	B1	Y2
	1ES	B2	Y1	B2	B2	B1	Y2
	2EC	B2	Y2	B2	B1	B1	Y2
	2ES	B2	Y1	B1	B2	B1	Y2
	3EC	—	Y1	B2	B2	B1	Y1
	3ES	—	Y1	B1	B2	B2	Y2
	4EC	B2	Y1	B2	B1	B1	Y1
	4ES	B2	Y2	B2	B2	B2	Y2
	5EC	B1	0	B2	B2	B1	Y1
	5ES	B2	Y1	B2	B2	B1	Y2
P. patula	1PC	B1	B1	B1	B1	B1	B1
	1PS	B1	B1	B2	B1	0	B1
	2PC	B1	B1	B1	B2	B2	B2
	2PS	B2	B1	B2	B2	B2	B1
	3PC	B1	B1	B1	B1	B1	0
	3PS	B2	Y1	B2	B1	B1	Y2
	4PC	B1	B1	B1	B1	B1	B1
	4PS	B2	B1	B1	B1	B1	B2
	5PC	B1	Y1	B2	B1	B1	B1
	5PS	B2	0	B1	B1	0	0
P. Taeda	1TC	B1	0	B1	0	0	0
	1TS	B1	Y1	B2	B2	B1	Y1
	2TC	B1	0	B1	B1	B1	Y1
	2TS	B1	0	B1	B1	0	Y2
	3TC	—	0	B1	B1	0	0
	3TS	B1	Y1	B1	B1	B1	Y2
	4TC	B1	0	B1	B1	0	0
	4TS	B2	Y2	B2	B2	Y2	Y2
	5TC	—	—	—	—	—	—
	5TS	B1	Y1	B1	B1	B1	Y1

Key: 1-5 = log no. per species; E = *Pinus elliottii*; P = *Pinus patula*; T = *Pinus taeda*; C = core board; S = side board; 0 = no stain; Y1 = mild yellow stain; Y2 = severe yellow stain; B1 = mild brown stain; B2 = severe brown stain; — = sample lost in production.

The F-values of significance for different independent variables and their interactions are given in Table 4 with their corresponding F-values at a 95% confidence level of significance. Evidently, the schedule was the

main determinant of the degree of discolouration, with species also having a considerable influence. Of all possible interactions, only the species-schedule interaction was found significant.

Table 4: Significance of various variables and variable interactions on the development of stain

Variable	Tabled F-value at a 95% confidence level of significance	Experimental F-value	Significance
Schedule	$F(5, 69) = 2.36$	33.40	Significant factor
Specie	$F(2, 12) = 3.89$	11.78	Significant factor
Board type	$F(1, 13) = 4.68$	3.22	Insignificant factor
Interacting variables	Tabled F-value at a 95% confidence level of significance	Experimental F-value	Significance
Specie-schedule	$F(10, 49) = 2.04$	3.32	Significant interaction
Specie-board type	$F(2, 11) = 4.00$	2.55	Insignificant interaction
Board type-schedule	$F(5, 63) = 2.37$	0.62	Insignificant interaction

Table 5: Discolouration means for the different schedules and species

Specie	Mean	Std. error
P. elliottii	3.889	0.140
P. patula	3.900	0.135
P. taeda	3.088	0.149
Schedule	Mean	Std. deviation
1	4.506	0.176
2	2.305	0.157
3	4.463	0.157
4	4.284	0.157
5	3.462	0.157
6	2.734	0.157

Since the assumption that the stain classifications could be treated as linear measurements was reasonable, the interpretation of effects and interactions could be based on the discolouration means. The discolouration means for the different schedules and species are given in Table 5. The mean discolouration of *P. taeda* was significantly less than that of the other two species. The means of *P. elliottii* and *P. patula* did not differ significantly. Table 6 shows that kilns 2 and 6, *i.e.* the two kilns operating at lower temperatures, produced exclusively yellow stained samples in the case of *P. elliottii* and *P. taeda* and predominantly brown stained samples in the case of *P. patula*. *P. patula* boards had a greater inclination to develop kiln brown stain than the other species. *P. elliottii* gave the smallest number of non-stained samples while *P. taeda* boards were least prone to discolour. The differences between species could be ascribed to the natural variation in chemical and anatomical properties of wood species.

Table 6: Stain occurrence by kiln and species

Kiln	Species	Number of pieces	No stain	Mild yellow stain	Severe yellow stain	Mild brown stain	Severe brown stain
1	*P. elliottii*	8	0%	0%	0%	13%	88%
2	*P. elliottii*	10	10%	70%	20%	0%	0%
3	*P. elliottii*	10	0%	0%	0%	30%	70%
4	*P. elliottii*	10	0%	0%	0%	30%	70%
5	*P. elliottii*	10	0%	0%	0%	80%	20%
6	*P. elliottii*	10	0%	30%	70%	0%	0%
Totals across all kilns		58	2%	17%	16%	26%	40%
1	*P. patula*	10	0%	0%	0%	60%	40%
2	*P. patula*	10	10%	20%	0%	70%	0%
3	*P. patula*	10	0%	0%	0%	60%	40%
4	*P. patula*	10	0%	0%	0%	80%	20%
5	*P. patula*	10	20%	0%	0%	60%	20%
6	*P. patula*	10	20%	0%	10%	50%	20%
Totals across all kilns		60	8%	3%	2%	63%	23%
1	*P. taeda*	8	0%	0%	0%	88%	13%
2	*P. taeda*	9	56%	33%	11%	0%	0%
3	*P. taeda*	9	0%	0%	0%	78%	22%
4	*P. taeda*	9	11%	0%	0%	67%	22%
5	*P. taeda*	9	44%	0%	11%	44%	0%
6	*P. taeda*	9	33%	33%	33%	0%	0%
Totals across all kilns		53	25%	11%	9%	45%	9%

Table 7: Stain occurrence by schedule

Schedule	Number of samples	No stain	Mild yellow stain	Severe yellow stain	Mild brown stain	Severe brown stain
1	26	0%	0%	0%	54%	46%
2	29	24%	41%	10%	24%	0%
3	29	0%	0%	0%	55%	45%
4	29	3%	0%	0%	59%	38%
5	29	21%	0%	3%	62%	14%
6	29	17%	21%	38%	17%	7%

The mean discolouration due to schedules 1, 3 and 4 did not differ significantly (Table 7). These schedules caused the greatest degree of discolouration and were followed, in order of decreasing discolouration means, by schedules 5, 6 and 2. Table 7 presents the results of the trials and indicates that of all the samples in kilns 1, 3, 4 and 5 only one sample was yellow stained. A few of these samples were not stained

while the rest showed kiln brown stain. These kilns operated at dry bulb temperatures above 80°C while the others (kilns 2 and 6) operated at temperatures below 80°C and produced almost all the yellow stained samples.

There seems to be a transition from yellow to brown stain when dry bulb temperatures exceed 80°C. As mentioned, the Maillard reactions also cause this colour progression in model solutions. It is, therefore, probable that yellow stains and kiln brown stains are chemically linked, both being products of predominantly Maillard reactions. Maillard reactions seem to proceed at a fast enough rate above 80°C for the yellow stains to turn brown before the end of the drying schedule. Kreber *et al.* (1999) also mentioned that the intensity of kiln brown stain increased dramatically in *in vitro* trials as temperatures went above 80°C. As a rule of thumb any chemical reaction rate, including the Maillard reaction rate, at least doubles when the temperature is increased by 10°C (Ledl and Schleicher 1990).

To examine the significant species-schedule interaction, the cross-tabulation of means in Table 8 was considered. *P. patula* samples discoloured more than those of the other species under schedules 2 and 6 (low temperature schedules). In all the other schedules, the degree of discolouration was higher in *P. elliottii* than in *P. patula* and least in *P. taeda*. It seemed that schedules with milder conditions tended to cause more severe stain in *P. patula* than *P. elliottii* while the opposite was true for schedules utilising high final dry bulb temperatures.

Table 8: A cross-tabulation of means for the species-schedule interaction. The standard errors of the means are not identical, but for practical purposes all of them can be taken as 0.250

Specie	Schedule					
	1	2	3	4	5	6
P. elliottii	4.935	2.100	4.700	4.700	4.200	2.700
P. patula	4.400	3.300	4.400	4.200	3.600	3.500
P. taeda	4.183	1.516	4.290	3.951	2.586	2.003

On average the effect of core and side boards on discolouration were inconclusive (Table 9). However, in the case of *P. taeda* the core boards produced significantly less stain. This may be due to differences in chemical composition and/or lower permeability in core boards because of pit aspiration. For the deposition of precursors of the Maillard reactions to take place at the surface, mass flow of water to the surface is a prerequisite. Reduced permeability would inhibit mass flow and thus stain development.

Table 9: Stain occurrence by board position and species

Specie	Position	Number of pieces	No stain	Mild yellow stain	Severe yellow stain	Mild brown stain	Severe brown stain
P. elliottii	Core	29	3%	21%	10%	34%	31%
	Side	29	0%	14%	21%	17%	48%
P. patula	Core	30	3%	3%	0%	80%	13%
	Side	30	13%	3%	3%	47%	33%
P. taeda	Core	23	48%	4%	0%	48%	0%
	Side	30	7%	17%	17%	43%	17%
Totals across all species	Core	82	16%	10%	4%	55%	16%
	Side	89	7%	11%	13%	36%	33%

3.2.5 Conclusions

The main determinants of severity of discolouration were kiln schedules and species. There was a significant schedule-species interaction. In high temperature schedules, *P. elliottii* discoloured to a greater degree than *P. patula*, while the opposite was true at lower temperatures. In both cases, *P. taeda* boards discoloured the least. In the event of discolouration, *P. patula* was more likely than the other species to develop kiln brown stain than yellow stain.

For all three species, core and side boards were almost equally inclined to discolour. However, *P. taeda* core boards were significantly less discoloured. This may be due to differences in chemical composition and/or permeability of core and side boards.

The results of this investigation as well as the characteristics of Maillard reactions in model solutions indicate that kiln brown stain and yellow stain development are chemically linked and largely influenced by dry bulb temperature. A transition from yellow to brown stain generally occurred when dry bulb temperatures rose above 80°C. The higher temperatures accelerated the chemical reaction rate, producing more severe and darker stains.

This investigation led to a more complete understanding of the mechanism of kiln brown stain and yellow stain formation. It also showed that commonly utilised South African grown softwood species from the Mpumalanga region are highly prone to discolouration. Kiln brown stain and yellow stain have already caused financial loss to some lumber producers in South Africa and depending on the future aesthetic preferences of the decorative market, it could have an even more detrimental effect. For the production of higher volumes of clear lumber, the use of low temperature schedules is recommended.

3.2.6 Acknowledgements

The authors wish to acknowledge Prof. J.S. Maritz and Mr. J. Dommisse of the Statistics Department at the University of Stellenbosch for the statistical analysis as well as the valuable contributions of Ndumiso Ngozo.

3.2.7 References

Boutelje, J.B. 1990. Increase in the content of nitrogenous compounds at lumber surfaces during drying and possible biological effects. *Wood Science and Technology.* 24, pp191-200.

Danehy, J.P. and Pigman W.W. 1951. Reactions between sugars and nitrogenous compounds and their relationship to certain food problems. *Advances in Food Research.* 3, pp241-290.

Ellis, G.P. 1959. The Maillard reaction. *Advances in Carbohydrate Chemistry.* 14, pp63-134.

Hodge, J.E. 1953. Dehydrated foods: chemistry of browning reactions in model systems. *Agricultural and Food Chemistry.* 1(15), pp928-943.

Kreber, B., Haslett, A.N. and McDonald A.G. 1999. Kiln brown stain in radiata pine: a short review on cause and methods for prevention. *Forest Products Journal.* 49(4), pp66-70.

Ledl, F. and Schleicher, E. 1990. New aspects of the Maillard reaction in foods and in the human body. *Angewandte Chemie: International Edition in English.* 29(6), pp565-594.

Long, K.D. 1978. Redistribution of simple sugars during drying of wood. *Wood Science.* 11(1), pp10-12.

Terziev, N., Boutelje, J.B. and Söderström, O. 1993. The influence of drying schedules on the redistribution of low-molecular sugars in *Pinus sylvestris L*. *Holzforschung*. 47, pp3-8.

Theander, O., Bjurman, J. and Boutelje, J.B. 1993. Increase in the content of low-molecular carbohydrates at lumber surfaces during drying and correlations with nitrogen content, yellowing and mould growth. *Wood Science and Technology.* 27, pp381-389.

3.3 Digital image analysis and colorimetric measurement of yellow and brown stained *Pinus elliottii*

3.3.1 Abstract

Yellow stain and kiln brown stain severity in *Pinus elliottii* due to two different kiln schedules was evaluated with both colorimeter measurements and digital image analysis. The colorimeter measurements correlated well with visual assessments of the colour of normal, yellow stained and kiln brown stained wood. Yellow stained wood did not differ much in colour on the greyscale when compared to the normal colour of wood. Consequently the method was not suited to the measurement of yellow stain.

Kiln brown stain and yellow stain occurred simultaneously in all boards; with kiln brown stain always closer to the surface. The high temperature schedule yielded more intense stain in the 1-2 mm depth zone than the low temperature schedule. However, the opposite was true at 3-5 mm depth. As a result more of the low temperature schedule samples fell outside the colour range of regular coloured wood at 3-5 mm depth.

3.3.2 Introduction

The demand for greater volumes of high quality softwood for furniture, joinery and decorative woodwork in South Africa has accentuated the problem of yellow stain and kiln brown stain. In a survey of several Southern African sawmills it was found that these stains were of geographically widespread and frequent occurrence in several commonly utilised softwood species (Scheepers and Rypstra 2001). These stains develop during kiln drying and are reportedly caused by Maillard reactions that occur between sugars and nitrogenous compounds present in softwoods. During drying the stain precursors, *i.e.* sugars and nitrogenous compounds, migrate to the wetline (fibre saturation line) where they accumulate and react to cause discolouration (McDonald *et al.* 2000). Keylwerth (1952) suggested and Wiberg and Morén (1999) confirmed that a wetline remains in the boundary layer close to the surface during the initial phases of drying. In the case of *Pinus sylvestris*, the wetline remained within 2 mm of the surface from the inception of drying at ±130% moisture content and down to ±50% moisture content, the point where capillary water flow diminishes rapidly (Wiberg and Morén 1999).

As yet there has not been a detailed quantitative description of the physical discolouration characteristics resulting from different drying conditions (Boutelje 1990; Kreber *et al* 1999; Long 1978; Terziev *et al.* 1993; Theander *et al.* 1993). At best the stains have been described as being in a boundary layer of ± 2 mm below the surface of a board and having a yellow and/or brown colour.

The aim of this study was to investigate methods to quantitatively describe the discolouration characteristics of *P. elliottii* flitches that were dried with two contrasting kiln-drying schedules.

3.3.3 Materials and methods

Pinus elliotii flitches (3.1 m long, 43 mm thick and of varying width) from 16-19 year old trees were collected from the Tsitsikamma region on the southern coast of South Africa. The flitches were cross-cut into sixty-four 1 m lengths and divided into two batches. Each batch (32 flitches per batch) was kiln dried to a final moisture content (after conditioning) of ±12% with a different kiln drying schedule for each batch.

Typically, Southern African softwoods are dried with dry bulb temperatures in the 70-90°C range (Scheepers and Rypstra 2001). Consequently, two schedules, one running at 90°C and another at 70°C dry bulb temperature, were selected to represent respectively severe and mild kiln drying conditions and used to dry the two batches.

Schedule 1:

a) Warm up phase for 5 hours at 90°C dry bulb and 87°C wet bulb temperature.

b) Drying phase at 90°C dry bulb and 60°C wet bulb until ±10% moisture content was reached.

c) Conditioning phase for 2 hours at 90°C dry bulb and 87°C wet bulb temperature until 12% MC was reached.

Schedule 2:

a) Warm up phase for 5 hours at 70°C dry bulb and 68°C wet bulb temperature.

b) Drying phase at 70°C dry bulb and 62°C wet bulb until ±30% moisture content was reached.

c) Drying phase at 70°C dry bulb and 50°C wet bulb until ±10% moisture content was reached.

d) Conditioning phase for 1½ hour at 70°C dry bulb and 68°C wet bulb temperature until 12% MC was reached.

The total time taken for the completion of schedules 1 and 2 was 40 and 121 hours, respectively.

The dried flitches were cross-cut into two halves (0.5 m in length). One half was discarded and the other was rip sawn into two halves, giving two boards of 43 mm thick, 500 mm length and varying width. The 0.5 m boards were rip sawn into two matched samples in such a manner as to give the most level surface possible on each sample. The surface of one sample was planed to its centre where little or no discolouration had taken place. This sample was used as a control that represented the regular colour of kiln dried wood. The discolouration of the other sample was compared to the matched control sample.

Two techniques were used to measure discolouration at various depths below the rough sawn surface of samples:

1. colour measurements at a number of preselected points; and

2. the measurement of the extent of, or area affected by, discolouration through digital image analysis.

The colour was assessed at the centre of the control samples and compared with the colour of their matched samples at different depths below the rough sawn surfaces. To measure the colour at various depths, a planer was set to 1 mm depth and the discoloured samples were passed over the planer until two thirds or more of the typically uneven surfaces were planed. This surface was chosen as the surface at 1 mm depth. Nine points were chosen by dividing the total planed surface area of the sample, in the length, into three blocks of equal size and measuring the colour of the three darkest points (a visual assessment) in each block. A Sheen Micromatch Plus colorimeter (Sheen Instruments Ltd.) with a 4 mm measurement aperture was used to assess the colour of the earlywood of the planed sample surface (1 mm depth) at these nine points. Only earlywood colour was evaluated since preliminary colorimetric tests showed that:

1. latewood colour is typically erratic within and between samples, while earlywood colour is more homogeneous;

2. latewood discolouration due to yellow and brown stain is not as distinct as earlywood discolouration; and

3. the latewood thickness is frequently less than the 4 mm measurement aperture diameter of the colorimeter, making it impossible to obtain a reliable colour reading.

After the 1 mm depth level of the discoloured sample was evaluated, the sample was planed down another 1 mm to reveal the 2 mm depth level and the colour of the earlywood was also measured. The colour was measured further at progressing 1 mm depth increments until the average colour of all the discoloured samples coincided with the average of all the matched control samples, indicating that no discoloured wood was left. The colour of the control sample (sample planed to centre) surface was assessed in the same manner as the discoloured sample.

The colorimeter (45°/0° instrument geometry) was set to D65/10° illumination/observation. Colours were measured using the CIE L*a*b* colour system (Figure 1). The L*-axis in Figure 1 indicates the lightness/darkness of the colour while the (a*, b*)-plane describes the hue and saturation.

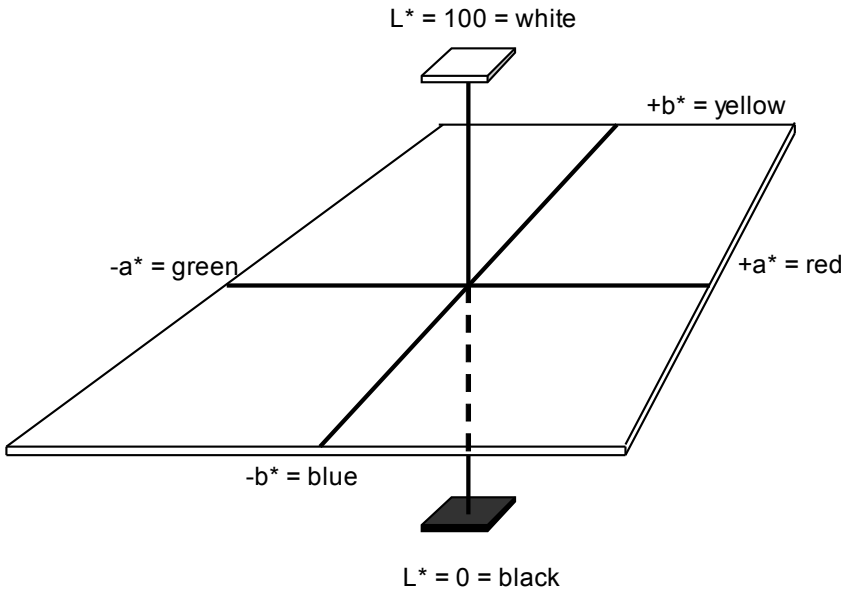

Figure 1: CIE L*a*b*-system of defining colour.

Discolouration is measured as a colour difference relative to a standard. In three dimensional colour space, the coordinates of a suitable standard should be such that any more discolouration gives a colour point with coordinates further away from the standard. Thus, to select a suitable standard, the colour points of regular wood as well as yellow stained and kiln brown stained wood first had to be plotted to determine the path of the colour progression in colour space. An increase in discolouration caused the colorimetric coordinates to move progressively further away from the defining coordinates of the colour white. Based on this result, it was decided to use the colour white (with L*-, a*- and b*-coordinates (100, 0, 0)) as the standard from which the total colour difference, ΔE^*, could be calculated. The total colour difference between sample and standard is calculated as with the Euclidian formula:

$$\Delta E^* = \sqrt{(\Delta L^*)^2 + (\Delta a^*)^2 + (\Delta b^*)^2}$$

Digital image analysis was performed by taking digital colour photos of the surface at each depth level of every sample using a Nikon Coolpix 880 camera. The matched control sample was included in the photo of each discoloured sample for comparative purposes. Image analysis of the digital images was executed with the ImageJ 1.21w freeware program available on the internet (http://rsb.info.nih.gov/ij/). Several earlywood sections of the control sample of the digital image were selected of which an example is shown in Figure 2. Then the greyscale (scale: 0 to 255, black to white) interval in which the pixels fell was determined (Figure 2). The greyscale interval of a colour was defined as the interval in which the middle 95% of pixels fell. In other words, 2.5% of the pixels at the lower and upper end of pixel occurrence were discarded. When the greyscale interval for the desired colour of the sample was determined from the control sample, the percentage of the sample pixels (discoloured earlywood) that was darker than (falling below the lower

limit of the desired greyscale interval) was determined. This percentage value was then taken as a measure of the area percentage of discoloured earlywood.

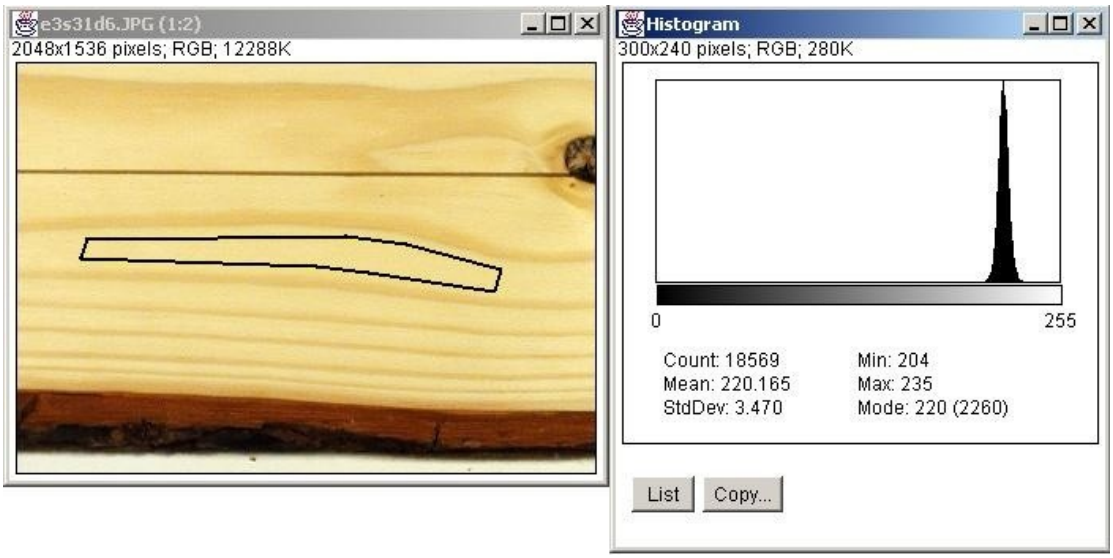

Figure 2: On the left, the selected area for greyscale interval determination. On the right, pixel occurrence on the greyscale for the selected area. Several areas were selected per control board and an average greyscale interval was determined for the non-stained earlywood of each sample.

Data obtained with the colorimeter was used to determine the colour of samples. During preliminary colorimetric measurements of earlywood it became apparent that there was considerable progression towards the darker end of the L*-axis as the wood colour progressed from the normal colour through yellow to dark brown. As a result, the greyscale differences alone might also be used as a measure of discolouration. The digital image analysis method only worked with the greyscale, a one-dimensional parameter, which measures the same property (lightness/darkness) as the L*-axis in the CIE L*a*b*-system.

3.3.4 Results

*3.3.4.1 The wood colour in the CIE L*a*b* colour space*

The colour change measured at the different depth levels followed a similar path in colour space for both Schedule 1 and Schedule 2 samples. The average colour at the different depth levels ranging from 1-5 mm as well as the regular wood colour of Schedule 1 samples is given in Figure 3a with a magnification of the plotted values in Figure 3b. As the rate of colour change in a certain axis direction increased, the standard deviation in that direction also increased. From the standard deviations it is evident that movement in the b*-direction is appreciable throughout the discolouration path, while movement in the a*-direction and L*-direction is maximal between points 4 and 1 and points 3 and 1 respectively. Yellow stained and kiln brown stained zones were simultaneously present in samples dried with Schedule 1 or Schedule 2. This points to the fact that yellow stain and kiln brown stain are closely associated. Usually, the 1-2 mm depth zone would be brown and the 3-5 mm depth zone yellow.

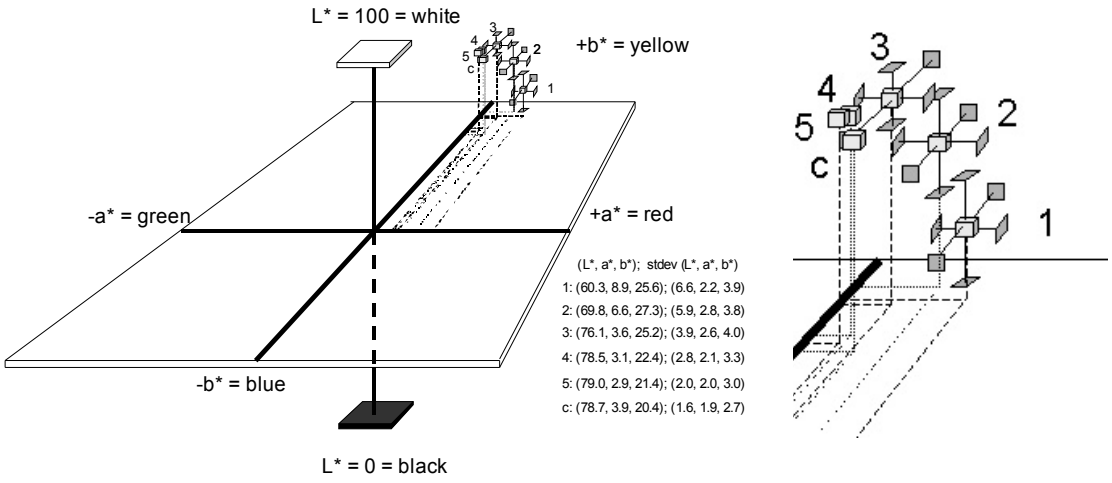

Figure 3: On the left, the average colour at different depths of Schedule 1 samples plotted in colour space. On the right a magnified view of the points is illustrated. The standard deviations of points 1-3 have been included in the graph, the rest were omitted for the sake of clarity. All coordinates and standard deviations are indicated in the figure. The values are averages of all samples and controls. Key: c = control samples; 1-5 = 1-5 mm depth levels of discoloured samples.

Figure 4 reflects the conclusions from the standard deviations indicated in Figure 3. It shows how the colour changed in the b*-direction throughout, but became more yellow between points C and 3 and then curved to the a*-direction (becomes brown). Simultaneously, it changed appreciably in the L*-direction (became darker). Schedule 2 revealed the same tendency, but the samples did not discolour to the same extent, as the positions of the 1 mm depth points in Figures 3, 4 and 5 indicate.

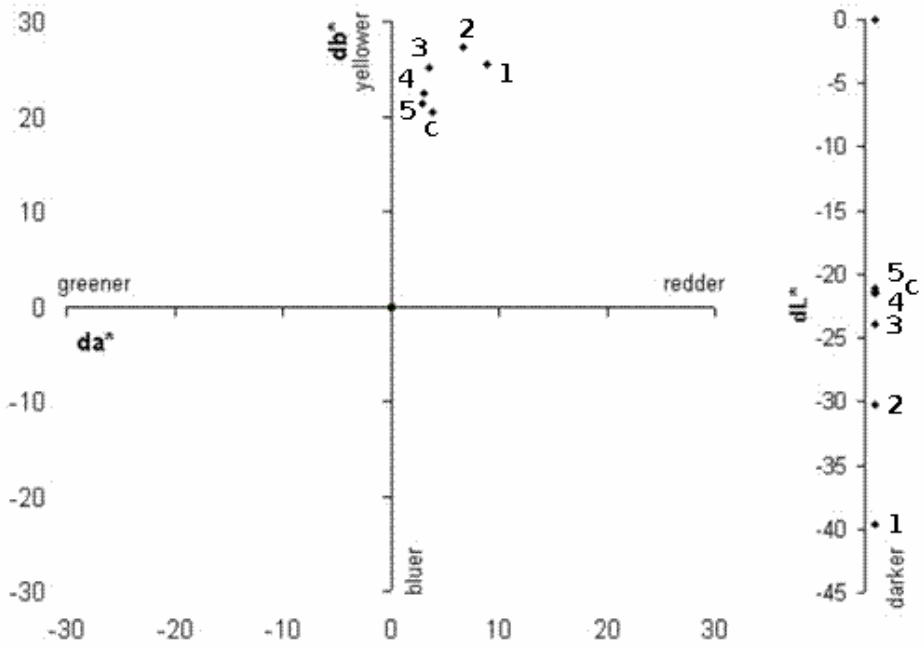

Figure 4: The average colour at different depths of Schedule 1 samples plotted in the (da*, db*)-plane and against the dL*-axis. All plots are in relation to white. Key: c = control samples; 1-5 = 1-5 mm depth levels of discoloured samples.

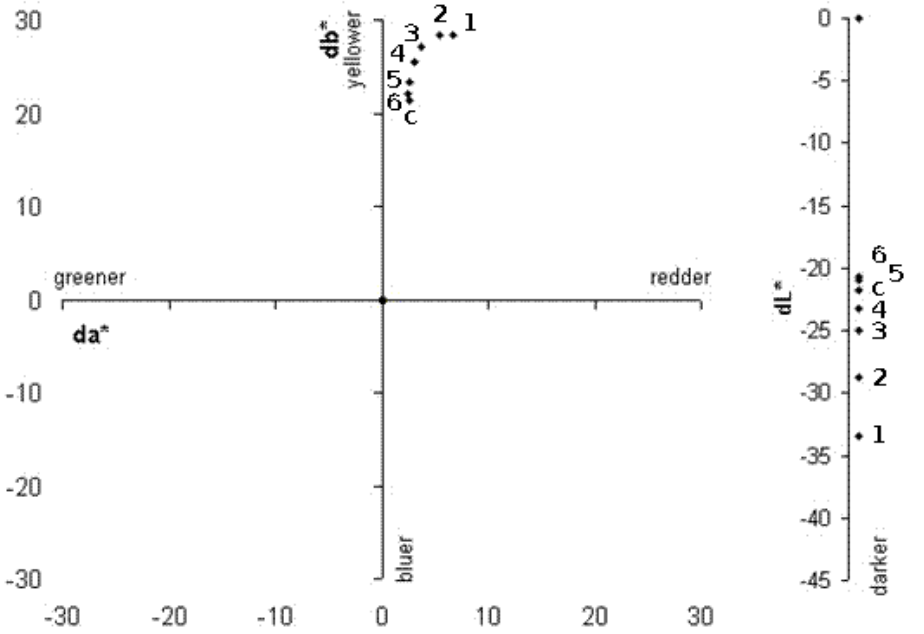

Figure 5: The average colour at different depths of Schedule 2 samples plotted in the (da*, db*)-plane and against the dL*-axis. All plots are in relation to white. Key: c = control samples; 1-5 = 1-5 mm depth levels of discoloured samples.

If it is assumed that the Maillard reaction was solely responsible for the discolouration (Hodge 1953), the colour progression would be caused by a combination of precursor reaction, accumulation of Maillard

intermediate products and polymerisation. All three factors would contribute at all stages of colour progression, but polymerisation would be responsible for most of the colour change (*i.e.* browning and darkening) towards the end of the colour pathway while the colour at the 5, 4 and 3 mm depths could mostly be ascribed to precursor reaction and pigment concentration .

3.3.4.2 Measurement of discolouration

The gradual decrease in ΔE*-values with increase in depth using drying Schedules 1 or 2 is illustrated in Figure 6. The ΔE*-averages, 29.90 and 30.00, of Schedule 1 and Schedule 2 control samples fell within the 25.91-34.29 and 26.33-31.94 ΔE*-ranges, respectively. From the colorimeter readings of samples it is evident that Schedule 1 caused more intense discolouration at the 1-2 mm depth level than Schedule 2. However, the discolouration gradient of Schedule 1 was steeper than that of Schedule 2 within the first four millimetres from the surface. As a result, the intensity of discolouration was higher in the Schedule 2 samples at the 3-5 mm depth level even though there was less severe discolouration at the surface.

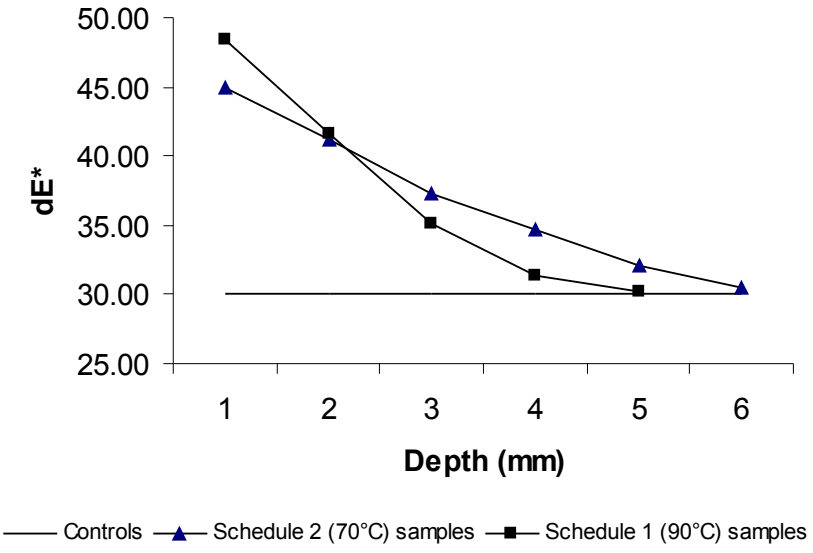

Figure 6: Total colour differences (with the colour white as standard) at progressing depths for samples kiln dried with Schedules 1 and 2. Key: dE* = ΔE*.

Table 1: Percentage of discoloured samples falling above the ΔE*-range of control samples at progressing depths. Schedule 1 yielded a wider ΔE*-range than Schedule 2 for its control samples. Consequently, discoloured samples from Schedule 2 were also tested against this wider range

Samples from:	ΔE*-range of control samples	Percentage of discoloured samples at various depths					
		1 mm	2 mm	3 mm	4 mm	5 mm	6 mm
Schedule 1	25.91-34.29	100%	91%	50%	19%	6%	No value
Schedule 2	26.33-31.94	100%	100%	97%	88%	53%	25%
Schedule 2	Tested against Schedule 1 control sample range: 25.91-34.29	100%	94%	81%	50%	19%	3%

The percentages of discoloured samples at the different depths falling outside the mentioned ΔE* control ranges are given in Table 1. Table 1 indicates that Schedule 2 caused deeper discolouration. The Δ E*-range of the Schedule 2 control samples was much narrower and fell within the control range for Schedule 1. When the control range of Schedule 1 was taken as the standard range for kiln dried wood, then the samples from Schedule 2 still were discoloured to a greater depth than the samples from Schedule 1.

Since Schedule 2 led to greater discolouration intensity in the 3-5 mm depth zone, more wood had to be planed off to attain a surface of regular colour (Table 1). Hence, a mild schedule actually could cause more wood to be lost due to discolouration should over-sizing followed by planing be used to remedially correct the problem of yellow stain and kiln brown stain.

3.3.4.3 Discoloured area

The brown stained surfaces were generally discoloured over the complete surface area with darker and lighter streaks of discolouration. Figure 7 reflects the more abrupt change in colour from dark to light with progressing depth of Schedule 1 samples.

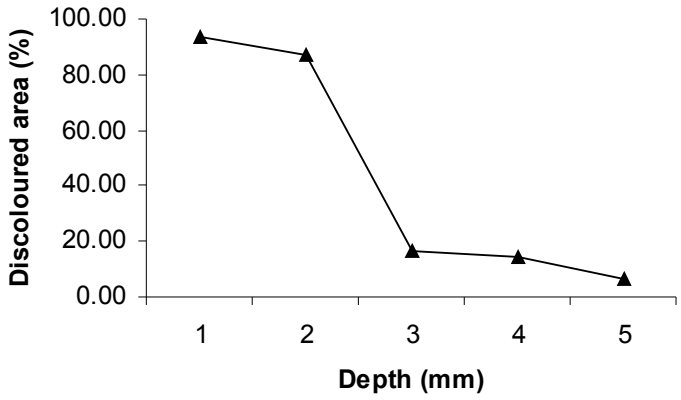

Figure 7: Discoloured area, on the basis of greyscale, at different depths of Schedule 1 samples.

Since the discoloured area was measured on a greyscale basis, measurement was simple when the sample areas that were much darker (much further down the L*-axis) were evaluated. Consequently, the standard deviation of Schedule 1 samples was also smaller at the 1-2 mm depth level. However, colours closer to the controls on the L*-axis were difficult to distinguish on a greyscale and gave high standard deviation values. Figure 8 reflects the smaller discolouration gradient of schedule 2 samples. The determination of the percentage of the discoloured area was more reliable for evaluating brown stain than yellow stain.

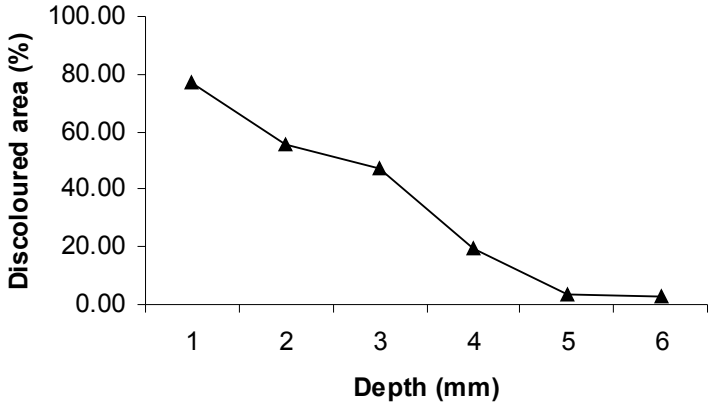

Figure 8: Discoloured area, on the basis of greyscale, at different depths of Schedule 2 samples.

3.3.5 Conclusions

Colour measurement of wood with the colorimeter described the amount and pattern of discolouration satisfactorily. The colour progression of the Maillard reaction in wood followed a definite path in colour space from the regular colour of kiln-dried wood through yellow to brown. Yellow stain and kiln brown stain occurred simultaneously in both Schedule 1 (90°C dry bulb) or Schedule 2 (70°C dry bulb) samples. The kiln brown stained zone of a board was always closer to the surface than the yellow stained zone. In the kiln brown stained depth zone, at 1-2 mm depth, the samples were generally discoloured over the full surface area but darker and lighter streaks of discolouration were present. Both schedules caused 91% or more discoloured samples at 2 mm depth and 100% at 1 mm depth. Schedule 1 yielded more intense staining at the surface while the lower temperatures and longer drying time of Schedule 2 yielded more intense discolouration than Schedule 1 deeper beneath the surface. The stains were characteristically formed in the ±0.5-4 mm depth zone in Schedule 1 samples and in the ±0.5-5 mm depth zone in Schedule 2 samples.

Digital image analysis was a reliable method when the percentage of brown stained area was measured because the colours were compared on a greyscale only. However, on a greyscale, yellow stained wood was not dark enough to differentiate from wood of regular colour.

3.3.6 Acknowledgements

The authors would like to thank the South African Lumber Millers' Association for its financial support of this project.

3.3.7 References

Boutelje, J.B. 1990. Increase in the content of nitrogenous compounds at lumber surfaces during drying and possible biological effects. Wood Science and Technology 24: 191-200.

Hodge, J.E. 1953. Dehydrated foods: Chemistry of browning reactions in model systems. Agricultural and Food Chemistry 1 (15): 928-943.

Keylwerth, R. 1952. Der Verlauf der Holztemperatur während der Furnier- und Schnittholztrocknung. Holz als Roh- und Werkstoff. 10 (3): 87-91.

Kreber, B.; A.N. Haslett and A.G. McDonald. 1999. Kiln brown stain in radiata pine: a short review on cause and methods for prevention. Forest Products Journal 49 (4): 66-70.

Long, K.D. 1978. Redistribution of simple sugars during drying of wood. Wood Science 11 (1): 10-12.

McDonald, A.G.; M. Fernandez; B. Kreber and F. Laytner. 2000. The chemical nature of kiln brown stain in radiata pine. Holzforschung 54: 12-22.

Scheepers, G.C. and T. Rypstra. 2001. Yellow and kiln brown stain in SA pine species and its effect on manufacturers of furniture and joinery products. South African Lumber Millers' Association research report.

Terziev, N.; J.B. Boutelje and O. Söderström. 1993. The influence of drying schedules on the redistribution of low-molecular sugars in *Pinus sylvestris* L. Holzforschung 47: 3-8.

Theander, O.; J. Bjurman and J.B. Boutelje. 1993. Increase in the content of low-molecular carbohydrates at lumber surfaces during drying and correlations with nitrogen content, yellowing and mould growth. Wood Science and Technology 27: 381-389.

Wiberg, P. and T.J. Morén. 1999. Moisture flux determination in wood during drying above fibre saturation point using CT-scanning and digital image processing. Holz als Roh- und Werkstoff 57: 137-144.

3.4 The occurrence of discolouration during kiln drying in South African grown *Pinus elliottii*

3.4.1 Abstract

The effect of different parameters on the surface discolouration (yellow stain and kiln brown stain) and thermal discolouration of *Pinus elliottii* during kiln drying was investigated. Boards were dried with different kiln schedules and discolouration was assessed at different depth levels from the surface of each board. The discolouration data were analysed using notched boxplots, multivariate analysis of variance and canonical variate analysis biplots. Thermal and surface discolouration were distinguishable by the distribution of colour data point plots in the CIE-L*a*b* colour system. Thermal discolouration was less intense and less varied than surface discolouration. The greatest degree of thermal discolouration occurred in one of the higher temperature (≥90°C T_{db} during first drying phase) schedules that was run for an excessively long period due to low air velocity. Discolouration progressively decreased as the boards were planed to a greater depth. Higher temperature schedules yielded 77.5-82.5% discoloured replicates at the 2 mm depth level. Lower temperature (≤71°C T_{db} during first drying phase) schedules yielded no discoloured wood at the surface or at the centre of the boards.

3.4.2 Introduction

During kiln drying of softwoods two types of non-microbial, non-enzymatic discolourations may take place. One discolouration type is caused by the reactions of wood polymers due to prolonged exposure to high temperature and humidity (kollmann *et al.* 1951). The effect is an even darkening of wood throughout the board. It usually occurs at elevated temperatures when drying is not rapid enough due to too low air velocity or too high relative humidity. For the purpose of clarity, this type of discolouration will be referred to as thermal discolouration in this article.

The second type of discolouration occurs when low molecular weight carbohydrates and nitrogenous compounds in wood accumulate and react with each other just beneath lumber surfaces (Boutelje 1990; Kapp *et al.* 2003, Kreber *et al*,. 1999; Long 1978; Terziev *et al.* 1993; Theander *et al.* 1993). The chemical reactions responsible for this type of discolouration are referred to as Maillard reactions and are well known in the food industry (Danehy and Pigman 1951). The discolouration is brown (called kiln brown stain) or yellow (called yellow stain) and often not visible on the rough sawn surfaces, but is exposed upon planing. These stains occur beneath the surface of a kiln dried board in a layer that is ± 4 mm deep. For the purpose of clarity, this type of discolouration will be referred to as surface discolouration.

The purpose of this investigation was to determine the effect of different kiln conditions on the occurrence of thermal discolouration as well as the effect of different kiln conditions and depth from surface on surface discolouration in South African grown *Pinus elliottii*.

3.4.3 Materials and methods

To evaluate a broad range of kiln conditions, an industrial kiln at a sawmill and an experimental kiln were utilised. The atmospheric conditions in the industrial kiln were conducive to the development of both surface and thermal discolouration, but much more prone to develop thermal discolouration than the experimental kiln due to the low air velocity and high temperatures employed. The low air velocity was due to baffling problems that the sawmill was struggling with at the time. The experimental kiln was used to dry softwood at low, intermediate and high temperatures with a sufficiently high air velocity to ensure proper drying.

3.4.3.1 Experimental kiln drying

Forty 1 m length *Pinus elliottii* flitches were cross-cut from twenty green boards (2.4 m × 43 mm × 160 mm) from the Tsitsikamma region on the southern coast of South Africa and dried in the experimental kiln using the three kiln schedules listed in Table 1. Each dried flitch was cross-cut into two halves (0.5 m in length). One half was discarded and the other was ripsawn into two halves, giving two matched replicate boards of ±40 mm thick, ±500 mm long and ±80 mm wide. One of each replicate pair was planed to the centre where no surface discolouration had occurred.

3.4.3.2 Industrial kiln drying

Green *Pinus elliotii* boards (2.4 m × 43 mm × 160 mm) from the Tsitsikamma region were dried in an industrial kiln using the kiln schedules listed in Table 2. Twenty flitches were randomly taken from each kiln charge and cross-cut in half yielding forty 1 m length boards. These 1 m boards were then machined in the same manner as the 1 m boards prepared for the experimental kiln to produce the same type and number of replicates per sample.

Table 1: Kiln schedules employed in the experimental kiln. The air velocity was 3.6 m/s

Schedule code	Duration	Final MC	T_{db} (°C)	T_{wb} (°C)	Emc (%)
90/60	5 hours	Warm up	90	87	14.3
		10%	90	60	3.0
	2 hours	Condition	90	87	14.3
Total duration:	40 hours				
71/65	4 hours	Warm up	71	69	17.5
		40%	71	65.5	12.0
		35%	71	63.5	10.3
		30%	71	60	8.3
		25%	76.5	62.5	7.1
		20%	76.5	60	6.3
		15%	82	62.5	5.4
		10%	82	54.5	3.6
	2½ hours	Condition	82	78	13.3
Total duration:	63 hours				
45/36	4 hours	Warm up	45	44	21.7
		55%	45	36	9.2
		40%	60	43	6.0
		25%	65	42	4.3
		9%	70	43	3.5
	2½ hours	Condition	70	66	13.8
Total duration:	123 hours				

Table 2: Kiln schedules employed in the industrial kiln. The air velocity was 2 m/s

Schedule code	Duration	Final MC	T_{db} (°C)	T_{wb} (°C)	Emc (%)
90/57	3½ hours	Ramp up to	90	88.5	17.4
		8%	90	57	2.5
	5½ hours	Equalize	95	84.5	8.1
Total duration:	70 hours				
102/67	3½ hours	Ramp up to	102	100	20.0
		8%	102	67	2.5
	8 hours	Equalize	110	100	7.3
Total duration:	55 hours				

3.4.3.3 Colour assessment

Colours were measured using the CIE L*a*b* colour system. A Sheen Micromatch Plus colorimeter (Sheen Instruments Ltd.) with a 4 mm measurement aperture was used to determine the colour of the earlywood of each planed surface. The colorimeter (45°/0° instrument geometry) was set to D65/10° illumination/observation. Nine points were chosen by dividing each planed surface area of the sample lengthwise into three blocks of equal size. The colour of the three darkest points (a visual assessment) was measured in each block. The colour of each replicate that was planed to the centre, was measured first. The other replicates were then planed in 1 mm increments to 5 mm depth while the colour was measured at each depth level.

Discolouration is normally measured as a colour difference relative to a standard. The colour white, with L*-, a*- and b*-coordinates (100, 0, 0), was chosen as the standard from which the total colour difference, ΔE^*,

could be calculated. The total colour difference between colour point and standard was calculated with the Euclidian formula:

$$\Delta E = \sqrt{(\Delta L^*)^2 + (\Delta a^*)^2 + (\Delta b^*)^2}$$

3.4.4 Results and discussion

Since ΔE is composed of three coordinates it follows that identical measurements may result from different underlying L*, a* and b* coordinates. Therefore, in order to obtain a detailed analysis of discolouration ΔE is treated as a separate variable, retaining the L*, a* and b* measurements. A detailed description of measurements obtained for these four variables by means of notched boxplots is given first. This is followed by multivariate analysis of variance (MANOVA) for testing equality of group mean vectors and associated simultaneous confidence intervals. The statistical analyses is concluded with canonical variate analysis (CVA) biplots as proposed by Gower and Hand (1996). These biplots display graphically the group structure together with information about all four variables, taking into account the interrelationships among the multivariate data. The above analyses will in turn be discussed for thermal discolouration, surface discolouration at varying depths and surface discolouration due to different schedules.

3.4.4.1 Thermal discolouration

The notches about the respective medians in Figure 1 demarcate approximate 95% confidence intervals for the medians. Therefore, if two notches do not overlap the hypothesis that the underlying two population medians are similar is rejected at an approximate 5% level of significance (McGill, Tukey and Larsen 1978).

The effect of different kiln schedules on the colour at the centre of the boards is clearly illustrated in Figure 1. The higher temperature (≥90°C T_{db} during first drying phase) and lower temperature (≤71°C T_{db} during first drying phase) schedule samples are grouped together. The darker colour of the higher temperature schedule samples, as indicated by the L*-axis, shows that a greater degree of thermal discolouration occurred in these samples. The 90/57 schedule showed the greatest degree of discolouration (statistically significant higher – the scalar difference from the colour white – and lower (darker) L* values). This could be due to the fact that it was the longest schedule of the higher temperature schedules. Note also that when the 45/36 schedule board centre ΔE*-range was taken as the desired colour, the 71/65 schedule yielded no replicates outside the range obtained for the 45/36 schedule.

However, the boxplots in Figure 1 are univariate displays of the results and a correlation analysis shows the four variables not to be uncorrelated. Therefore, a MANOVA was performed to investigate the differences between the mean values of the different kiln schedules for the four variables. The MANOVA results in rejection of the null hypothesis (p-value approaching zero) of similar population mean values for the five schedules. Therefore, 99% Roy's largest root simultaneous confidence intervals (Morrison 1976) were calculated. These intervals are given in Table 3.

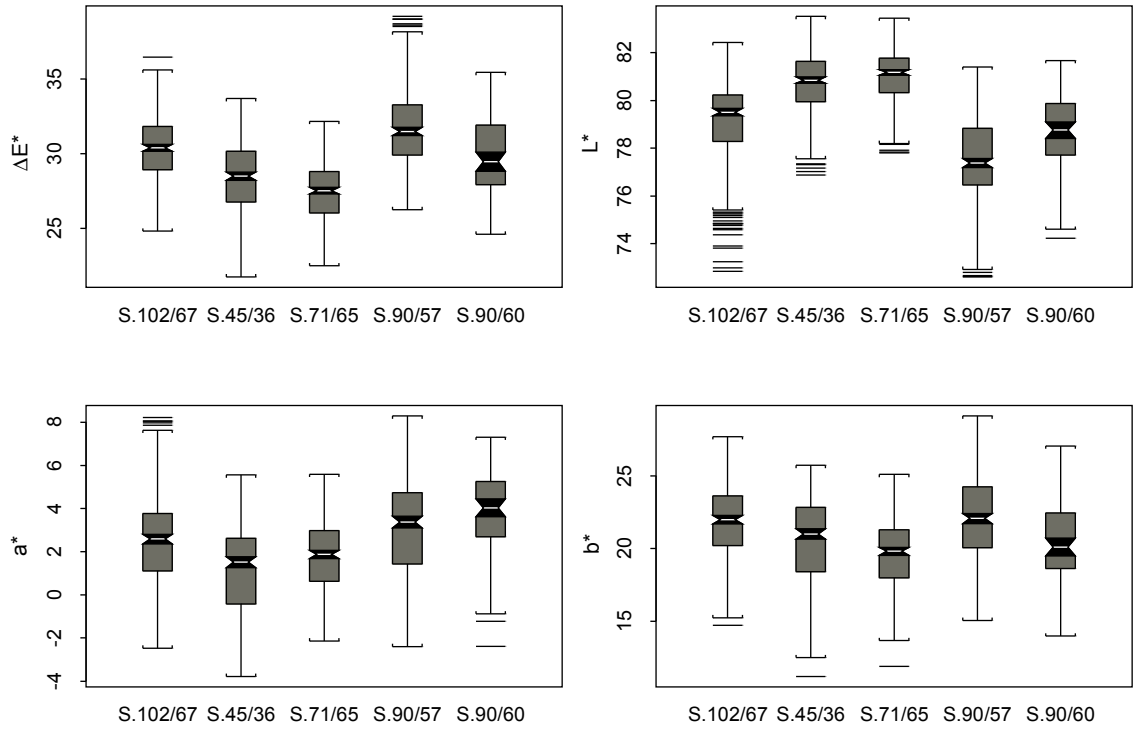

Figure 1: Notched boxplots of the CIE-L*a*b* defined colour at the centre of the boards produced by five different kiln schedules.

Table 3: 99% simultaneous confidence intervals for all pairwise contrasts among mean thermal discolouration at the centre of the boards produced by five kiln schedules. Intervals excluding zero are highlighted

Contrast	ΔE^* Conf interval		L* Conf interval		a* Conf Interval		b* Conf Interval	
S.102/67 S.45/36	-1.346	2.961	-2.206	-1.142	0.745	2.129	0.331	2.259
S.102/67 S.71/65	-2.18	3.798	-2.452	-1.388	0.123	1.506	1.221	3.149
S.102/67 S.90/57	-2.113	-0.498	0.982	2.046	-1.353	0.031	-1.192	0.736
S.102/67 S.90/60	-0.688	1.801	-0.381	1.258	-2.422	-0.290	-0.061	2.911
S.45/36 - S.71/65	0.029	1.644	-0.778	0.286	-1.314	0.069	-0.074	1.854
S.45/36 - S.90/57	-4.267	-2.651	2.656	3.720	-2.790	-1.406	-2.487	-0.559
S.45/36 - S.90/60	-2.842	-0.353	1.293	2.932	-3.859	-1.727	-1.356	1.616
S.71/65 - S.90/57	-5.103	-3.488	2.902	3.966	-2.167	-0.784	-3.377	-1.449
S.71/65 - S.90/60	-3.678	-1.189	1.539	3.179	-3.236	-1.104	-2.246	0.726
S.90/57 - S.90/60	0.618	3.107	-1.895	-0.255	-1.761	0.371	0.167	3.139

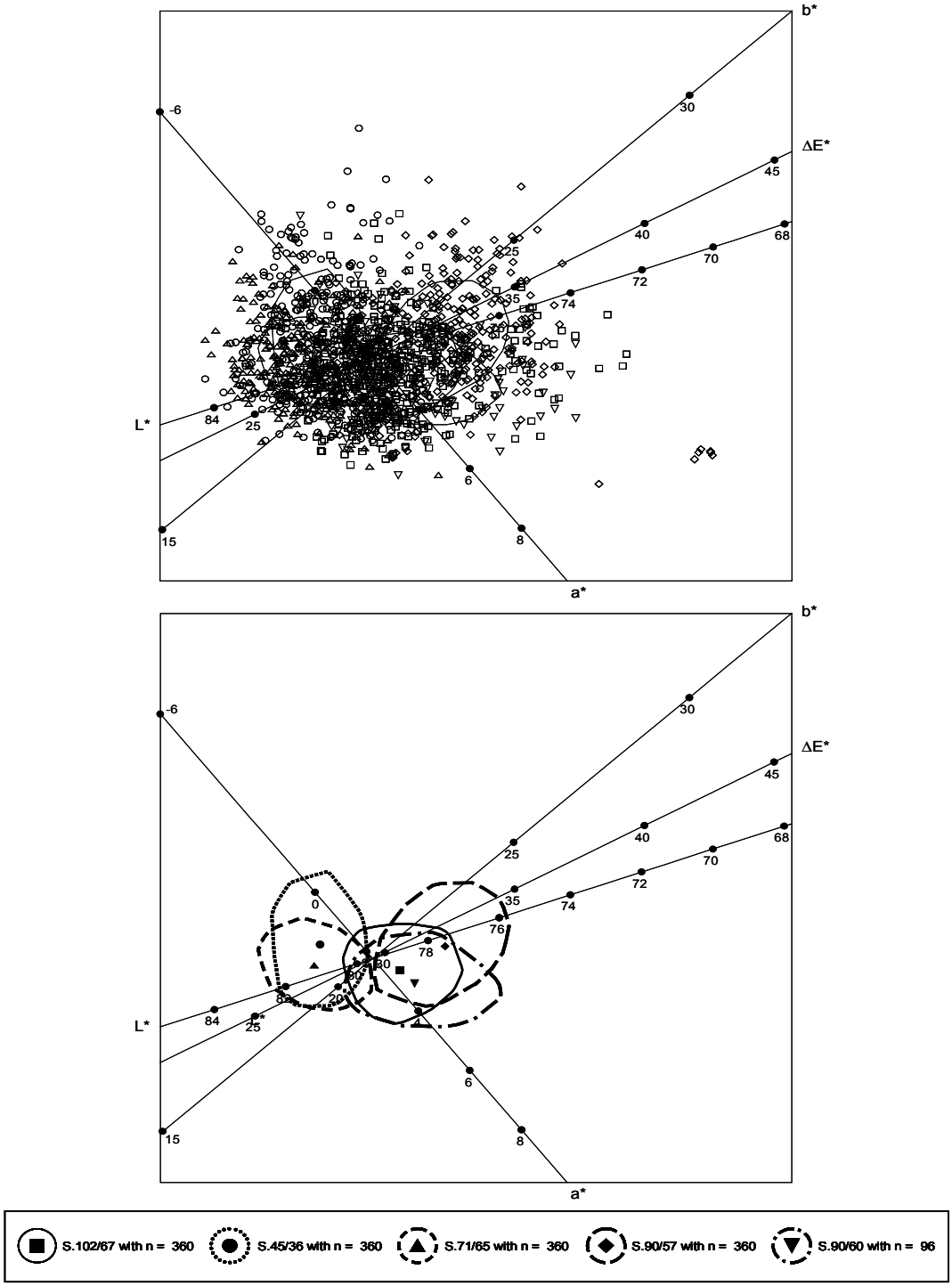

Figure 2: Top panel shows a CVA biplot of the thermal discolouration at the centre of the boards of all samples in the five different kiln schedules. The same biplot is repeated in the bottom panel but only the mean values of the different schedules together with the respective 50% bags are shown.

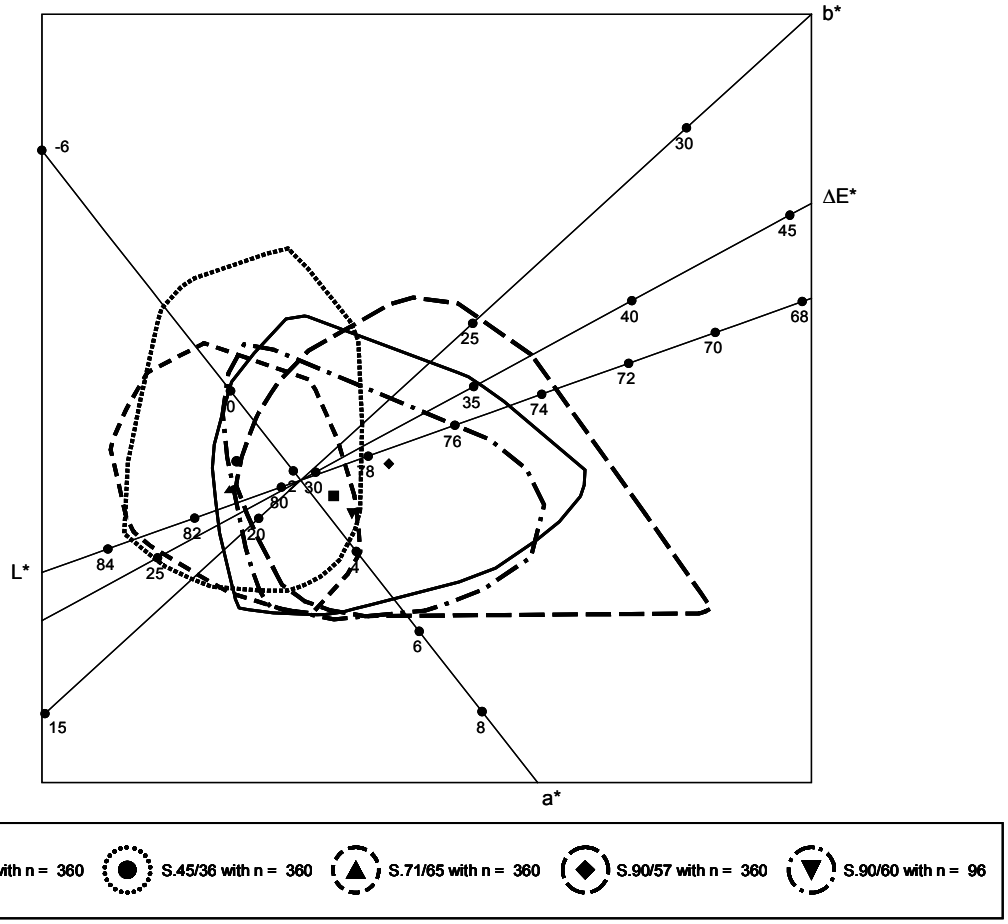

Figure 3: CVA biplot displaying thermal discolouration at the centre of the boards associated with five kiln schedules. Mean values together with 95% bags are shown.

The biplots displayed in Figures 2 and 3 are simultaneous displays of the sample values and the four variables denoting discolouration. The differences among the five kiln schedules are visually displayed. Note that the mean values for all four variables in the case of each kiln schedule can easily be obtained from the biplot by dropping a line perpendicular to each axis representing the individual variables. Since the CVA biplot in the top panel of Figure 2 shows all the replicates, it provides visual evidence of the differences and variation among the replicates originating from the five schedules with respect to the four measurements describing discolouration. Unfortunately, due to overplotting, the use of this biplot is limited. Therefore, the group structure is described in terms of alpha-bags about each mean. An alpha-bag demarcates the inner α percent of the observations. 50% and 95% bags are shown. The results of the simultaneous confidence intervals in Table 3 are confirmed by perusal of the biplots in Figures 2 and 3: Schedules S.45/36 and S.71/65 are similar and completely separated from schedule S.90/57. It is clear from Figure 3 that the latter schedule leads to the largest values and the smallest L* (i.e. darkest) values. The S.102/67 and S.90/60 schedules show also significant discolouration and occupy positions on the biplot close to each other between schedules S.45/36 and S.71/65 on the one hand and S.90/57 on the other. Note also that S.102/67, S.90/60 and S.90/57 have similar a*-values; more red than the other two schedules.

Photographs of the replicates which most closely resembled the average colour of each sample as well as the darkest (lowest L*-value) replicates from each sample are shown in Figure 4. The thermal discolouration yielded a homogenous darkening that was not distinctly noticeable when comparing the average sample colours. However, some replicates from the higher temperature samples were clearly much darker as illustrated by the photos of the darkest (lowest L*-value) replicates in Figure 4.

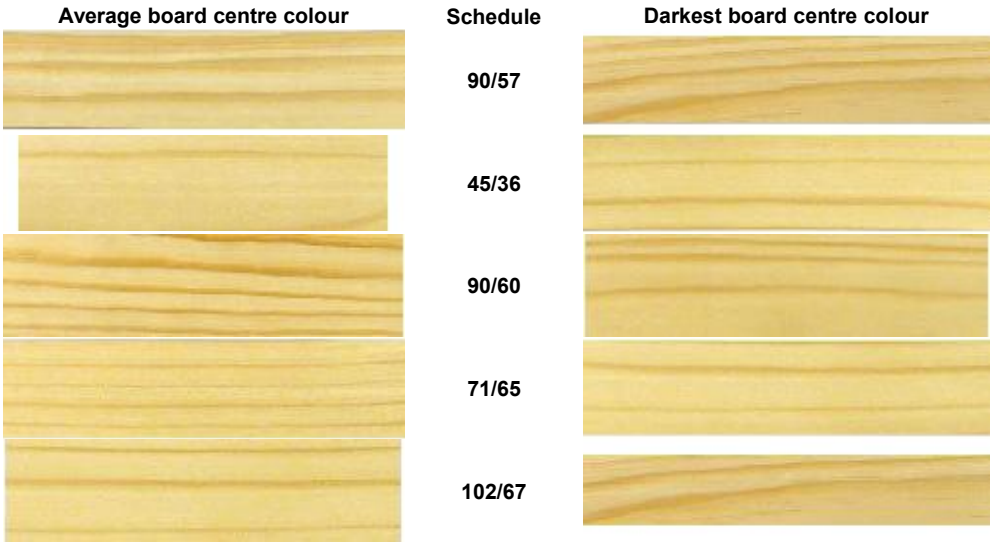

Figure 4: Replicates that closely resembled the colour of the average and darkest (lowest L*-value) board centre colours produced by each kiln schedule.

3.4.4.2 Surface discolouration at varying depths

The boxplots in Figure 5 of the CIE-L*a*b* defined colour at varying depths of the 90/60 schedule samples show that a progressively weaker surface discolouration is exhibited as the depth from the surface increased. Samples that showed brown surface discolouration at the 1 mm depth level always showed yellow surface discolouration at greater depths, indicating that yellow stain and kiln brown stain were chemically linked. At the 5 mm depth level the wood colour was much the same as at the centre. Yellow surface discolouration mainly occurred at the 3-4 mm depth with a transition to predominantly brown discolouration at the 1-2 mm depth level. A significant difference in direction of variation was evident between yellow and brown surface discolourations. This variation also indicated the direction of surface colour progression in the CIE-L*a*b* colour system.

A MANOVA conducted on these data leads to rejection of the null hypothesis (p-value approaching zero) of no significant differences among the six population group mean vectors. Therefore, a more detailed statistical analysis was performed by calculating 99% simultaneous confidence intervals for all pairwise contrasts for all four variables. These intervals are given in Table 4.

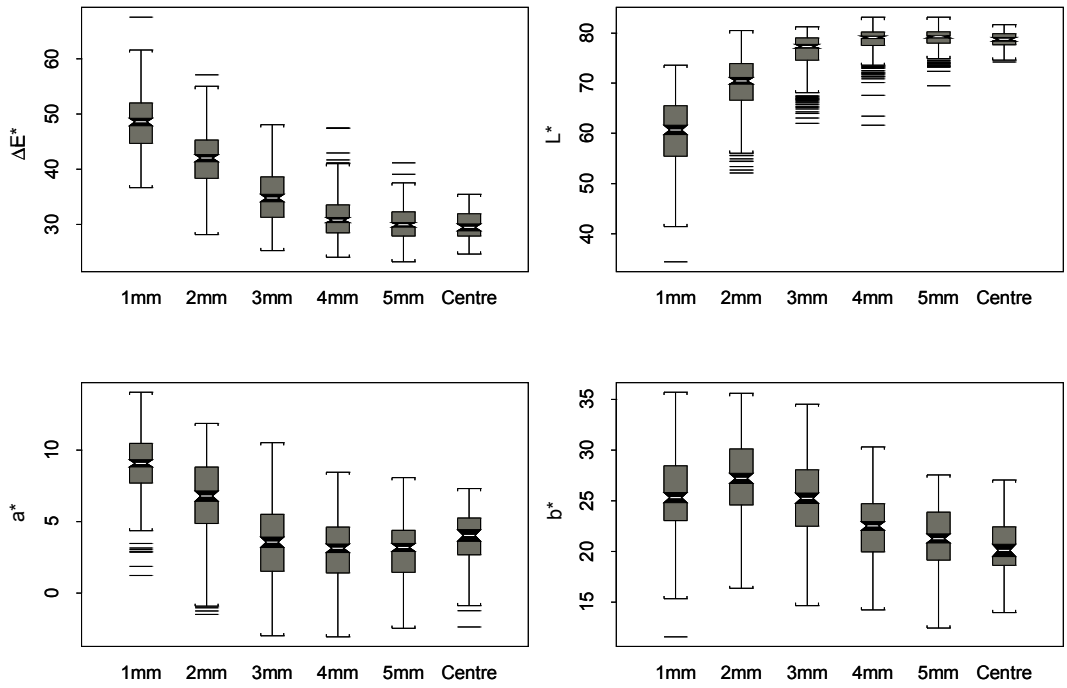

Figure 5: Notched boxplots of four variables depicting surface discolouration produced by the S.90/60 kiln schedule at varying depths.

Table 4: 99% simultaneous confidence intervals for all pairwise contrasts among mean thermal discolouration at varying depths. Intervals excluding zero are highlighted

Contrast	ΔE^* Conf interval		L* Conf interval		a* Conf Interval		b* Conf Interval	
1mm – 2mm	4.907	8.764	-11.35	-7.52	1.297	3.300	-3.285	-0.217
1mm – 3mm	11.430	15.280	-17.67	-13.84	4.357	6.360	-1.128	1.940
1mm – 4mm	15.170	19.030	-20.08	-16.25	4.842	6.845	1.633	4.701
1mm – 5mm	16.250	20.110	-20.57	-16.74	4.993	6.996	2.650	5.718
1mm – Centre	15.810	21.270	-21.05	-15.63	3.633	6.465	3.002	7.341
2mm – 3mm	4.590	8.448	-8.23	-4.40	2.059	4.061	0.623	3.691
2mm – 4mm	8.337	12.190	-10.64	-6.81	2.544	4.546	3.384	6.452
2mm – 5mm	9.415	13.270	-11.13	-7.30	2.695	4.698	4.400	7.468
2mm – Centre	8.978	14.430	-11.61	-6.19	1.335	4.167	4.753	9.092
3mm – 4mm	1.818	5.676	-4.32	-0.49	-0.516	1.486	1.227	4.295
3mm – 5mm	2.896	6.754	-4.82	-0.98	-0.365	1.638	2.243	5.311
3mm – Centre	2.459	7.915	-5.29	0.13	-1.725	1.107	2.596	6.935
4mm – 5mm	-0.851	3.007	-2.41	1.42	-0.850	1.153	-0.518	2.551
4mm – Centre	-1.288	4.168	-2.89	2.54	-2.210	0.622	-0.165	4.174
5mm – Centre	-2.366	3.090	-2.39	3.03	-2.362	0.470	-1.182	3.157

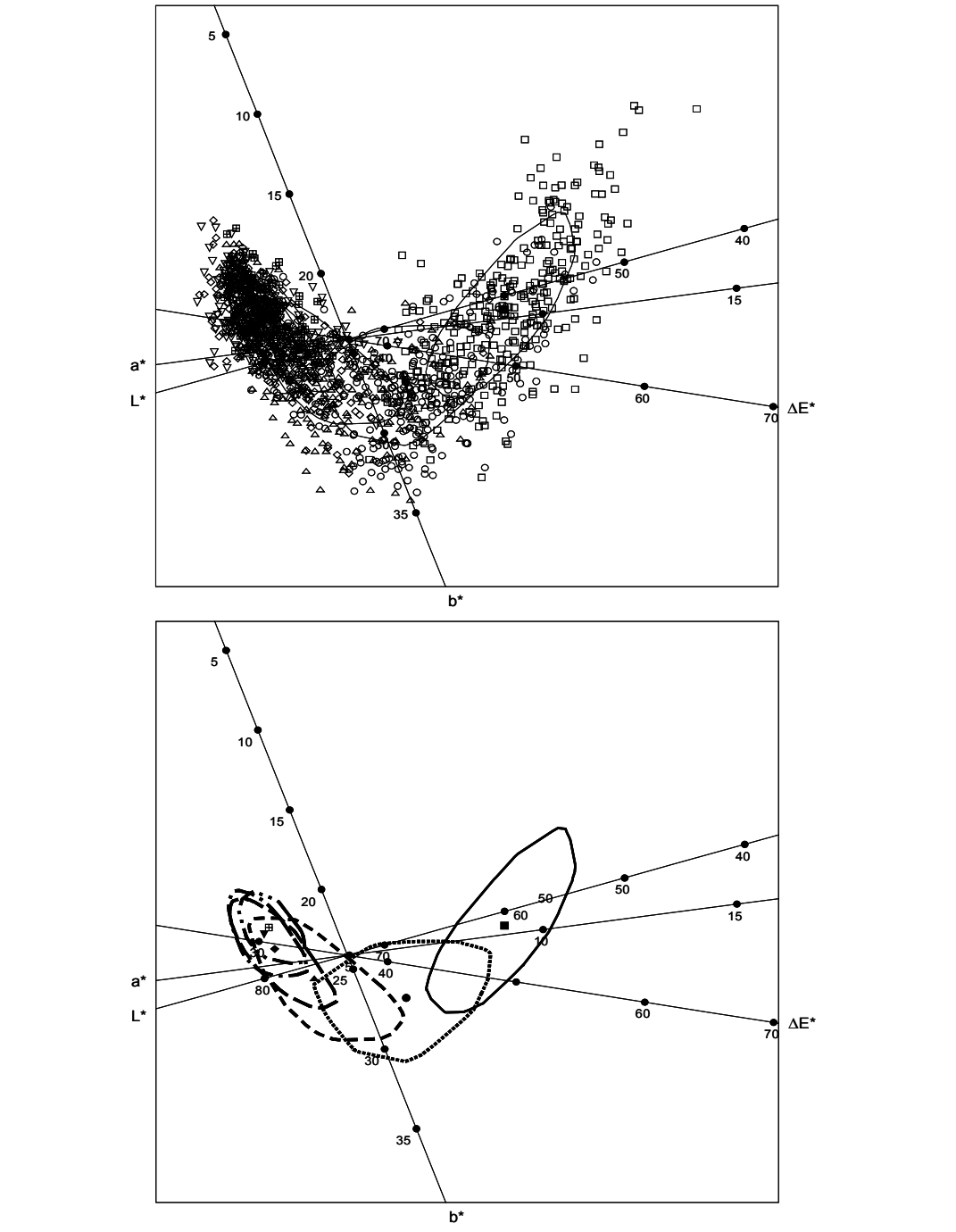

Figure 6: Top panel shows a CVA biplot of the CIE-L*a*b* defined colour produced by the S.90/60 schedule at different depths from the surface of the boards. The same biplot is repeated in the bottom panel but only the respective mean values at the different depths together with the respective 50% bags are shown.

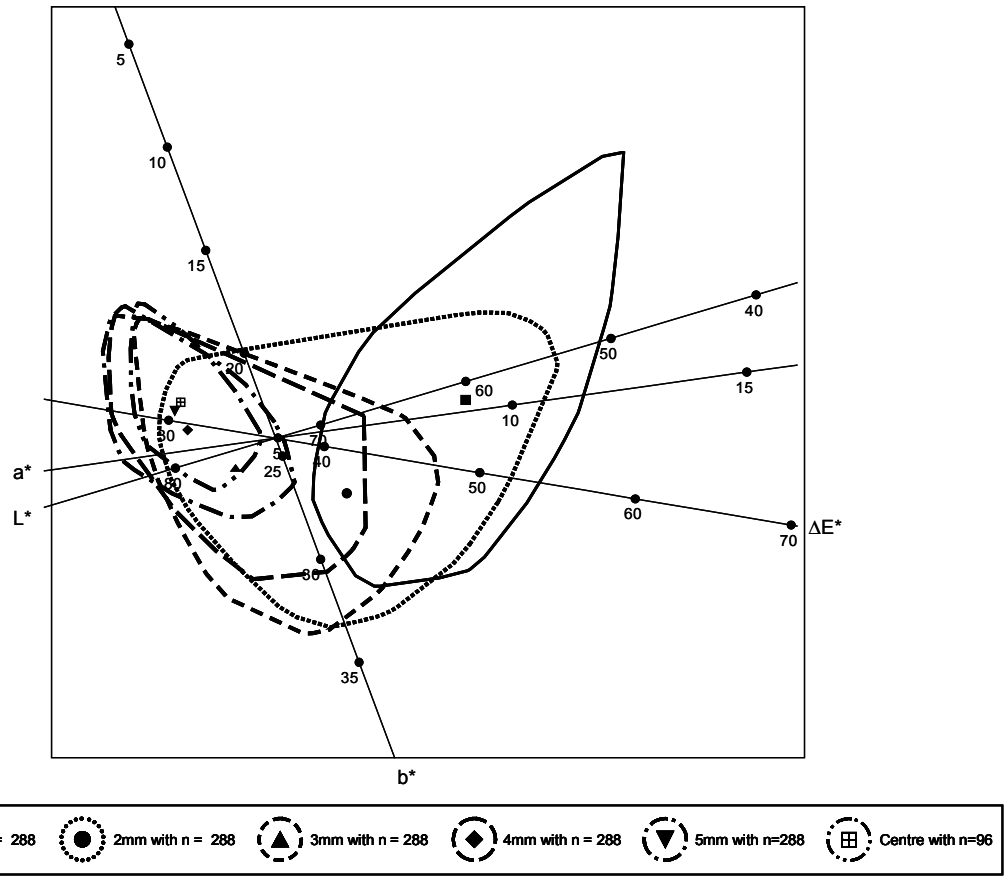

Figure 7: CVA biplot of the CIE-L*a*b* defined colour produced by the S.90/60 schedule at different depths from the surface of the boards. The mean values at the different depths together with the respective 95% bags are shown.

It follows from Table 4 and Figures 6 and 7 that there is very little difference between the mean values obtained for the , L*, a* and b* measurements at depths of 4 mm, 5 mm and centre of boards. At 3 mm, the mean values of and b* become larger with a decrease in the mean values of L* and a*. These changes are more pronounced at 2 mm. Discolouration as measured by , L* and a* is strongest at 1 mm. Note that even the 95% bag at 1 mm has no overlap with those at board centre and 5 mm. However, while the largest mean b* value occurs at 2 mm, there is a significant drop in the mean b*value at 1mm, returning to a value similar to that found at 3 mm. This is confirmed by the corresponding confidence interval for the contrast between the mean b* value at 1 mm and 3 mm depths in Table 4 that includes zero. Notice also how insight into the progression of the discolouration with increasing distance away from the centre of the boards can be gained by connecting the successive mean points on the biplot with straight lines.

The CVA biplots in Figures 6 and 7 suggest negative correlations between ΔE* and L* as well as between L* and a*. These biplots also suggest b* to be weaker correlated with the other variables while in the case of thermal discolouration the biplots in Figures 3 and 4 suggest a* to be weaker correlated with the other variables.

When the ΔE*-range of the 90/60 board centre samples are taken as the desired colour, the notched boxplot in Figure 5 shows a steady decrease in discolouration as the samples were planed to a greater

depth. The notched boxplot for L* in Figure 5 shows a similar trend. It is also clear that both the ΔE* and L* values at 5 mm and 4 mm closely match those of the board centre samples. This phenomenon is consistent with the theory that capillary water movement concentrates Maillard reaction precursors close to the surface of a board (Terziev *et al.* 1993; Theander *et al.* 1993) while the wetline remains just beneath the board surface (Wiberg and Morén 1999). Progressively lower concentrations of precursors would be deposited at greater depths from the surface.

Figure 8 illustrates the average and darkest colours yielded by the 90/60 schedule at different depth levels. At 1-2 mm depth, the average colour of the samples was a dull brown that did not even closely resemble the colour at greater depths. At 3 mm depth, the average sample displayed yellow stain with a slight tinge of brown stain. The average sample colour at 4 mm depth was more similar to the colour of the 5 mm depth and centre samples. However, there were some replicates in the 4 mm sample that were discoloured, as indicated by the photograph of the darkest replicate and Table 4. Note how the shape of the corresponding bag along the ΔE*-axis in Figure 7 is in agreement with the evidence provided by the photograph in Figure 8.

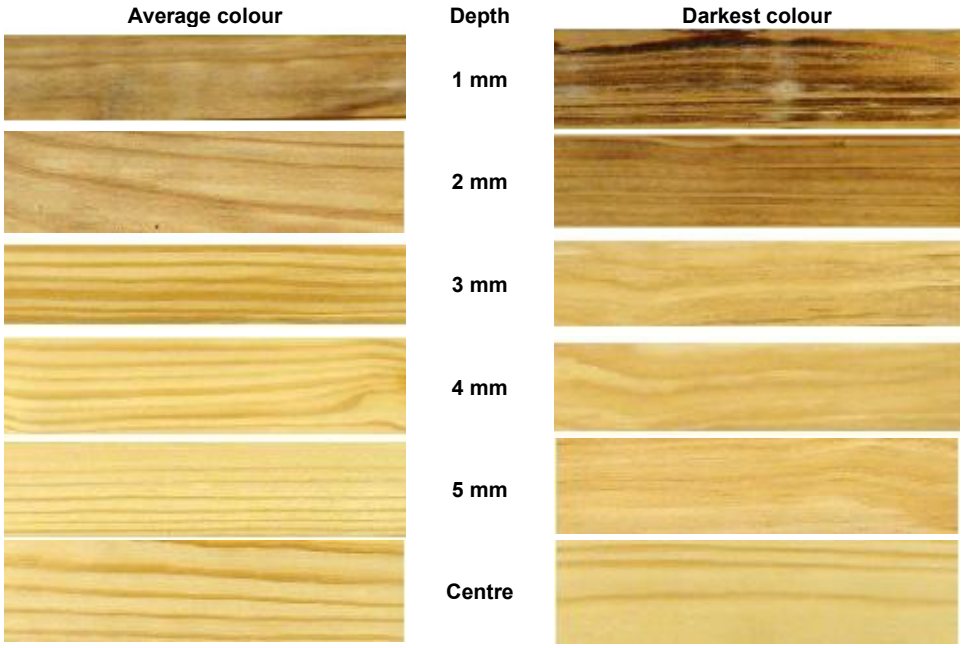

Figure 8: Replicates that closely resembled the colour of the average and darkest (lowest L*-value) board centre colours at progressing depth as produced by the 90/60 schedule.

3.4.4.3 Surface discolouration due to different schedules

Since it is known that the higher temperature schedules yielded thermal discolouration, the colour produced by these schedules at the surface would be a combination of thermal and surface discolouration. Therefore, the effect of the different schedules was investigated at the 2mm depth level.

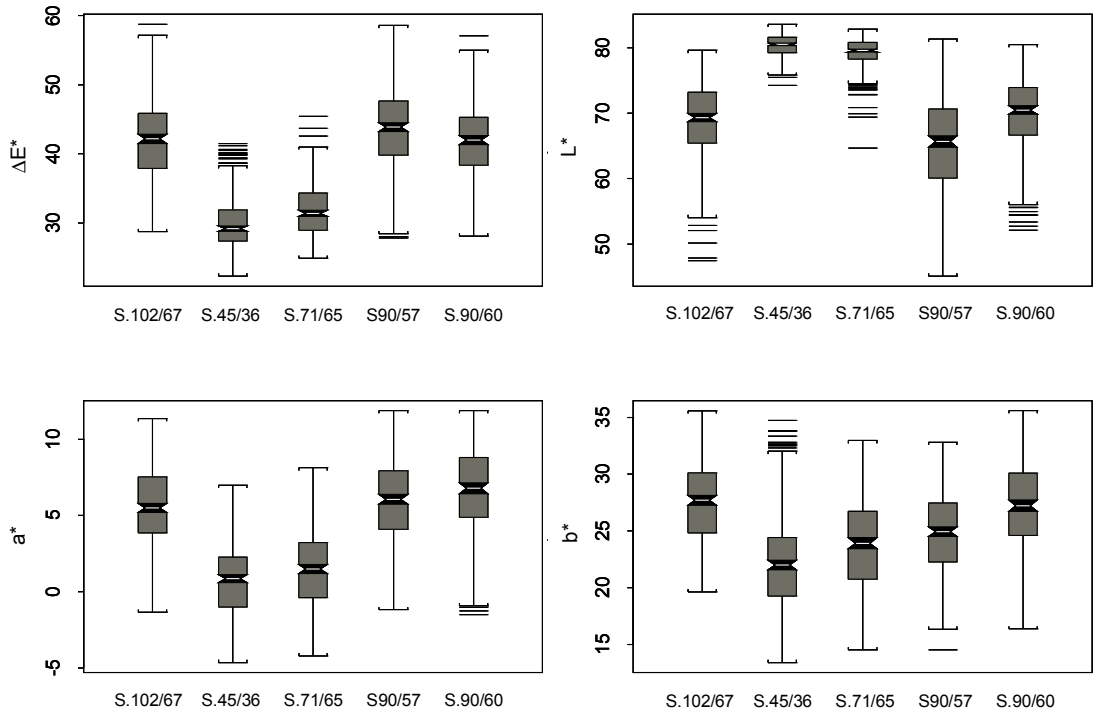

Figure 9: Notched boxplots showing thermal discolouration corresponding to the different schedules at 2mm depth level.

Figure 9 suggests that the 71/65 schedule yielded no surface discoloured replicates at the 2 mm depth level when the 45/36 ΔE*-range is taken as the desired colour. However, there is an abrupt change in the median values of ΔE*, L* and a* (and to a lesser extent also of b*) in the case of the higher temperature schedules. This suggests an increase in discolouration for the latter cases, indicating that a ≥90°C dry bulb temperature during the first drying phase would yield surface discolouration, while a ≤71°C dry bulb temperature during the first drying phase would produce a light coloured surface. A MANOVA was performed to test the above suggestions. The hypothesis that the population mean vectors of the five schedules are similar at a depth of 2 mm was rejected (p-value approaches zero). Therefore, all pairwise contrasts were investigated by the simultaneous confidence interval procedure of Roy (Morrison 1976). The results of this analysis are given in Table 5.

Table 5: 99% simultaneous confidence intervals for all pairwise contrasts among mean thermal discolouration for five kiln schedules at 2mm depth. Intervals excluding zero are highlighted

Contrast	ΔE * Conf interval		L* Conf interval		a* Conf Interval		b* Conf Interval	
S.102/67 - S.45/36	10.470	14.140	-13.17	-9.45	3.967	5.798	4.070	6.807
S.102/67 - S.71/65	8.455	12.130	-12.09	-8.36	3.268	5.100	2.333	5.070
S.102/67 - S.90/57	-3.327	0.346	1.94	5.67	-1.156	0.676	1.286	4.023
S.102/67 - S.90/60	-1.519	2.376	-2.71	1.24	-1.983	-0.040	-1.305	1.598
S.45/36 - S.71/65	-3.847	-0.174	-0.78	2.95	-1.614	0.217	-3.105	-0.368
S.45/36 - S.90/57	-15.630	-11.960	13.25	16.98	-6.039	-4.207	-4.152	-1.415
S.45/36 - S.90/60	-13.820	-9.925	8.60	12.55	-6.865	-4.923	-6.743	-3.84
S.71/65 - S.90/57	-13.620	-9.945	12.17	15.89	-5.340	-3.508	-2.415	0.321
S.71/65 - S.90/60	-11.810	-7.915	7.52	11.47	-6.167	-4.224	-5.006	-2.104
S.90/57 - S.90/60	-0.028	3.867	-6.51	-2.56	-1.743	0.200	-3.959	-1.057

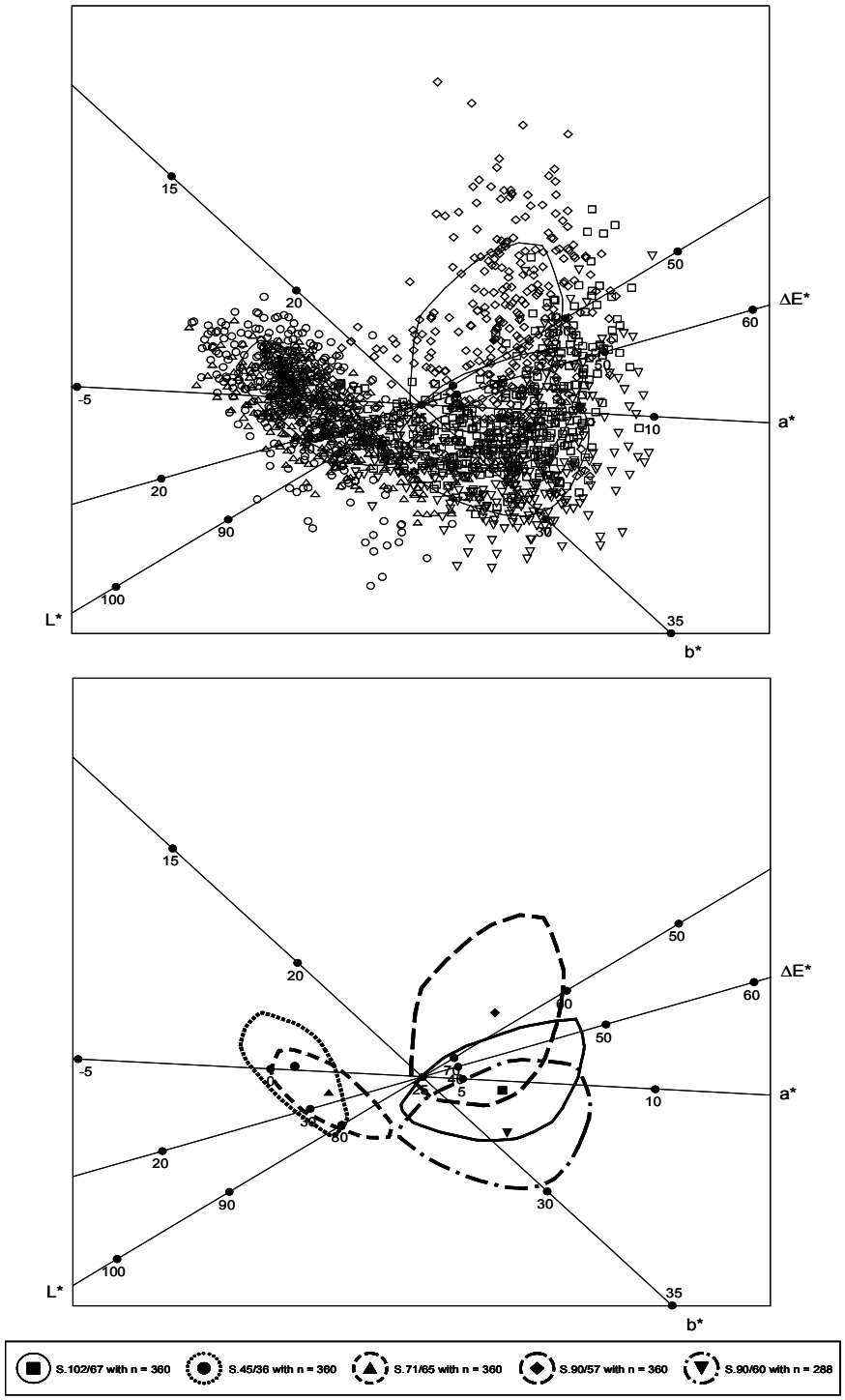

Figure 10: CVA biplot showing the effect of different schedules on colour at 2mm depth. Biplot in upper panel show the variation in all the samples while mean values together with 50% bags are shown in the biplot in the bottom panel.

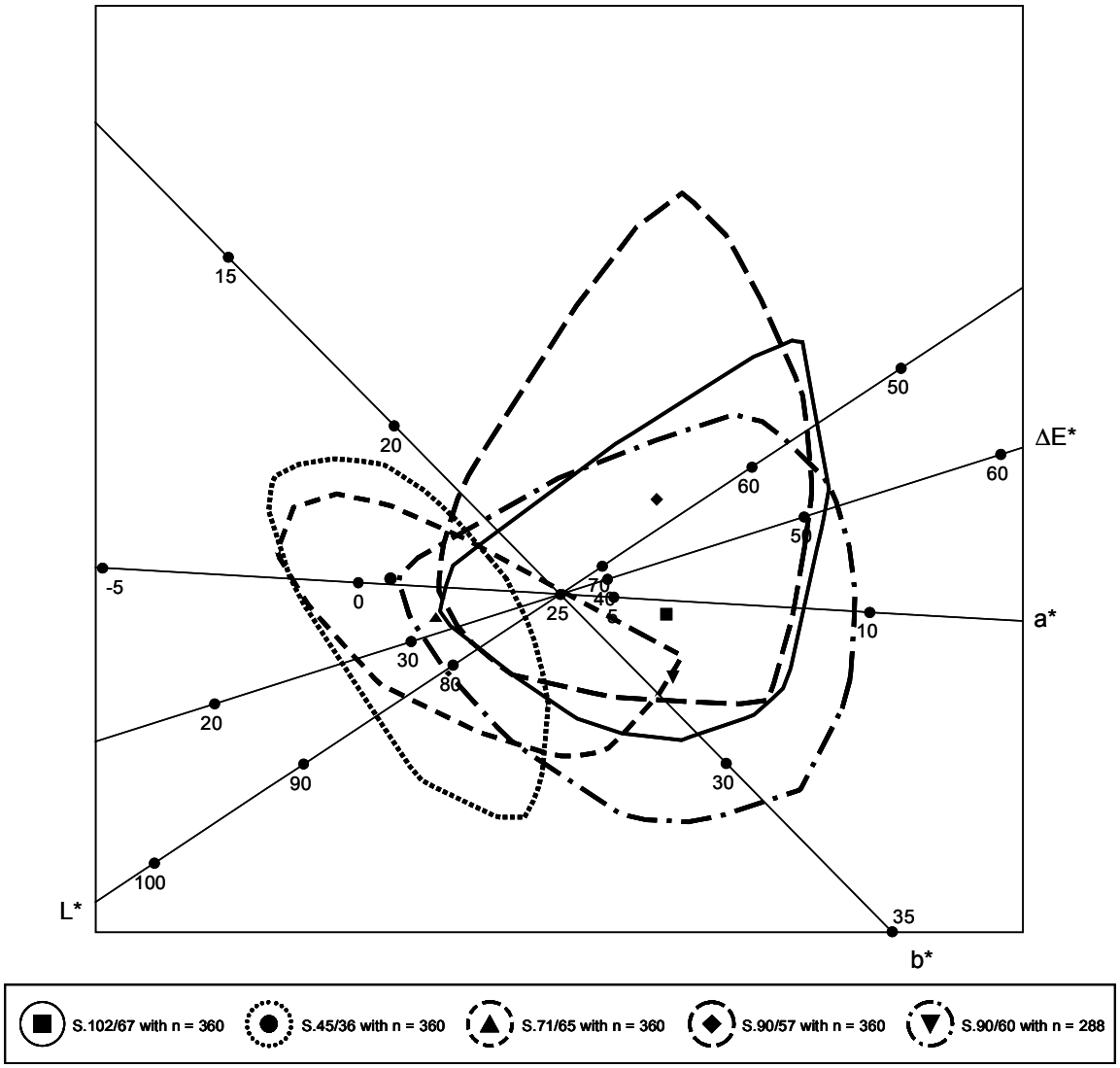

Figure 11: CVA biplot showing the mean values of five different schedules for four colour measurements at 2mm depth together with 95% bags.

It follows from Table 6 and Figures 10 and 11 that schedules S.45/36 and S.71/65 are almost of the same darkness (L*) with the ΔE*-mean for S.71/65 slightly larger and also more yellow (larger b* mean). However, the differences between these two schedules are slight in comparison with the other three schedules. The mean ΔE*-value for these three schedules are similar but appreciably higher than those of S.45/36 and S.71/65. Similarly S.102/67, S.90/57 and S.90/60 are appreciably darker than S.45/36 and S.71/65 (mean L* significantly smaller). The main difference between S.102/67, S.90/57 and S.90/60 occurs in the mean b*-values – S.90/60 more yellow than S.102/67 that in turn is more yellow than S.90\57. Note that the mean b*-value of S.90/57 is similar to that of S.71/65. The complete separation in the 50% bags of S.45/36 and S.71/65 on the one hand and the 50% bags of S.102/67, S.90/57 and S.90/60 on the other hand, is conspicuous.

If the scales of the axes in Figure 11 are compared to those of Figure 3, it is evident that the variation in surface discolouration is much greater. As with thermal discolouration, the 90/57 schedule showed the

greatest degree of surface discolouration. This may be ascribed to the fact that this schedule took longer to finish than the other higher temperature schedules.

The above conclusion is corroborated by the work of Kapp *et al.* (2003), which showed that a transition from yellow to brown stain occurred at about 80°C dry bulb temperature for the first drying phase.

Figure 12 illustrates the much lighter colour wood produced by the lower temperature schedules at a 2 mm depth. The colour variation between the darkest replicates from each sample was even more distinct and reflected the greater within-sample colour variation of the higher temperature schedule samples.

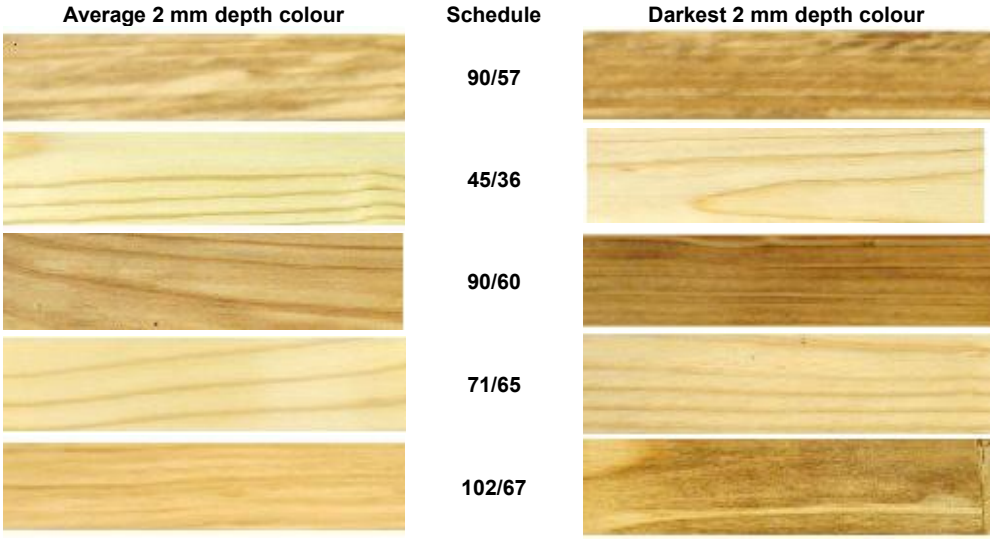

Figure 12: Replicates that closely resembled the colour of the average and darkest (lowest L*-value) 2 mm depth colours produced by each kiln schedule

3.4.5 Conclusions

Thermal and surface discolouration were distinguishable by the distribution of colour data point plots in the CIE-L*a*b* colour system. Thermal discolouration was much less varied and correlations among the CIE-L*a*b* colour system components differed for the two discolouration types.

Higher temperature schedules (≥90°C T_{db} during first drying phase) yielded more thermal discolouration. The thermal discolouration was uniform and generally not conspicuous. However, in a higher temperature schedule that takes a long time to finish, like the 90/57 schedule with low air velocity, a large percentage of discoloured samples may result. In the case of the 90/57 schedule, 45% of the replicates were discoloured.

The degree of surface discolouration was greatly dependent on the planing depth and schedule temperatures. The greatest number of discoloured samples was found close to the surface, with progressively less discolouration at greater depths. Higher temperature schedules yielded 77.5-82.5% discoloured replicates at the 2 mm depth level, while lower temperature (≤71°C T_{db} during first drying phase) schedules yielded no discoloured wood at the surface or at the centre of the boards.

The use of CVA biplots with superimposed alpha bags was found to provide valuable insights into the overlap and separation of the different schedules. In particular, the biplots provide visual evidence of the role played by the various components of the CIE-L*a*b* colour system in discolouration produced by the different kiln schedules at the measured depths in this study.

3.4.6 References

Boutelje, J.B. 1990. Increase in the content of nitrogenous compounds at lumber surfaces during drying and possible biological effects. Wood Science and Technology 24: 191-200.

Danehy, J.P. and W.W. Pigman. 1951. Reactions between sugars and nitrogenous compounds and their relationship to certain food problems. Advances in Food Research 3: 241-290.

Gower, J.C. and D.J. Hand. 1996. *Biplots*. London: Chapman & Hall.

Kapp, S., G.C. Scheepers and T. Rypstra. 2003. Factors influencing the development of yellow stain and kiln brown stain in South African grown *Pinus spp.* Journal of the Institute of Wood Science 16 (2): 113-118.

kollmannn, F., R. Keylwerth and H. Kübler. 1951. Verfärbungen des Vollholzes und der Furniere bei der künstlichen Holztrocknung. Holz als Roh- und Werkstoff 9 (10): 382-391.

Kreber, B., A.N. Haslett and A.G. McDonald. 1999. Kiln brown stain in radiata pine: a short review on cause and methods for prevention. Forest Products Journal 49 (4): 66-70.

Long, K.D. 1978. Redistribution of simple sugars during drying of wood. Wood Science 11 (1): 10-12.

McGill, R., J.W. Tukey, and W.A. Larsen. 1978. Variations of box plots, *The American Statistician*, 32, 12-16.

Morrison, D.F. 1976. *Multivariate Statistical Methods*, 2nd edition. Tokyo: McGraw-Hill Kogakusha.

Terziev, N., J.B. Boutelje and O. Söderström. 1993. The influence of drying schedules on the redistribution of low-molecular sugars in *Pinus sylvestris* L. during kiln and air drying. Holzforschung 47: 3-8.

Theander, O., J. Bjurman and J.B. Boutelje. 1993. Increase in the content of low-molecular carbohydrates at lumber surfaces during drying and correlations with nitrogen content, yellowing and mould growth. Wood Science and Technology 27: 381-389.

Wiberg, P. and T.J. Morén. 1999. Moisture flux determination in wood during drying above fibre saturation point using CT-scanning and digital image processing. Holz als Roh- und Werkstoff 57: 137-144.

3.5 The effect of surface tension on liquid water flow and discolouration in softwood

3.5.1 Abstract

Two end-matched *P. sylvestris* boards, of which one was treated with a surfactant, were kiln-dried while taking X-ray CT-scan density images. The density images showed that the liquid water flow pattern was significantly altered by a reduced surface tension. Subsequently, green *P. elliottii* boards were treated with a surfactant to determine whether the development of discolouration by yellow stain and kiln brown stain would be influenced by the altered liquid flow pattern observed in the *P. sylvestris* boards. The treatment did have a significant effect on the colour at 1-2 mm depth in especially the L*- and b*-dimensions of the CIE L*a*b* colour space.

The results highlighted the influence of the cohesive forces within the liquid water on the liquid flow pattern. The results also support the connection between the wetline phenomenon, liquid water movement and surface discolouration in softwood.

3.5.2 Introduction

Drying above the fibre saturation point (FSP) has been described as a two-stage process (Keey 1999). In the first stage, the border of the free water region, or wetline, remains close to the surface and liquid water is drawn from the core to the surface. The second stage follows when liquid continuity ceases and the wetline starts moving towards the core. This type of wetline movement has been shown to be true for various wood species (Wiberg and Morén 1999). During the drying of lumber above fibre saturation point, capillary water flow to the wetline deposits precursors of the Maillard reaction close to the surface, which leads to surface discolouration in softwoods (Kreber *et al.* 1999, and Terziev 1995), referred to as yellow stain and kiln brown stain.

The most effective liquid flow pathways are dictated by the cellular structure of the wood (Siau 1984). The cellular structure is also the foundation of the invasion percolation theory of drying (Prat 2002), which predicts the existence of a receding wetline during drying. Recently, it was also suggested that cavity-size distribution influences the drying characteristics of different wood species (Scheepers *et al.* 2005).

The purpose of this study was to determine the effect of the liquid water surface tension on the moisture flow pattern above FSP in *P. sylvestris* and the associated surface discolouration found in *P. elliottii*. Swedish *P. sylvestris* was selected for the X-ray CT-scan component of the investigation because it was a readily available softwood in the proximity of the experimental equipment. South African *P. elliottii* was selected for the discolouration component of the study because of its inclination to discolour (Kapp *et al.* 2002). The results are discussed in terms of the current understanding of the drying mechanism above FSP.

3.5.3 Materials and methods

3.5.3.1 Drying and CT-scanning of Pinus sylvestris boards

Two end-matched *Pinus sylvestris* boards were dried at 80°C dry bulb and 40°C wet bulb temperature. Prior to drying, one of the boards was soaked in a 5% aqueous surfactant (sodium lauryl sulphate, SLS) solution for 5 days, while the other was kept in a freezer at -20°C. While drying, a Siemens Somatom AR.T X-ray Computed Tomography (CT) scanner captured a density image of the same 10 mm thick cross-section in each replicate at 10 minute intervals. Each density image was a 512×512 matrix with a density value (kg/m^3) for each matrix element. To determine the average moisture content of the replicate at every point in time where a density image was captured, the oven-dry density value of the scanned wood volume at the end of kiln-drying was first determined. This final kiln-dry density value was then adjusted to compensate for the difference in replicate size at the end of kiln-drying and the respective previous points in time. With the dry density values for each point in time known, and the wet density at each point in time determined by calculating the average matrix element value for matrix elements representing wood, the moisture content at each point in time could be calculated.

3.5.3.2 Yellow stain and kiln brown stain of Pinus elliottii boards due to drying

Green 43×121×2400 mm^3 (wet dimensions) *P. elliottii* boards from the Tsitsikamma region of South Africa were cross-cut to 700 mm lengths and end-sealed with a polyurethane waterproofing compound. The boards were divided into four groups of 20 boards each. Each group was treated as follows:

1. Group 1: 3 day water dip;
2. Group 2: 10 second SLS dip (shortly before drying);
3. Group 3: 3 day 5% SLS dip; and
4. Group 4: 3 day 2% SLS dip.

Subsequently, the boards were loaded into an experimental kiln and dried with the schedule shown in Figure 1.

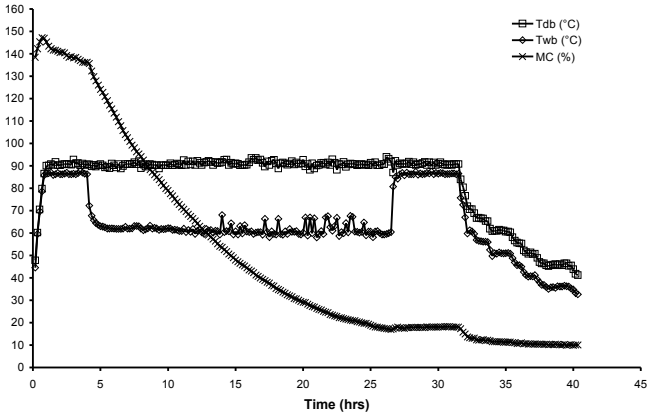

Figure 1: Kiln schedule employed to investigate surface discolouration.

The kiln dried boards were passed over a planer set at 1 mm depth until two thirds of the typically uneven surface was planed. This surface was defined as the 1 mm depth level. The planed surface was divided into 3 equal sized areas along the full length of the board, and colour measurements of the three darkest earlywood spots were taken in each area, yielding nine colour measurements per planed board surface. Each board was again passed once over the planer set at 1 mm depth, the newly exposed surface was designated the 2 mm depth level, and the colour of this surface was measured in the same manner. This process was repeated every 1 mm up to 5 mm depth. The replicates were then ripsawn at approximately 20 mm depth (board centre depth) and planed to determine the colour of the wood where no yellow stain or kiln brown stain had occurred.

Colours were measured using the CIE L*a*b* colour system. A Sheen Micromatch Plus colorimeter (Sheen Instruments Ltd.) with a 4 mm measurement aperture was used to determine the colour of the earlywood of each planed surface. The colorimeter (45°/0° instrument geometry) was set to D65/10° illumination/observation. The dE*-value, the scalar difference from white with (L*, a*, b*)-coordinates (100, 0, 0) and L*, a* and b* values were used as measures of discolouration.

3.5.4 Results

3.5.4.1 X-ray CT-scans

In the X-ray CT scan images shown in Figure 2, darkness indicates low density and whiteness high density. The presence of free water greatly influences the density of wood. At the start of drying, both boards showed a high-density sapwood region (free water present) and a low-density heartwood region (free water not present). At an average MC of about 54%, there was little difference in density between sapwood and heartwood as most of the free water had evaporated. Hence, the white areas in the images indicate the presence of free water in the cells.

In the control, a clearly defined wetline was developed a few millimeters under the surface of the board at about 80% MC. The board then dried homogeneously throughout its thickness and width, as evidenced by

the density image at 54% MC. However, in the SLS-treated board the liquid water split up into four distinct zones (free-water pockets) at 80% MC. These free-water pockets were bordered by the board surface. At 54% MC the last remnants of these zones could still be seen at the board surface, indicating that these wet zones were emptied by evaporation at the surface and the resulting capillary action. Hence, the wetline did not develop a few millimeters under the surface as with the control.

Since cell walls are fully saturated with water at moisture contents above FSP, the behaviour of the liquid water within the cell lumens would be a function of the cohesive forces within the liquid body and the adhesive forces to the saturated cell wall. The work of cohesion needed to break a column of liquid water is described by:

$$W_c = 2\gamma$$

Where γ is the surface tension of the liquid water.

Hence, in the SLS-treated board less work was needed to break cohesive forces in continuous columns of water compared to the control. This may explain why the SLS-treated board developed liquid separation into four distinct pockets of water. The position of these pockets of water seemed to be dictated by the easiest liquid transport route: tangentially along the earlywood cells of the year rings to the site of evaporation at the board surface. Also, the wetline position was influenced by the surface tension (cohesive forces) within the body of water. Evidently, a reduction in surface tension caused the wetline to remain closer to the board surface.

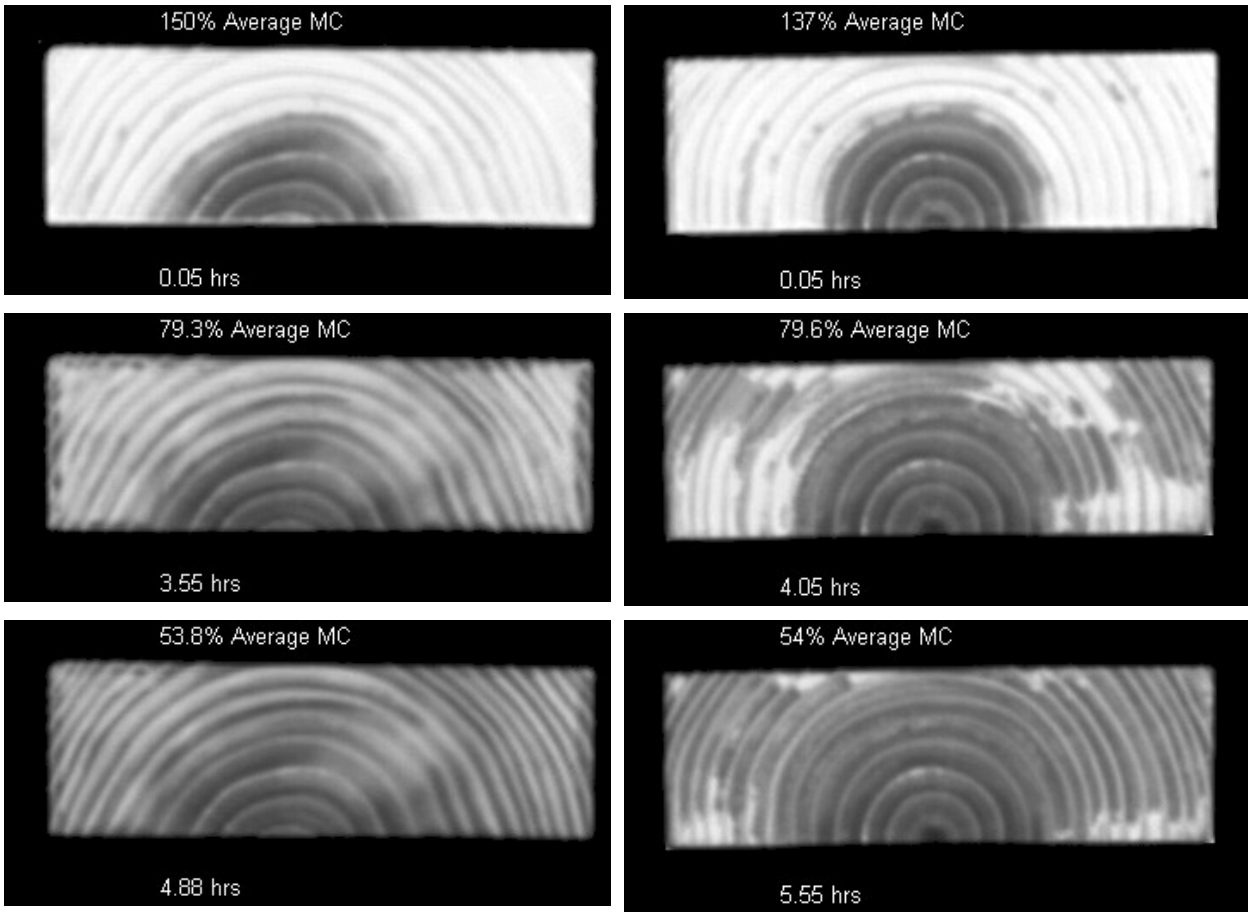

Figure 2: Moisture distribution patterns during drying of the *P. sylvestris* control on the left, and a 5% SLS surfactant treated board on the right. Low density areas are dark, and high density areas (with much free water) are white.

3.5.4.2 Surface discolouration

As previously mentioned, the surface discolouration of softwood due to yellow and brown stain is partly attributed to the wetline phenomenon. If the surfactant treatment causes the wetline to remain close to the surface, and discolouration is more prevalent because of concentration of precursors at the wetline, one could expect less discolouration reactions deeper into the board and thus more of the discolouration to be removed when planing the surface. The colour at different depths for the different groups of *P. elliottii* is depicted in Figure 3. The colour at the centre of the boards can be considered to be the "normal" colour of the kiln dried wood. Evidently, compared to the colour of the board centre, the surface discolouration is represented by lower L*-values and higher dE*-, a*- and b*-values. The lower L*-values indicate a darker colour.

The ten second SLS dip had a negligible, if any, effect on the colour of the wood when compared to the control group. Only in the a*-dimension at 1 mm and 5 mm depths was there a significant difference between these to groups. The two groups that were treated with 3 day SLS dips yielded a similar colour that was distinctly different from the other two groups at 1-2 mm depth. The most distinct differences were in the L*- and b*-dimensions. At 3 mm or greater depth, the differences were negligible.

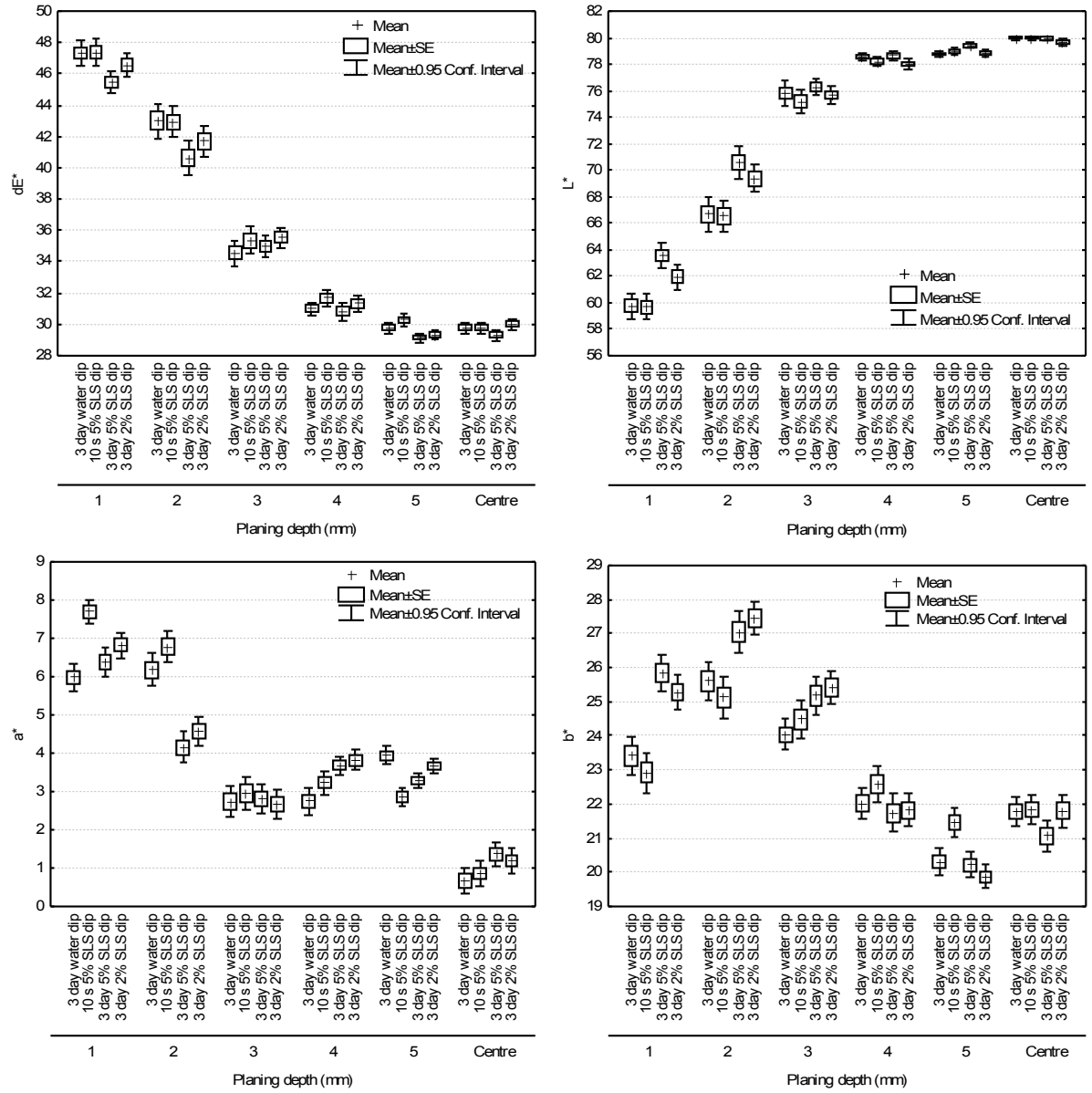

Figure 3: Effect of treatment on wood colour measured at different depths in boards. Values shown in the CIE L*a*b* colour space. The dE*-value is the scalar difference from the colour white at L*a*b*-coordinates (100, 0, 0).

3.5.5 Discussion

The drying behaviour of the *P. sylvestris* control was similar to what the invasion percolation theory of drying would predict: a distinctive wetline retracting into the board while the cells in the inner part of the boards were emptied of liquid water through evaporation and capillary action, thus creating a situation where presumably only the smaller cells were still filled with water. A reduction in the cohesive forces within the body of liquid water caused a deviation from this moisture movement pattern. The liquid water split up into large wet pockets that bordered the surface of the board and these pockets were also much closer to the board surface than that of the untreated board. This could possibly be attributed to a relaxation of the cohesive forces within the liquid body of each wet pocket, thus increasing the spreading ability of the liquid

water and resulting in a wetline closer to the surface. The treated board showed that liquid water was mainly transported tangentially within a growth ring to the wetline at the board surface by capillary forces.

A change of surface tension also influenced the surface colour. Evidently the distribution of discolouration reaction precursors at the surface was influenced by a change of the liquid flow pattern. The two 3-day SLS dips caused a significantly lighter colour, or greater L*-values, at 1-2 mm depth. The b*-values were also higher, *i.e.* the colour became more yellow at this depth. It is possible that more precursors were deposited close to the board surface due to a modified wetline position, and planed off on the first pass over the planer.

3.5.6 Conclusions

The results pointed out the influence of the cohesive forces within the liquid water to the liquid flow pattern. Both the discolouration and CT-scan results showed that a lower surface tension influenced liquid water movement in the selected two softwoods during drying. A reduced surface tension led to distinct liquid water pockets, caused the wetline to be closer to the surface, and as a result, yielded less discolouration at 1-2 mm depth. The results also support the connection between the wetline phenomenon, liquid water movement and surface discolouration in softwood.

3.5.7 References

Kapp, S., G.C. Scheepers and T. Rypstra. 2003. Factors influencing the development of yellow stain and kiln brown stain in South African grown *Pinus spp*. Journal of the Institute of Wood Science 16(2): 113-118.

Keey, R.B., T.A.G. Langrish and J.C.F. Walker. 1999. Kiln-Drying of Lumber. Springer-Verlag, Berlin.

Kreber, B, Haslett, AN, and AG McDonald. 1999. Kiln brown stain in radiata pine: a short review on cause and methods for prevention. *Forest Products Journal*, 49(4): 66-70.

Prat, M. 2002. Recent advances in pore-scale models for drying of porous media. *Chemical Engineering Journal* 86: 153-164.

Scheepers, GC, J Danvind, T Morén and T Rypstra. 2005. An investigation of liquid water movement in Birch during drying through variation of wood sap surface tension and initial average moisture content. *Proceedings of the 9th International IUFRO Wood Drying Conference*, Nanjing, China. p. 57-62.

Siau, J.F. 1984. Transport Processes in Wood. Springer-Verlag. New York.

Terziev, N. 1995. Migration of low-molecular sugars and nitrogenous compounds in *Pinus sylvestris* L. during kiln and air drying. *Holzforschung* 49: 565–574.

Wiberg, P and TJ Morén. 1999. Moisture flux determination in wood during drying above fibre saturation point using CT-scanning and digital image processing. *Holz als Roh- und Werkstoff* 57: 137-144.

3.6 Liquid water movement in Birch during drying

3.6.1 Abstract

End-sealed 60×60×250 mm^3 Birch (*Betula verrucosa*) pieces were dried at 65/45°C (dry bulb/wet bulb temperature). The Birch pieces were pretreated to yield varying initial average moisture contents and wood sap surface tensions. While drying, data was collected with an X-ray Computed Tomography (CT) scanner measuring density data and probes measuring wood temperature and liquid pressure. The data from the CT-scanner was used to determine moisture content, moisture loss from the core of the wood pieces, wetline (boundary between water-filled and non-filled cells) depth and sample dimensions. The temperature, pressure and X-ray density-data showed varying patterns, which were affected by initial average moisture content and wood sap surface tension in this study. The results are discussed in terms of present theories of capillary moisture movement in wood.

3.6.2 Introduction

During lumber drying above fibre saturation point (FSP), capillary flow frequently leads to drying defects like cell collapse (Innes 1995) and surface discolouration (Kreber *et al.* 1999) in various wood species. Drying above FSP has been described as a two-stage process (Keey 1994). In the first stage, the wetline (or evaporative front) remains close to the surface and liquid water is drawn from the core to the surface by capillary forces. The second stage follows when liquid continuity ceases and the wetline starts moving towards the core. This type of wetline movement has been shown to be true for various wood species (Wiberg and Morén 1999). Spolek and Plumb (1981) also showed that the capillary forces present in softwood were dependent on the liquid water saturation level, with progressively stronger capillary forces at decreasing saturation levels.

According to this theory, the capillary flow that moves free water to the surface should result in a decreasing moisture content at the core while the wetline is stationary at the surface. Due to the expected dependency of the core moisture rate loss on capillary suction, it could be a function of the surface tension of the liquid water and the water saturation level. A continuously decreasing or constant (but not increasing) rate of moisture loss from the core could be expected while the wetline is at the surface since the potential supply of free water from the core and number of intact capillary pathways should decrease continuously. The objective of this investigation was to study the core moisture loss rate in a wood specie that is known to have a relatively open porous structure.

The core drying rates of Birch (*Betula verrucosa*) pieces during drying above FSP were monitored with an X-ray Computed Tomography (CT) scanner. The samples differed in initial moisture content and wood sap surface tension. Core drying rate profiles are discussed in relation to other drying phenomena.

3.6.3 Materials and methods

A fresh Birch log was sawn into 60×60×250 mm^3 pieces and stored at -20°C before use.

3.6.3.1 Determination of Drying Patterns

Three types of Birch samples were prepared in triplicate:

1. High MC: 130-140% MC replicates at normal surface tension of water;
2. Low Surface Tension: 130-140% MC replicates with low surface tension; and
3. Low MC: 70-75% MC green wood replicates with a normal surface tension.

The High MC replicates was prepared by submerging the frozen green replicates in a 90°C water bath for three days so air trapped in the pieces would bubble out, and then letting the water bath cool down. The Low Surface Tension sample was prepared similarly, but with the exception that an aqueous 3% sodium lauryl sulphate (SLS, Merck & Co., Inc.) solution was used in stead of water only. The Low MC sample was prepared by letting the frozen replicates thaw for 24 hours at room temperature in tightly wrapped plastic bags.

The three sample groups were dried in three separate drying runs. The replicates were end-sealed with silicone and dried in an atmoshpere constantly controlled at 65/45°C (dry bulb/wet bulb temperature) and a 4 $m.s^{-1}$ air speed while a Siemens Somatom AR.T X-ray CT-scanner captured a density image of the same 10 mm thick cross-section in each replicate at 10 minute intervals. To prevent any possible external influence on drying patterns, none of the replicates from these samples (*i.e.* the replicates referred to in Figures 1-5 of the results section) had any probes inserted or any holes drilled into them.

3.6.3.2 Processing the density data

Each density image was a 512×512 matrix with a density value (kg/m^3) for each matrix element. The successive density images were used to calculate (as illustrated in Figure 1):

1. The rate of moisture loss from the core;
2. The wetline (evaporative front) depth; and
3. The cross-cut area of each replicate.

The selected core area was a 15×15 mm^2 square at the centre of each replicate. The difference in the average density of the core of two successive images was divided by the elapsed drying time to provide the rate of moisture loss. The average wetline depth was calculated through its relationship to the cross-cut circumference of each replicate and the size of the above-FSP area. The cross-cut and above-FSP areas were obtained through determining the number of matrix elements above selected threshold density values.

These threshold density values were calculated according to the method employed by Wiberg and Morén (1999).

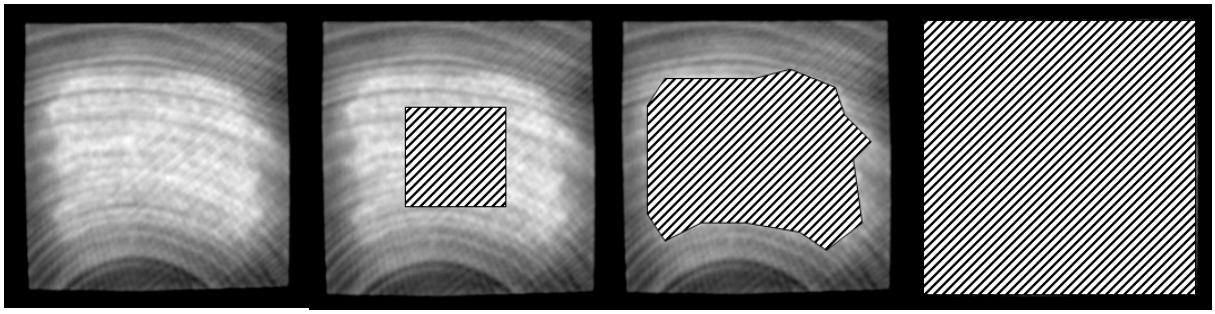

Figure 1: From left to right: the basic CT-scan density image, the selected core region, the selected above-FSP region for determination of the average wetline depth, and the cross-cut area of the wood piece.

To determine the average moisture content of the replicate at every point in time where a density image was captured, the oven-dry density value of the scanned wood volume at the end of drying was first determined. Then this final dry density value was adjusted to compensate for the difference in replicate size at the end of drying and the respective previous points in time. With the dry density values for each point in time known, and the wet density at each point in time determined by calculating the average matrix element value for matrix elements representing wood, the MC at each point in time could be calculated.

3.6.3.3 Study of a Separate High MC Birch Piece

To study the wood core temperature and liquid pressure during drying, a separate green Birch piece was taken from the freezer. Two holes were drilled to the core of the frozen green Birch piece; one for a pressure probe and one for a temperature probe. The piece was submerged in a 90°C water bath for three days and then allowed to cool down while in the water bath. It attained a final MC of 138%. Subsequently, a pressure and temperature probe were inserted into the drilled holes and sealed at the wood surface with silicone. The pressure probe was filled with de-aerated water in an attempt to create a continuous water column from the wood sap to the pressure probe diaphragm. The Birch piece was dried at 65/45°C (dry bulb/wet bulb temperature) while the X-ray CT-scanner captured a density image of the same 10 mm thick cross-section in each replicate every 10 minutes. The same data was extracted from this Birch piece as with the replicates of the previously mentioned three sample groups.

3.6.4 Results

3.6.4.1 Drying Patterns

3.6.4.1.1 Moisture loss from the core

Similar patterns of moisture loss from the core were shown by the three replicates of the High MC sample (Figure 2). Repeating peaks and troughs were evident. Shortly after drying started, a short sharp increase in moisture loss, indicated as Peak 1, occurred in all three replicates (Figure 2). Following Peak 1, all three replicates showed a steady increase in the rate of moisture loss to approximately 100% MC, when it steadily decreased to a trough at 70% MC. From 70% MC on, an increase in the rate of moisture loss from the core occurred in all three replicates; peaking at 60-65% MC and then continually decreasing as the average MC of the replicates approached FSP.

Unfortunately there was some data loss during the drying of the Low Surface Tension sample (Figure 3). However, the same peaks appeared to be present in these replicates as with those of the high MC sample. The first peak in the Low Surface Tension replicates was more distinct and separated by a deep trough from the second peak.

The Low MC replicates that were dried from green started out at approximately 70% MC (Figure 4). Replicates 2 and 3 showed two well-defined phases of drying, with the transition point close to 60% MC. Replicate 1 also showed two peaks, but the transition point was not as clear.

3.6.4.1.2 Wetline depth

In the replicates from all three samples the wetline stayed close to the wood surface to approximately 50% MC (Figure 5). The Low MC sample showed more variability, where the wetline of Replicate 3 stayed close to the surface to a lower average MC. The slope of the graph repesenting Replicate 1 was smaller than that of the other two replicates.

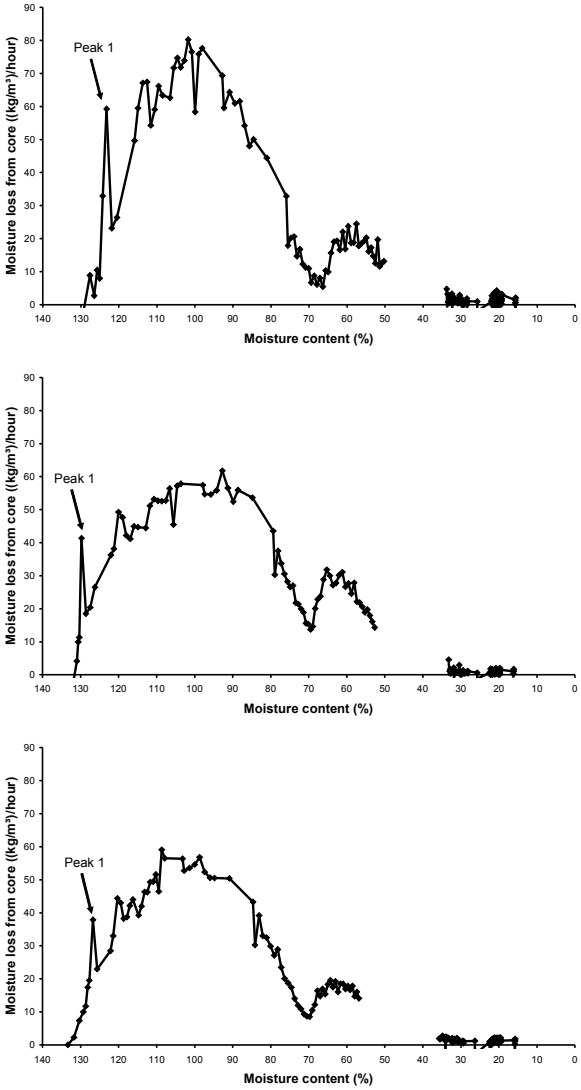

Figure 2: The rate of moisture loss from the core vs. the average moisture content of Replicates 1-3, top to bottom, of the High MC sample.

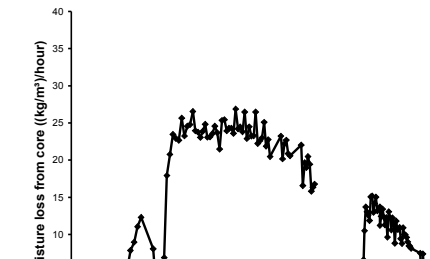

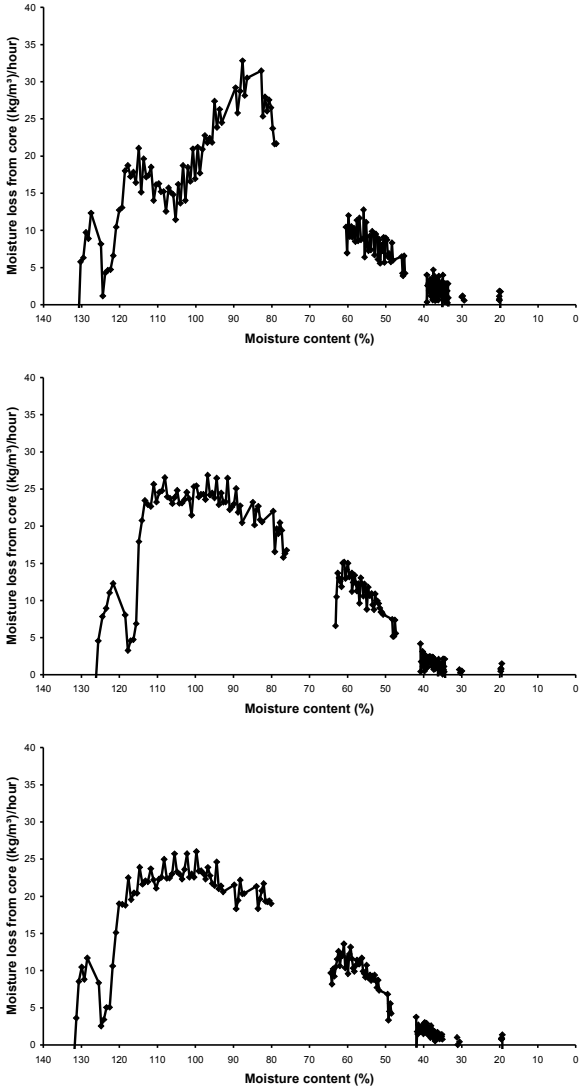

Figure 3: The rate of moisture loss from the core vs. the average moisture content of Replicates 1-3, top to bottom, of the Low Surface Tension sample.

3.6.4.1.3 Cross-cut area

The shrinkage progress, as indicated by the cross-cut area graphs (Figure 6), shows a unique pattern for each sample. The cross-cut area graphs of the replicates of the High MC sample showed different slopes at different stages: 140-130% MC, 120-70% MC, 70-50% MC and 40%-final MC. The replicates of the Low Surface Tension sample initially showed a greater slope at 140-120% MC. Subsequently, the cross-cut area graph stabilised at 120-50% MC and sloped again at 50%-final MC. The Low MC sample once again showed greater variation, but all three replicates seemed to exhibit a change in shrinkage characteristics at 40% MC, especially Replicates 2 and 3.

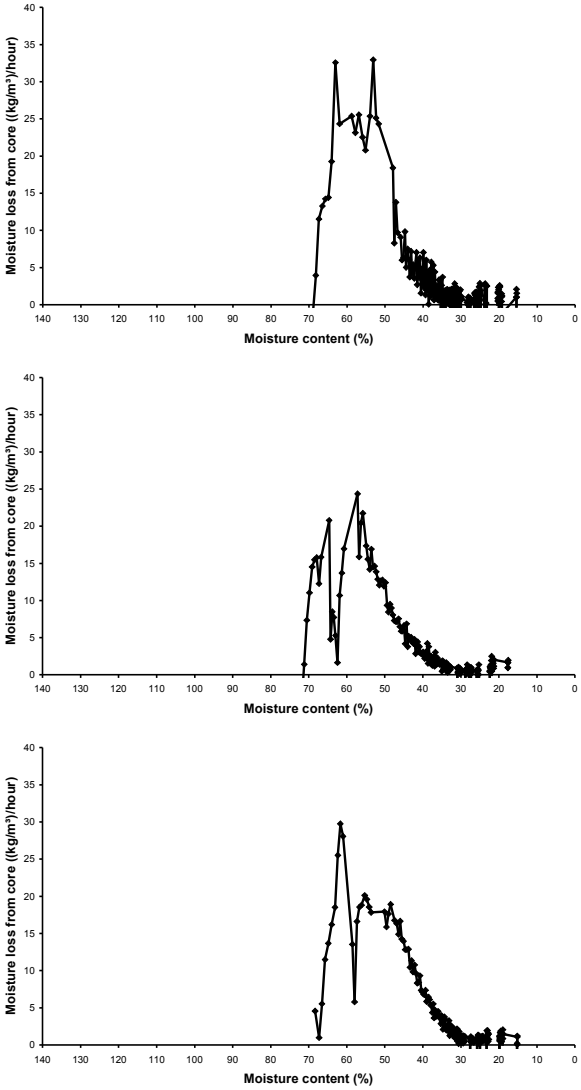

Figure 4: The rate of moisture loss from the core vs. the average moisture content of Replicates 1-3, top to bottom, of the Low MC sample.

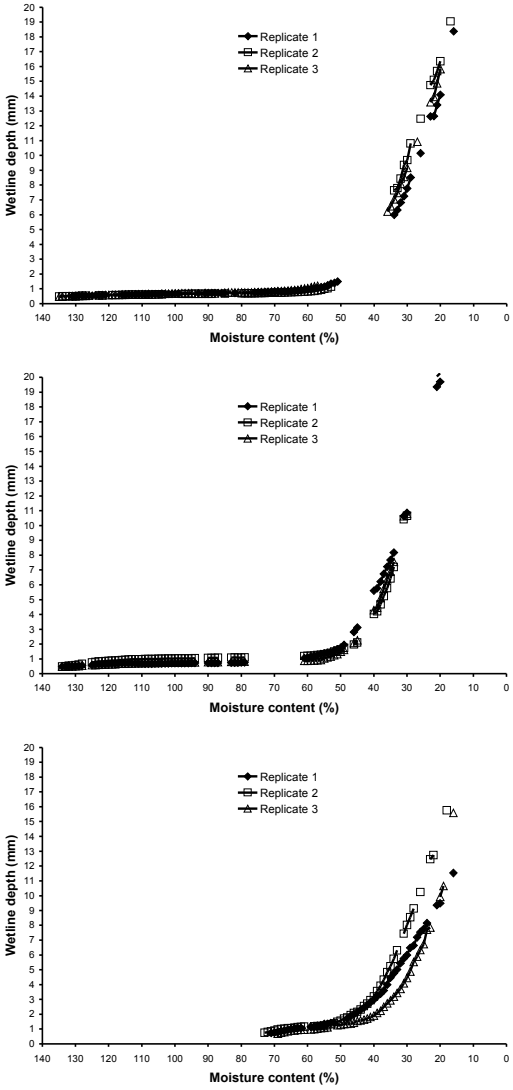

Figure 5: Wetline depth vs. average moisture content of the replicates from the High MC, Low Surface Tension and Low MC samples, top to bottom.

3.6.4.2 Study of a Separate High MC Birch Piece

Noticeable relationships became evident when the drying patterns of a single 138% MC Birch piece was plotted together with the liquid pressure and core temperature (Figure 7). The initial high rate of change of the cross-cut area when the wood surface layer quickly lost free and bound water, is thought to be an artefact of the thresholding method employed to determine the cross-cut area. The abrupt change in cross-cut area at about 130% MC coincides with a peak in the rate of moisture loss from the core, a sharp core temperature increase and low liquid pressure (*ca.* -50 kPa relative pressure). The second abrupt change in cross-cut area at about 70% MC coincides with the start of a peak in the rate of moisture loss from the core. The end of this peak coincides with an increasing wetline depth and shrinkage rate.

It should be noted that the liquid pressure plot is only useful at a high saturation level. It is also probable that the sharp increase in pressure at 130% MC was due to cavitation inside the pressure chamber,

subsequently rendering the pressure probe useless for the rest of the drying process, and slightly changing the size and shape of the first two peaks.

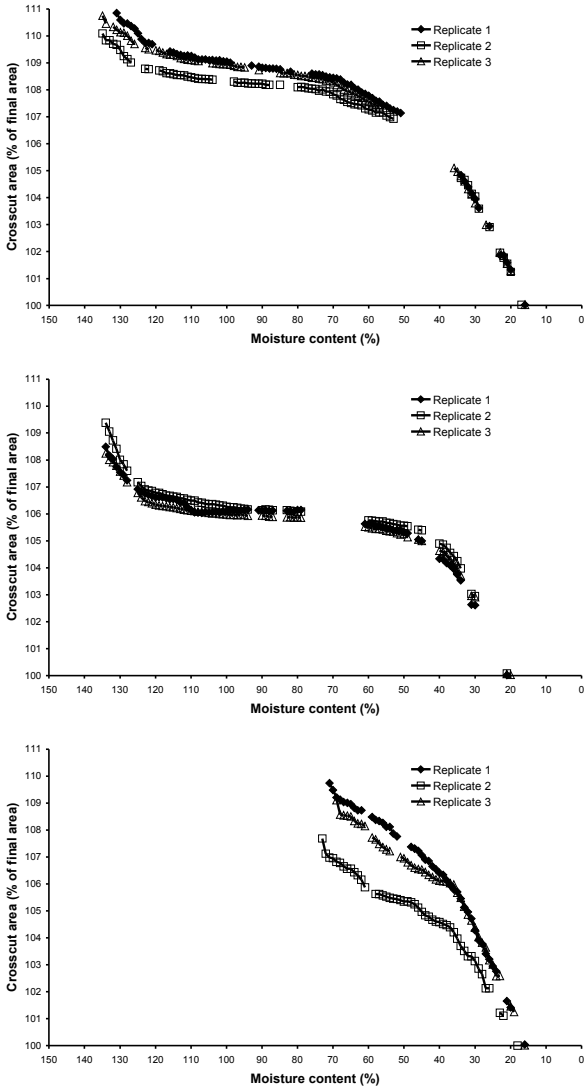

Figure 6: cross-cut area vs. average moisture content of the replicates from the High MC, Low Surface Tension and Low MC samples, top to bottom.

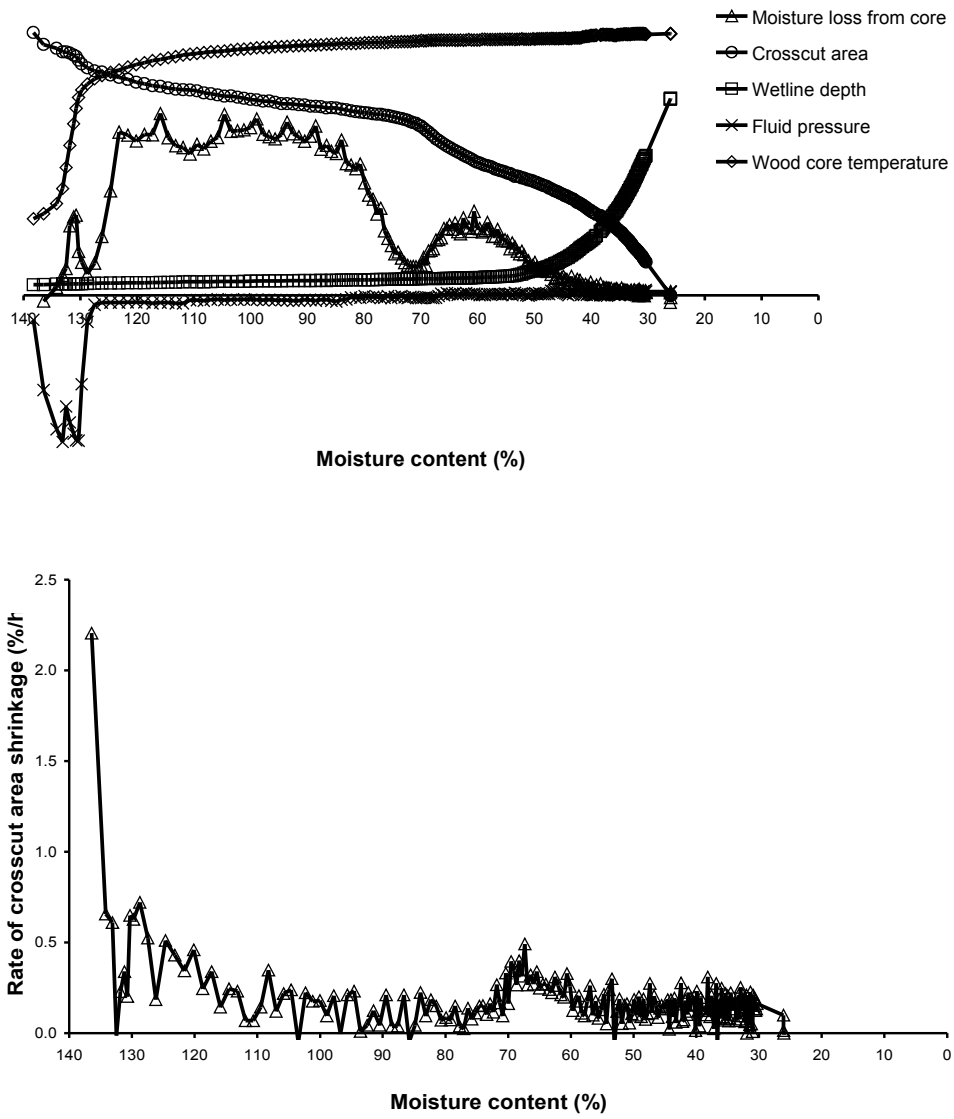

Figure 7: A plot of the measured drying patterns, core temperature and liquid pressure of a single 138% MC Birch piece at the top; and a plot of the rate of cross-cut area change vs. average MC for the same piece (bottom).

3.6.5 Discussion and conclusion

3.6.5.1 Relationships Between Drying Patterns

When the drying patterns of the High MC sample are scrutinised, it becomes apparent that the relationships pointed out with the aid of the simultaneous plot in Figure 7 hold true for the replicates of this sample. As mentioned, all three replicates showed a sharp peak in moisture loss from the core, Peak 1, shortly after drying started at about 130% MC (Figure 1). In every replicate this peak coincides with an abrupt cross-cut size decrease (Figure 6). The first peak of the Low Surface Tension replicates also coincides with a sharp change in cross-cut area (Figures 3 and 6). The drying phase following this first peak and ending at approximately 70% MC coincides with a period of relatively stable cross-cut area in

both the High MC and Low Surface Tension samples (Figures 2, 3 and 6). At 70-50% MC the change in cross-cut area of the High MC replicates (Figure 6) coincides with the last peak in moisture loss from the core. However, the Low Surface Tension replicates did not show the same shrinkage tendency (Figures 3 and 6). Among the Low MC replicates, only Replicate 2 showed a similar relationship between a peak in moisture loss from the core and a change in cross-cut area. This occurred at approximately 60% MC (Figures 4 and 6).

3.6.5.2 The Classification of Drying Phases

Cell walls within the wetline perimeter should theoretically be fully saturated with water. Consequently, most of the shrinkage that occurred during the period that the wetline was close to the surface may be attributed to full or partial cell collapse and not cell wall dehydration.

The High MC Birch samples exhibited three distinct phases of drying above FSP, which are indicated on the example in Figure 8. The existence of these phases at characteristic moisture content (saturation) levels and their effects on shrinkage profiles indicate that different capillary drying regimes were at work during different phases and that some phases may be associated with full or partial cell collapse. At least two of these phases seemed to be present in green Birch. The Low Surface Tension sample made transition between the first and second phase more distinguishable.

The first phase included the mentioned sharp peak, Peak 1, in moisture loss from the core at approximately 130% MC. Subsequently, the second phase started and continued to 70% MC. The third phase then continued until the average MC reaches 50%, at which point the wetline started moving into the sample.

The rising core temperature and low pressure at about 130% MC in Figure 8 led to accelerated moisture loss from the core and an abrupt shrinkage of the cross-cut area. This is in agreement with the theory of collapse: due to a combination of thermal plasticization of cell walls and strong capillary forces, water-filled cells may collapse during drying (Innes 1995). A second possible example of full or partial cell collapse occurred at 70-50% MC in the high MC sample. The Low Surface Tension sample also showed a decrease in cross-cut area above 50% MC, with the difference being that it occurred largely during the first phase of drying above 120% MC.

Contrary to expectation, the core moisture loss rate showed periods of increasing rate loss while the wetline was close to the surface. It is possible that differing capillary forces were at work at the different stages since the transition from one drying phase to the next coincided with an abrupt decrease in the cross-cut area. Thus, in a network of varying capillary types (ray cells, vessels, parenchyma, etc.) like that of Birch, it is possible that capillary forces due to different capillary size classes were causing the variation in the rate of capillary flow from the core. A comparison of these moisture loss patterns with that of wood species with more or less heterogeneous capillary networks, *e.g. Pinus spp.*, may show whether this theory of drying above FSP is viable.

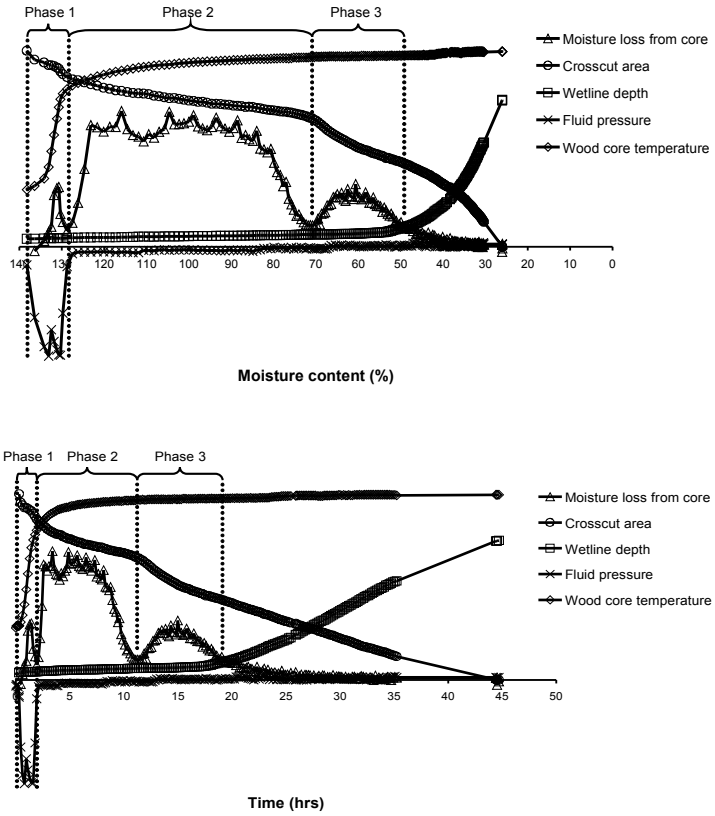

Figure 8: The three drying phases that repeatedly show up in high MC Birch pieces on a MC scale (top), and time scale (bottom). The drying patterns of the Birch piece that had temperature and pressure probes connected to it, is used as an example.

3.6.6 References

Innes, T. C. 1995: Stress model of a wood fibre in relation to collapse. Wood Science & Technology 29: 363-376.

Keey, R. B. 1994: Heat and mass transfer in kiln drying: a review. Proc 4th Int IUFRO Wood Drying Conf, Rotorua, New Zealand, 22-44.

Kreber, B., Haslett, A. N., McDonald, A. G. 1999: Kiln brown stain in radiata pine: A short review on cause and methods for prevention. Forest Products Journal 49 (4): 66-70.

Spolek, G. A.; Plumb, O. A. 1981: Capillary pressure in softwood. Wood Science & Technology 15: 189-199.

Wiberg, P., Morén, T. J. 1999: Moisture flux determination in wood during drying above fibre saturation point using CT-scanning and digital image processing. Holz als Roh- und Werkstoff 57: 137-144.

3.7 Liquid water flow in *Pinus radiata* during drying

3.7.1 Abstract

End-sealed 60×60×250 mm^3 *Pinus radiata* pieces were dried at 65/37°C (dry bulb/wet bulb temperature) and 4 $m.s^{-1}$ air speed to study various drying phenomena above fibre saturation point. While drying, an X-ray Computed Tomography (CT) scanner captured a cross-cut density image every ten minutes. The density data was used to determine moisture content, rate of moisture loss from the core of the wood pieces, wetline (boundary of the free water region) depth and cross-cut area. Repeating patterns were observed, which indicated that the cavity-size distribution of the wood pieces dictated fluctuations in the rate of moisture loss from the core and cross-cut area shrinkage during drying in the free water phase.

It is hypothesised that, while drying an interconnected capillary network in the free water phase, the largest meniscus penetrates a wood piece through the largest cavities, thus also allowing air into the capillary network. The largest meniscus would always get smaller as it penetrates the wood piece until it is not the largest meniscus in the network anymore. Then the new largest meniscus would start penetrating the capillary network, etc. The largest meniscus would also determine the liquid tension in the capillary network. When the largest meniscus gets small enough, and the liquid tension strong enough, deformation and collapse of the remaining liquid-filled cavities can occur. A large liquid-filled interconnected capillary network would eventually fragment into a number of smaller liquid-filled interconnected networks, at which point a receding wetline could be observed.

3.7.2 Introduction

Drying above fibre saturation point (FSP) has been described as a two-stage process (Keey 1994). In the first stage the wetline, or evaporative front, remains close to the surface and liquid water is drawn from the core to the surface. Machining results in damaged cells at lumber surfaces, thus creating a thin layer at the surface of a board with large apertures in the cellular structure of the wood. As a consequence, the large menisci of free water in this region quickly retracts into the wood to a point where the original anatomical structure of the wood is still intact. This would happen shortly after machining of green wood, creating the 0.5 mm thick dry shell at the surface (Salin 2003). Studies on yellow stain and kiln brown stain have shown that the concentration of water soluble extractives and the intensity of discolouration is the greatest at what would be the inner border of the dry shell where a lot of free water is evaporated (Kreber *et al.* 1999, Terziev 1993), which also supports the current understanding of the initial drying phase.

The second stage of drying follows when liquid continuity ceases and the wetline starts moving towards the core. This type of wetline movement has been shown to be true for various wood species (Wiberg and Morén 1999). Spolek and Plumb (1981) also showed that the capillary forces present in softwood were dependent on the liquid water saturation level, with progressively stronger capillary forces at decreasing saturation levels.

The most effective liquid flow pathways are dictated by the cellular structure of the wood (Siau 1984). The cellular structure is also the foundation of the invasion percolation theory of drying (Prat 2002), which predicts the existence of a wetline above FSP. A study on the drying of *Betula verrucosa* above FSP (Scheepers *et al.* 2005) has indicated that the cavity-size distribution yields a predictable pattern in the rate of moisture loss from the core as drying progresses. If this is true, softwoods, which have a fundamentally different anatomical structure to hardwoods, should yield a different but also predictable pattern in the rate of moisture loss from the core. In this investigation the drying phenomena of *Pinus radiata* above FSP were studied.

3.7.3 Materials and methods

Fresh *P. radiata* sapwood from the Western Cape in South Africa was sawn into 60×60×250 mm^3 pieces and stored at -20°C before use.

Three types of *P. radiata* samples were prepared:

1. Four green wood replicates;
2. Four water-soaked replicates; and
3. Four soap-soaked replicates.

The water-soaked replicates were prepared by submerging green replicates in a 90°C water bath for 24 hours so that air trapped in the pieces could bubble out, and then letting the water bath cool down. The soap-soaked replicates were prepared similarly, with the exception that an aqueous 2% sodium lauryl sulphate (SLS, Merck & Co., Inc.) solution was used. Green replicates were prepared by letting the frozen replicates thaw for 24 hours at room temperature in tightly wrapped plastic bags.

All the replicates were end-sealed with silicone prior to drying. Each one of the four drying runs consisted of one water-soaked, one soap-soaked and one green replicate, which were dried at 65/37°C (dry bulb/wet bulb temperature) and 4 $m.s^{-1}$ air speed while a Siemens Somatom AR.T X-ray CT-scanner captured a density image of the same 10 mm thick cross-section in each replicate at 10 minute intervals.

Each density image was a matrix consisting of 512×512 elements, with each element representing a density value (kg/m^3) for each matrix element. Successive density images were used to calculate the rate of moisture loss from the core; the wetline (boundary of the free water region) depth; and the cross-cut area of each replicate (Figure 1).

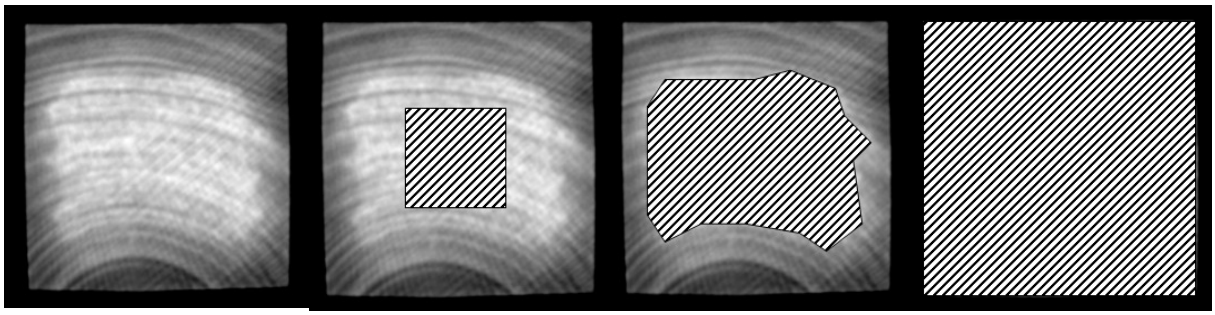

Figure 1: From left to right: the basic CT-scan density image, the selected core region, the selected above-FSP region for determination of the average wetline depth, and the cross-cut area of the wood piece.

The selected core area was a 15×15 mm^2 square at the centre of the cross-cut area of each replicate. The difference in the average density of the core of two successive images was divided by the elapsed drying time to provide the rate of moisture loss. The average wetline depth was calculated from the relationship of the cross-cut circumference of each replicate with the size of the below-FSP area:

$$d = \frac{c}{8} - \frac{\left|\sqrt{\frac{c^2}{16} - A}\right|}{2}$$

where *d* is the wetline depth, *c* is the cross-cut circumference of the wood piece, and *A* is the area below FSP.

The cross-cut area was obtained through determining the number of matrix elements above a selected threshold density value. This threshold density value were calculated according to the method employed by Wiberg and Morén (1999). The above-FSP elements of the image matrix were defined as those elements in the image which were 70 kg/m^3, and more, dense than the corresponding elements at the end of the drying run. This value was empirically determined by monitoring the drying rate *vs.* the density difference. This definition is only applicable to the replicates of this study dried to a final moisture content of about 10%.

The oven-dry density value of the scanned wood volume at the end of drying was determined. This final dry density value was then adjusted to compensate for the difference in replicate size at the end of drying and the respective previous points in time when density images were captured. With the dry density values for each point in time known, and the wet density at each point in time determined by calculating the average matrix element value for matrix elements representing wood, the average MC at each point in time could be calculated.

3.7.4 Results

The wetline in the green, water-soaked and soap-soaked pieces receded from the surface at 80-50% MC (Figure 2), which is a similar result to that shown by Wiberg and Morén (1999) for various species.

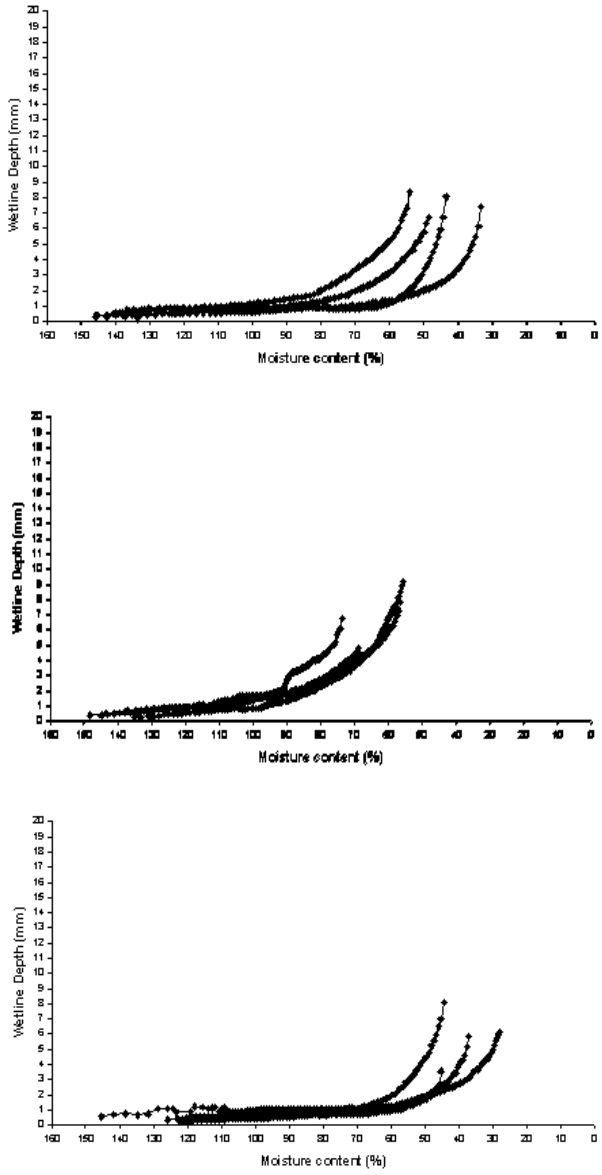

Figure 2: The distance from the wood surface to the wetline during drying. From top to bottom: water-soaked replicates, soap-soaked replicates and green replicates.

There seemed to be two distinct phases in the rate of moisture loss from the core of the water-soaked replicates. These phases were separated by a trough at *ca.* 100% MC (Figure 3). In the phase above 100% MC, the rate of moisture loss from the core was fast relative to the second phase. At about 40-30% average MC the rate of moisture loss finally dropped off again.

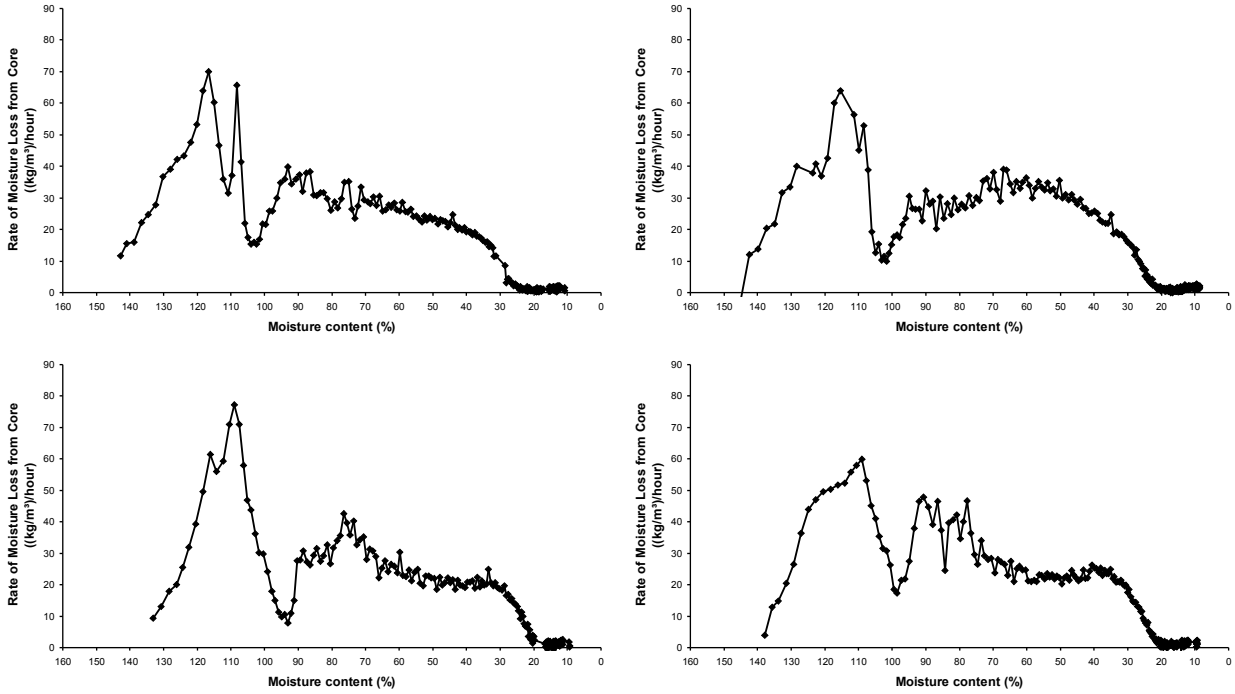

Figure 3: Rate of moisture loss from the core versus MC of the water-soaked *P. radiata* pieces. The pieces were dried in separate drying runs.

The initial sharp drop in cross-cut area of the water-soaked replicates at 140-130% MC was probably an artifact of the measurement method (Figure 4). The thresholding method would have detected a shrinking cross-cut area because of the excess free water that evaporated from the surface at that stage. At *ca.* 110% to 100% MC there was a drop in cross-cut area, followed by a period of relative stability down to 30% MC when there was a sharp drop to the final cross-cut area.

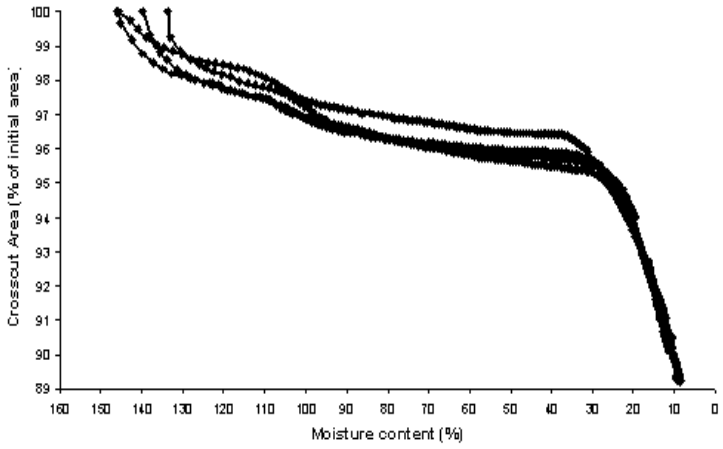

Figure 4: Cross-cut area, as a percentage of the initial wet cross-cut area, versus MC of the water-soaked *P. radiata* replicates.

In general, the rate of moisture loss from the core of the soap-soaked replicates was lower than that of the water-soaked replicates (Figure 5). As with the water-soaked replicates, the rate was high until *ca.* 100% MC was reached. However, the soap treatment seemed to give more distinct peaks in the rate. So much

so, that three of the four replicates, which were all dried in different drying runs, showed three peaks above 100% MC. Below 100% MC the plots had a particularly different shape to that of the water-soaked replicates, with the rate gradually tapering off until the final moisture content was reached.

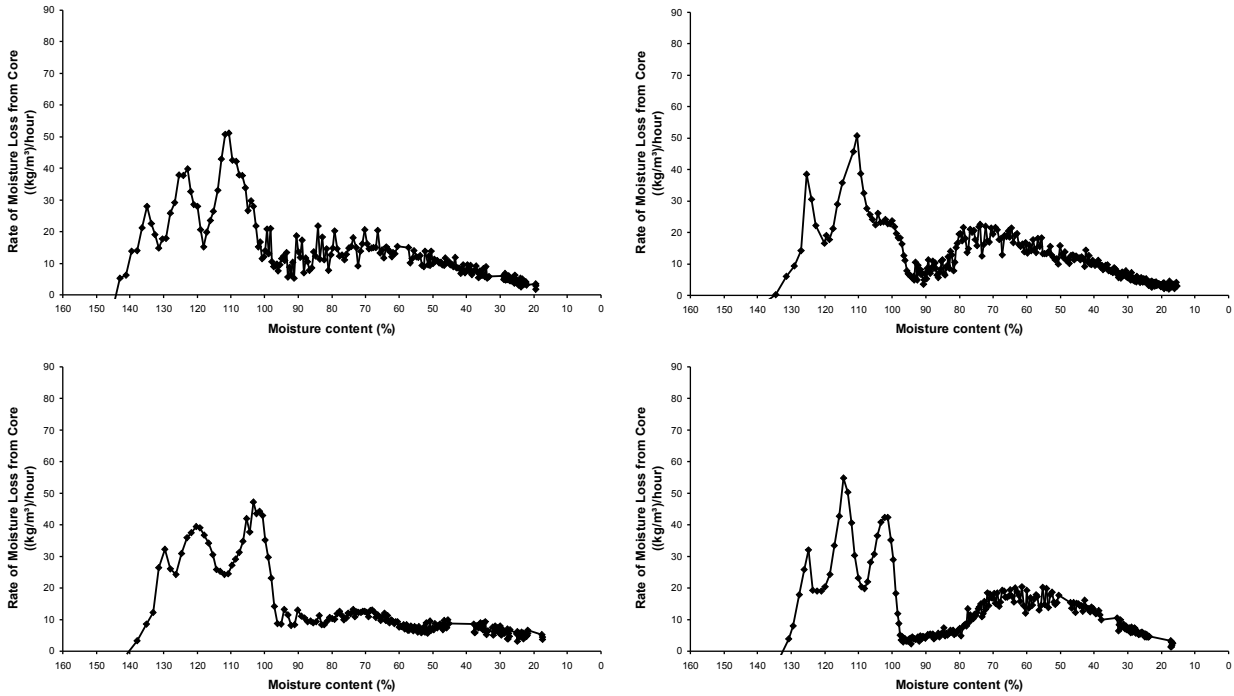

Figure 5: Rate of moisture loss from the core versus MC of the soap-soaked *P. radiata* pieces. The pieces were dried in separate drying runs.

Three of the four soap-soaked replicates showed a drop in cross-cut area at *ca.* 100% MC (Figure 6). In general the total percentage of shrinkage was less than that of the water-soaked replicates. This would be because the soap-soaked replicates dried slower and reached a higher final moisture content than the water-soaked ones.

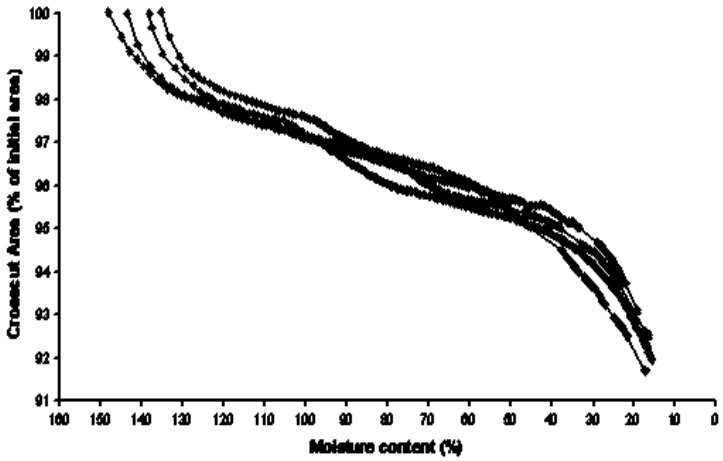

Figure 6: Cross-cut area, as a percentage of the initial wet cross-cut area, versus MC of the soap-soaked *P. radiata* replicates.

The rate of moisture loss from the core of green *P. radiata* replicates showed a more variable result. However, all replicates had a distinct trough at about 100% MC, followed by a peak in the rate of moisture loss from the core (Figure 7).

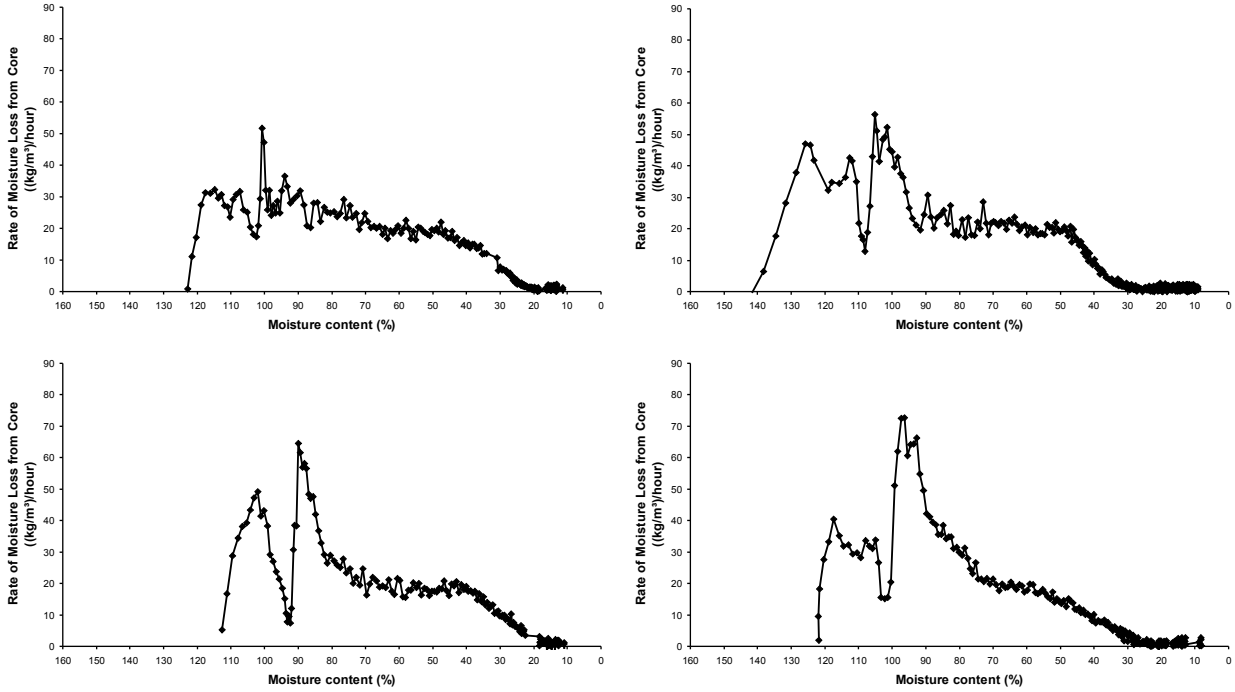

Figure 7: Rate of moisture loss from the core versus MC of the green *P. Radiata* pieces. The pieces were dried in separate drying runs.

The change in the cross-cut area of the green replicates were also more variable (Figure 8). However, there was a period of stability between *ca.* 100% and 30% MC, which was a similar result to the water- and soap-soaked replicates.

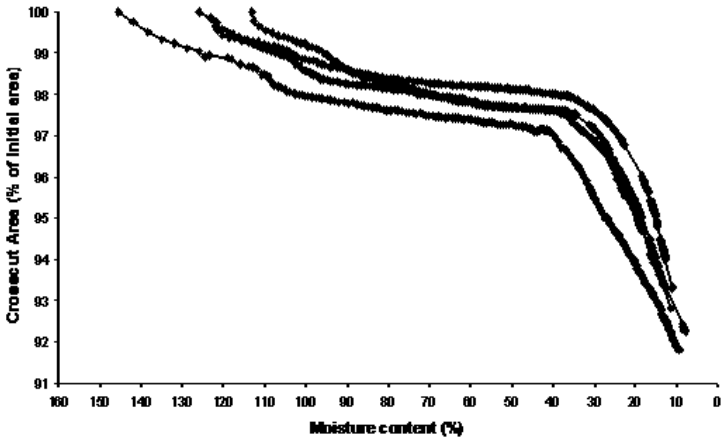

Figure 8: Cross-cut area, as a percentage of the initial wet cross-cut area, versus MC of the green *P. radiata* replicates.

3.7.5 Discussion

While the wetline was still close to the surface, changes in cross-cut area and the rate of moisture loss from the core were observed. The changes in the rate of the moisture loss from the core above 80% MC have to be attributed to mostly capillary flow and not diffusive moisture loss because of the level of water saturation and wetline position. Due to the same reason, the changes in cross-cut area above 70% MC have to be attributed to mostly deformation of cells due to capillary forces and not the drying of cell walls. These changes can, therefore, only be explained by the action of capillary phenomena.

In most of the replicates, a repeated fluctuation in the rate of moisture loss from the core at *ca.* 100% MC coincided with a drop in cross-cut area. This is similar to the results found with *B. verrucosa* (Scheepers *et al.* 2005), with the exception that *B. verrucosa* showed the same behaviour at *ca.* 70% MC when the wetline was still close to the surface. In both cases the change in cross-cut area has to be attributed to the deformation of the replicates due to the action of capillary forces. If deformation occurred during a high level of water saturation, it indicates that the suctional capillary force had increased. The only way this could have happened was if the largest meniscus in the existing interconnected capillary network became significantly smaller so that a large number of cells could be deformed, thus making the overall deformation observable.

The soap-soaked replicates dried slower than the water-soaked ones, and had a slower rate of moisture loss from the core, indicating the importance of liquid surface tension and capillary forces to drying rate. Interestingly, the soap-soaked replicates yielded a clearer separation of peaks in the rate of moisture loss from the core than the water-soaked pieces. Thus revealing three distinct peaks above 100% MC, which could not be seen in the water-soaked replicates.

In a liquid-filled, interconnected, capillary network with varying cavity sizes, one would expect the smallest meniscus to exert the greatest force while the largest meniscus, which lies in the largest cavity, exerts the weakest force. The liquid tension, or suctional force, observed in the liquid should be controlled by the force exerted by the largest meniscus. When evaporation occurs, the largest meniscus should move into the capillary network along the biggest cavity it can find until it is no longer the largest meniscus, and the process should repeat itself with the new largest meniscus, and so forth. So as drying continues the largest meniscus always should get smaller, thus increasing the liquid tension in the network.

In the case of wood, different cell- and cavity types yields a capillary network of distinguishable size-classes. With the major anatomical differences between hard- and softwoods, one could expect a significant difference in the distribution of cavity size-classes. Therefore the noticeable differences in the drying patterns in this investigation from that of *B. verrucosa* can be expected. The fluctuation in the rate of moisture loss from the core at 100% MC and 70% MC, in respectively *P. radiata* and *B. verrucosa*, coincided with a drop in cross-cut area. This was probably because the largest meniscus in the network became a size-class smaller as it moved to a smaller type of cavity. The resultant increase in liquid tension could have caused deformation of a large number of the remaining liquid-filled cavities.

The penetration of the largest meniscus into the capillary network also would allow air into the system. Initially, columns of humid air may extend deep into the network along the largest capillary pathways. As drying continues, the volume ratio of air to liquid water would increase and eventually result in a state where only isolated pockets of liquid water still exist in the smallest cavities. At this point, liquid transport to the meniscii at the surface would not be possible anymore, and the wetline would have to recede. This type of behaviour is also in agreement with predictions made by the invasion percolation theory of drying (Prat 2002).

3.7.6 Conclusion

P. radiata showed a fluctuation in the rate of moisture loss from the core and a drop in cross-cut area at *ca.* 100% MC. The result was very similar to that observed with *B. verrucosa* (Scheepers *et al.* 2005) with the exception that *B. verrucosa* showed the same behaviour at *ca.* 70% MC. It may have been, that while evaporation takes place, the largest meniscus penetrated the wood pieces through the largest cavities, thus also allowing air into the capillary network. This hypothesis is also in agreement with the invasion percolation theory and predicts the existence of a wetline close to the surface during the capillary flow stage of drying. The observed differences between the drying phenomena of *P. radiata* and *B. verrucosa* can be explained by the fundamental difference in anatomical structure and cavity-size distribution between hard- and softwoods.

The typical cavity-size distribution of a specie has to be taken into account to accurately model drying while the wetline is close to the surface. A similar study on other softwoods and hardwoods could help to pinpoint the specific cavity types that are emptied of liquid water at different phases of drying. It may also shed new light on the occurrence of collapse in susceptible species.

3.7.7 References

Keey, R. B. 1994: Heat and mass transfer in kiln drying: a review. Proc 4th Int IUFRO Wood Drying Conf, Rotorua, New Zealand, p. 22-44.

Kreber, B., A.N. Haslett and A.G. McDonald. 1999. Kiln brown stain in radiata pine: a short review on cause and methods for prevention. Forest Products Journal 49 (4), 66-70.

Prat, M. 2002. Recent advances in pore-scale models for drying of porous media. Chemical Engineering Journal 86: 153-164.

Salin, J.-G. 2003. External heat and mass transfer – some remarks. Proceedings of the 8th International IUFRO Wood Drying Conference, Brasov, Romania, p. 343-348.

Scheepers, GC, J Danvind, T Morén and T Rypstra. 2005. An investigation of liquid water movement in Birch during drying through variation of wood sap surface tension and initial average moisture content. Proceedings of the 9th International IUFRO Wood Drying Conference, Nanjing, China. p. 57-62.

Siau, J.F. 1984. Transport Processes in Wood. Springer-Verlag. New York.

Spolek, G. A.; Plumb, O. A. 1981: Capillary pressure in softwood. Wood Science & Technology 15: 189 199.

Terziev, N., J.B. Boutelje and O. Söderström. 1993. The influence of drying schedules on the redistribution of low-molecular weight sugars in *Pinus sylvestris* L. Holzforschung 47, 3-8.

Wiberg, P., Morén, T. J. 1999: Moisture flux determination in wood during drying above fibre saturation point using CT-scanning and digital image processing. Holz als Roh- und Werkstoff 57: 137-144.

3.8 Classification and regression tree analysis as a tool for predicting wood colour

3.8.1 Abstract

Classification and regression tree analysis was used to categorise 14 418 colour measurements from *P. elliottii* obtained over a period of a number of years, from a large geographical area in South Africa, and dried with nine different kiln schedules. Despite the variability of the data, the resulting decision trees corroborated the results of previous studies on the discolouration of wood, and are useful tools for the control of processing variables and wood colour in industrial wood processing. Kiln temperature variables and the planing depth depth variable were commonly present in the constructed decision trees.

3.8.2 Introduction

In South African sawmills incoming logs are classified mainy according to log size. However, South Africa is a country where contrasting climates can be separated by relatively short distances due to the interaction of weather systems with mountains and valleys. Due to space and production volume constrictions it is simply not possible to handle lumber differently according to these variables even though dried lumber quality could be influenced by them. Sawmill management's point of control lies in the processing variables they can manipulate. In this study 14 418 colour measurements on *P. elliottii* lumber harvested over a large area of the southern coast of South Africa, over a period of three of years, incorporating different seasons and dried with nine different kiln schedules were statistically analysed with various multivariate techniques to determine the influence of various processing variables. It was found that the classification and regression tree method was the best for producing reliable decision models for predicting dried and planed softwood colour.

A decision tree is a predictive model and describes a tree structure wherein leaves represent classifications and branches represent a combination of features that lead to those classifications. In statistics, classification and regression trees can be built for predicting continuous dependent variables (regression) and categorical predictor variables (classification) (Breiman et al. 1984; Ripley 1996). In general terms, the purpose of the analyses via tree-building algorithms is to determine a set of if-then logical (split) conditions that yield accurate prediction or classification of cases.

In most cases, the interpretation of results summarized in a tree is very simple. This simplicity is useful for purposes of rapid classification of new observations. It is easier to evaluate just one or two logical conditions, than to compute classification scores for each possible group, or predicted values, based on all predictors and possibly using some complex non-linear model equations. It can also often yield a much simpler model for explaining why observations are classified or predicted in a particular manner. It is much easier to present a few simple if-then statements to management, than some elaborate equations. There is

also no assumption that the relationships between the predictor variables and the dependent variable can be mathematically described, either linear or non-linear.

In general terms, the split at each node will be found that will generate the greatest improvement in predictive accuracy. This is usually measured with some type of node impurity measure, which provides an indication of the relative homogeneity (the inverse of impurity) of cases in the terminal nodes. If all cases in each terminal node show identical values, then node impurity is minimal, homogeneity is maximal, and prediction is perfect.

In previous studies on the discolouration of wood during kiln drying, the importance of kiln temperatures and planing depth has been pointed out (Boutelje 1990, Kapp *et al*. 2003, Kreber *et al.* 1999, Long 1978, McDonald *et al.* 2000, Scheepers 2006a, 2006b, 2006c and 2006d, Theander *et al.* 1993, Terziev *et al.* 1993). It has also been hypothesised that kiln conditions above or below 50% MC, when the wetline starts receding into the lumber board, may be of special importance to the different discolouration types (Scheepers *et al.* 2005, Scheepers 2006e, Wiberg and Morén 1999). To effectively use statistical tools like classification and regression tree analysis in industrial decision making on colour control, it is essential to be acquainted with these publications.

In this study, the colour close to the board surface was analysed (with the classification and regression tree method) separately from the colour at the board centre of kiln-dried *P. elliottii* because of the known difference in discolouration mechanism between these regions. One could say that this is a manually induced first node in the classification tree of the whole data set.

3.8.3 Materials and Methods

Nine different kiln schedules were employed to dry nine different batches of *P. elliottii* boards from wet to dry. From this data many independent variables could be defined. The defined independent variables are described in Table 1. Some of the variables were defined in terms of their values above or below 50% MC. This was done because 50% MC represents a turning point in the flow of liquid water and wetline movement, as first described by Wiberg and Morén (1999). Conditions above or below this point could potentially be used as predictors of discolouration.

The kiln dried boards were passed over a planer set at 1 mm depth until two thirds of the typically uneven surface was planed off. This surface was defined as the 1 mm depth level. The planed surface was divided into 3 equal blocks along the length, and colour measurements of the three darkest earlywood spots were taken in each block, yielding nine colour measurements per planed surface. Each board was again passed once over the planer set at 1 mm depth, the newly exposed surface was designated the 2 mm depth level, and the colour of this surface was measured in the same manner. This process was repeated every 1 mm up to 5 mm depth. The replicates were then split at approximately 20 mm depth (board centre depth) and planed to determine the colour of the wood where no yellow stain or kiln brown stain had occurred.

Colours were measured using the CIE L*a*b* colour system. A Sheen Micromatch Plus colorimeter (Sheen Instruments Ltd.) with a 4 mm measurement aperture was used to determine the colour of the earlywood of

each planed surface. The colorimeter (45°/0° instrument geometry) was set to D65/10° illumination/observation. The ΔE*-value, the scalar difference from white with (L*, a*, b*)-coordinates (100, 0, 0), was used as a measure of discolouration.

The data was analysed using the classification and regression tree module of Statistica 7.1 (StatSoft, Inc.). Eighty percent of the 14 418 cases was randomly selected to function as the training-subset to define statistical models. These models were then evaluated on the remaining 20% of observations, which functioned as the test-subset. To limit the final tree size, a minimum category size was specified. Also, large trees were pruned by evaluating the cost of the tree. The cost was determined based on the difference between the actual and predicted values. The idea was to identify the smallest tree that gives the best predictions. A larger tree with more categories will of course yield greater prediction accuracy and have a lower cost, but if the cost of an incrementally larger tree did not decrease substantially, the smaller tree was selected. For more information on classification and regression tree analyses and algorithms, see Breiman (1984) and Ripley (1996). The results are, of course, only valid for *P. elliottii* from the southern coast of South Africa and the range of variable values shown in Table 1.

Table 1: Description of the defined independent variables and their values for the different kiln schedules

Independent variable	Description	Kiln schedule #								
		1	2	3	4	5	6	7	8	9
Planing depth (mm)	Planed depth from the rough sawn surface of the dried board	1-5mm, board centre	1-5mm, board centre	1-5mm, board centre	1-5mm, board centre	1-5mm, board centre	1-5mm, board centre	1-5mm, board centre	1-5mm, board centre	1-5mm, board centre
Initial MC (%)	Average moisture content of the batch of boards at the start of drying	176	160	170	142	130	105	105	170	110
Avg. Tdb (°C)	Average dry bulb temperature over the whole length of the drying run	64.52	70.45	89.00	90.24	104.31	98.45	88.87	89.40	74.89
Avg. Tdb above 50% (°C)	Average dry bulb temperature over the period when the average MC of the batch of boards were above 50% MC	64.33	68.42	88.94	89.43	104.62	88.04	84.25	88.31	71.15
Avg. Tdb below 50% (°C)	Average dry bulb temperature over the period when the average MC of the batch of boards were below 50% MC	70.00	72.22	89.06	90.94	104.00	103.66	91.18	90.97	78.00
Avg. Twb (°C)	Average wet bulb temperature over the whole length of the drying run	49.54	49.66	65.95	68.21	94.91	81.70	65.45	67.75	62.70
Avg. Twb above 50% (°C)	Average wet bulb temperature over the period when the average MC of the batch of boards were above 50% MC	49.86	49.20	67.29	67.75	95.60	77.40	68.70	67.46	64.11
Avg. Twb below 50% (°C)	Average wet bulb temperature over the period when the average MC of the batch of boards were below 50% MC	49.23	50.04	64.62	68.61	94.21	81.70	61.65	68.16	61.54
Tdb.dt (°C.hr)	Integral of the dry bulb temperature in time over the whole length of the drying run	3000.00	2771.68	2551.37	2842.65	3911.57	5418.10	6229.01	2413.67	4518.50
Tdb.dt above 50% (°C.hr)	Integral of the dry bulb temperature over the period when the average MC of the batch of boards were above 50% MC	1436.63	1242.98	1274.80	1296.72	1970.28	1615.05	1968.39	1413.00	1944.65
Tdb.dt below 50% (°C.hr)	Integral of the dry bulb temperature over the period when the average MC of the batch of boards were below 50% MC	1563.37	1528.70	1276.57	1545.93	1941.28	3803.05	4260.62	1000.67	2573.85
Twb.dt (°C.hr)	Integral of the wet bulb temperature over the whole length of the drying run	2212.85	1953.10	1890.70	2148.68	3559.00	4496.16	4587.32	1829.18	3783.17
Twb.dt above 50% (°C.hr)	Integral of the wet bulb temperature over the period when the average MC of the batch of boards were above 50% MC	1113.43	893.85	964.53	982.37	1800.45	1498.72	1706.66	1079.38	1752.30
Twb.dt below 50% (°C.hr)	Integral of the wet bulb temperature over the period when the average MC of the batch of boards were below 50% MC	1099.42	1059.25	926.17	1166.32	1758.55	2997.44	2880.65	749.80	2030.87
Total time (hrs)	Total time taken to dry the wood	44.67	39.33	28.67	31.50	37.50	55.03	70.09	27.00	60.33
Time above 50% (hrs)	Time taken to dry the wood down to 50% MC	22.33	18.17	14.33	14.50	18.83	18.34	23.36	16.00	27.33
Time below 50% (hrs)	Time taken to dry the wood from 50% MC to the final moisture content	22.33	21.17	14.33	17.00	18.67	36.69	46.73	11.00	33.00

3.8.4 Results and discussion

When evaluating the results, it should be kept in mind that lower values of L* and greater values of ΔE*, a* and b* indicate greater discolouration. A ΔE*-value of equal to or less than 34 can be considered as an acceptable colour (Scheepers 2006b). Also, it should be understood that, for instance, a low dry bulb temperature does not necessarily imply less discolouration. If the relative humidity is high, even a low dry bulb temperature would yield appreciable discolouration because of the resulting long period of drying. However, kiln schedules are designed in such a manner as to get the wood dry in a reasonable time with reasonably little defects. Thus, one would not prolong a kiln schedule by employing an excessively high relative humidity. To design a kiln schedule for colour control based on the decision trees presented in this study requires knowledge and understanding of the mechanisms of discolouration presented in other publications. Also, atmospheric conditions that control discolouration might exacerbate other types of defects, like surface checking. The use of decision trees and statistics, as with any other tool, requires background knowledge and common sense.

Figures 1 to 4 show that kiln conditions above 50% MC greatly influenced the board centre colour. Generally speaking, prolonged exposure to high temperatures above 50% MC produced greater discolouration. The ΔE*-value is a good indicator of colour quality and higher values indicate greater discolouration (Scheepers 2006c). Little discolouration occurred if the integral of the dry bulb temperature over the time above 50% MC was lower than 1956.5°C.hr while the average dry bulb temperature was below 89.2°C.

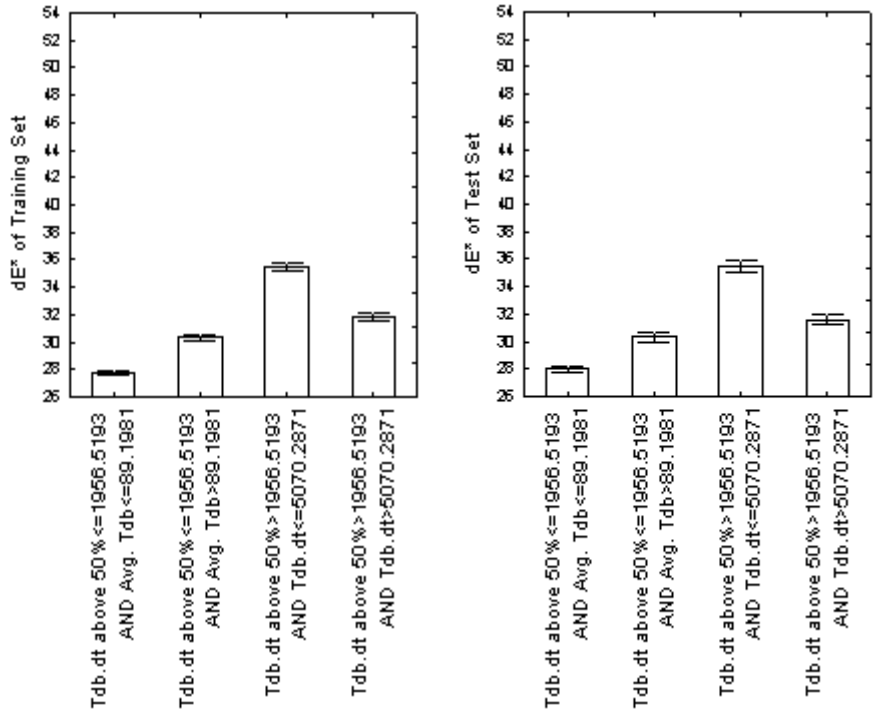

Figure 1: Board centre ΔE*-values of the training and test data sets.

The lightness or darkness of the board centre is indicated by the L*-values. Low values of L* indicates greater discolouration. Figure 2 shows that an average dry bulb temperatures above 50% MC greater than 97°C would produce significantly worse colour at the board centre.

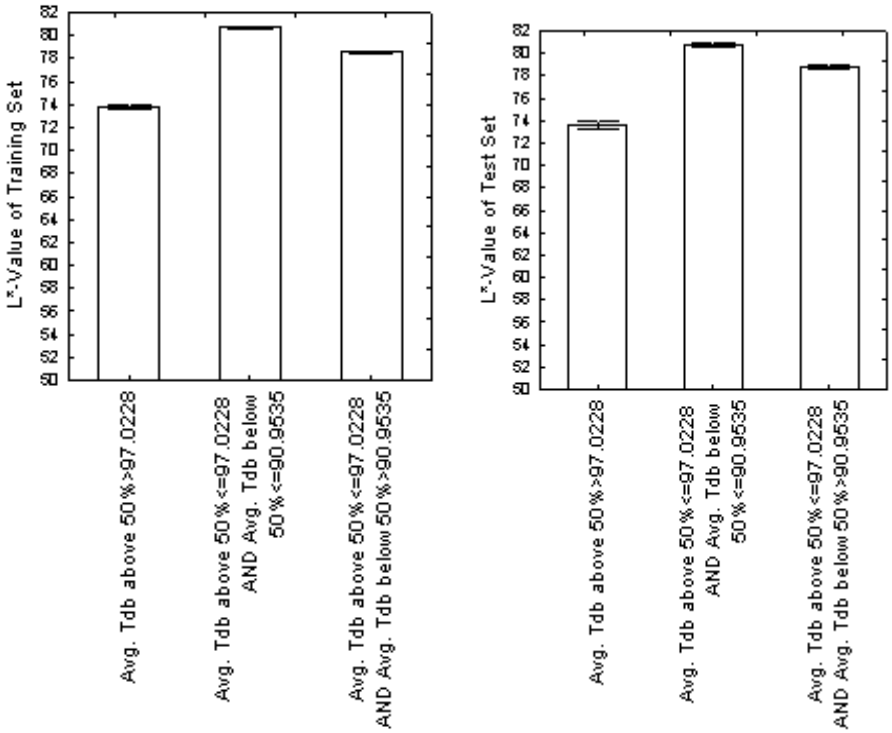

Figure 2: Board centre L*-values of the training and test data sets.

Figures 3 and 4 shows that the chroma at the board centre was firstly defined by the average wet bulb temperature above 50% MC. The average wet bulb temperature above 50% MC had to be lower than 68.2°C and 65.7°C, respectively, to yield a*- and b*-values that were close to that of normal wood.

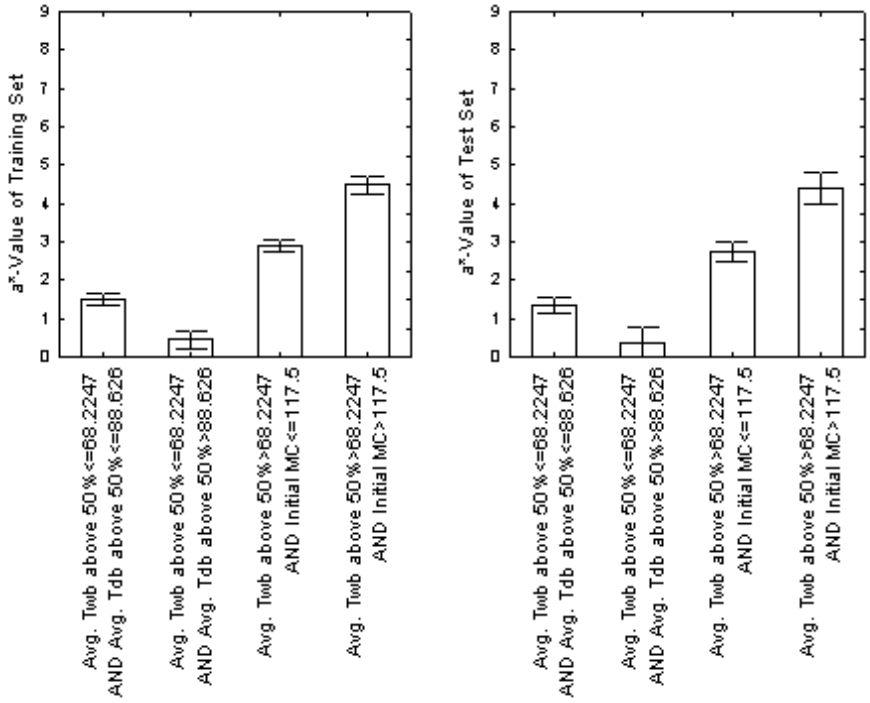

Figure 3: Board centre a*-values of the training and test data sets.

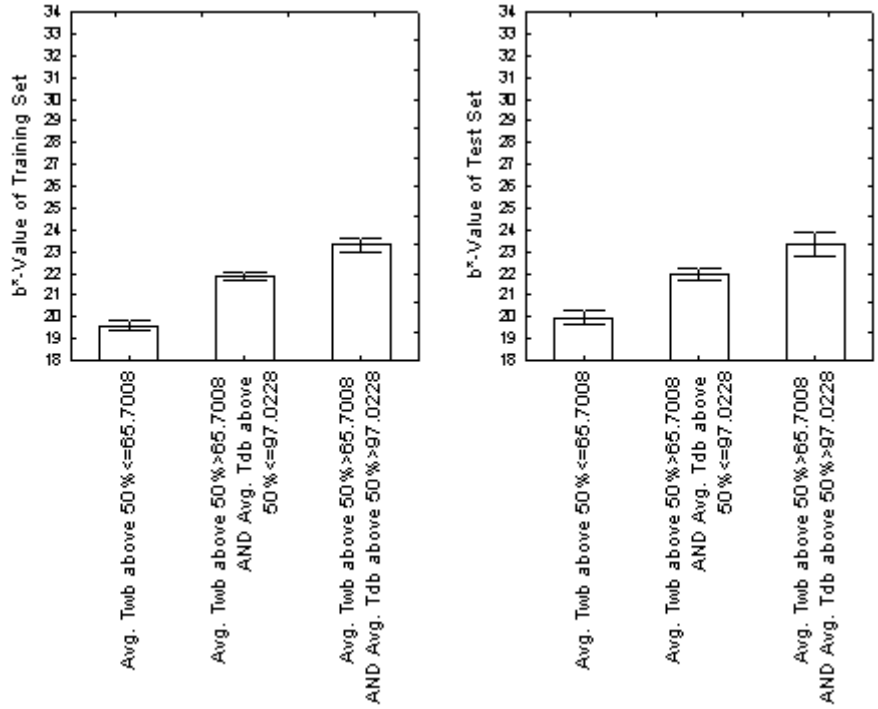

Figure 4: Board centre b*-values of the training and test data sets.

Figures 5 to 8 show that the 1-5 mm depth colour was mostly dependent on planing depth. Generally speaking, significantly better colour was yielded by planing deeper than 2.5 mm from the rough sawn

surface and keeping the dry bulb temperature below 80-90°C. The highest ΔE*-values was yielded by a planing depth shallower than 2.5 mm when the dry bulb temperature was greater than 81.88°C (Figure 5). The ΔE*-values closest to the normal colour of wood was produced by a planing depth greater than 2.5 mm and an average web bulb temperature above 50% MC lower than 68.22°C.

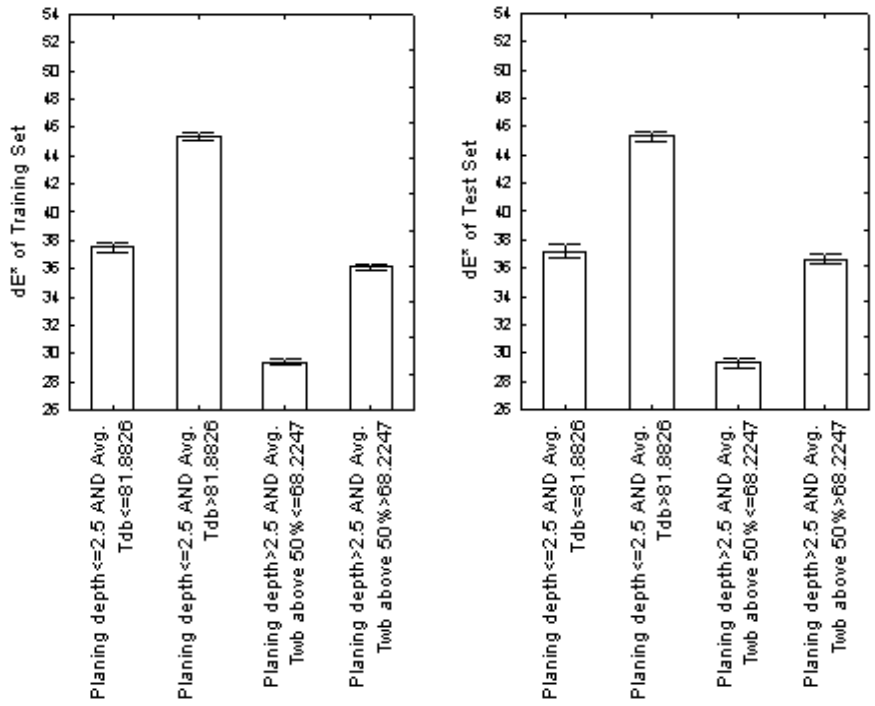

Figure 5: 1-5 mm ΔE*-values of the training and test data sets.

A comparison of Figures 5 and 6 shows that the conditions that were specified for classification of the ΔE*-values was similar to those that effectively classified L*-values. This reflects the inverse relation of these values (Scheepers 2006c).

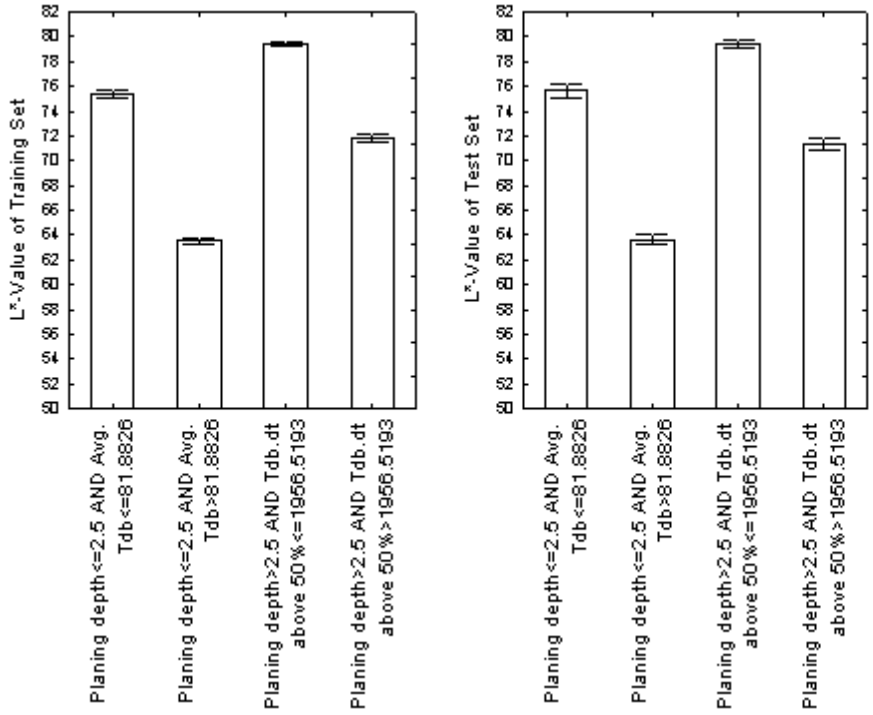

Figure 6: 1-5 mm L*-values of the training and test data sets.

In the case of the a*-values at the 1-5 mm depth level there were five categories of which two categories were defined by three conditions (Figure 7). The a*-values were greatly dependent on dry bulb temperature and planing depth. Less discolouration was yielded by an average dry bulb temperature below 50% MC lower than 90°C and a planing depth beyond 1.5 mm. The b*-values were closest to that of normal coloured wood when the planing depth was greater than 2.5 mm and the average dry bulb temperature below 91°C (Figure 8).

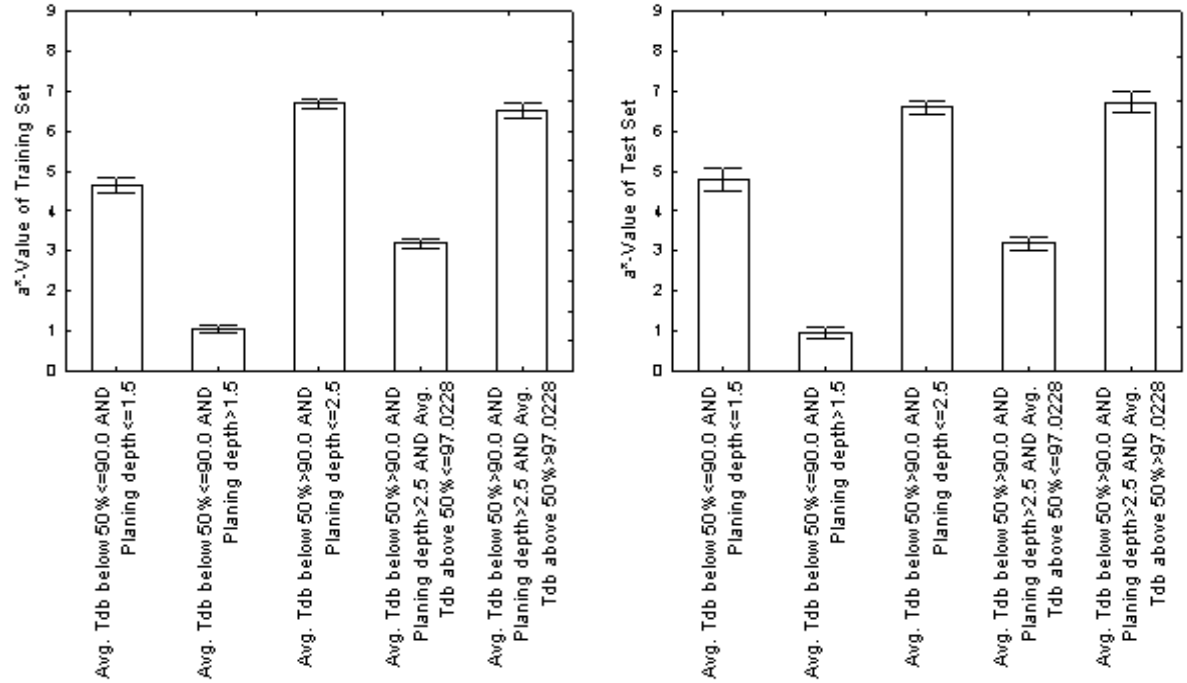

Figure 7: 1-5 mm a*-values of the training and test data sets.

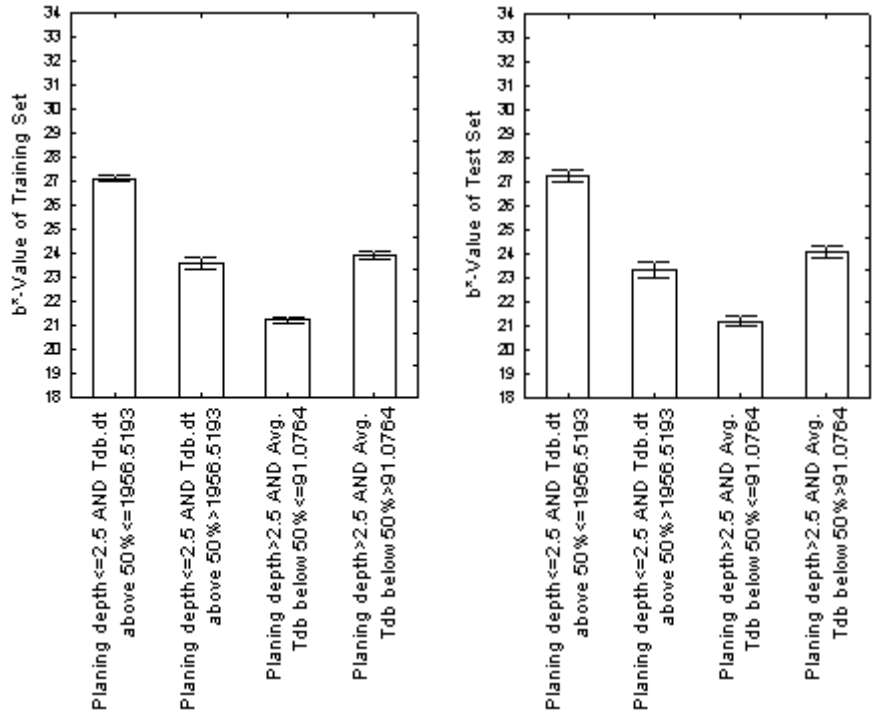

Figure 8: 1-5 mm b*-values of the training and test data sets.

If the ΔE*-values measured at the board centre (Figure 1) and in the 1-5 mm depth region (Figure 5) are taken as examples, the decision trees for the two datasets would be as presented in Figures 9 and 10. At 1-5 mm depth (Figure 10), there is a choice between one good (low ΔE*-values), two moderate and one poor processing solution for colour control. Evidently, a good planed surface colour can be achieved

through planing off a lot of wood and keeping temperatures low. When the opposite is done, it would yield the poor processing solution, and the planed surface would be severely discoloured. A moderately good planed surface colour can be achieved in two ways: shallow planing depth and low temperature, or deep planing depth and high temperatures. Thus, if a moderately good surface quality is acceptable, sawmill management would have to decide whether processing time or recovery volume is more important, and make a decision accordingly.

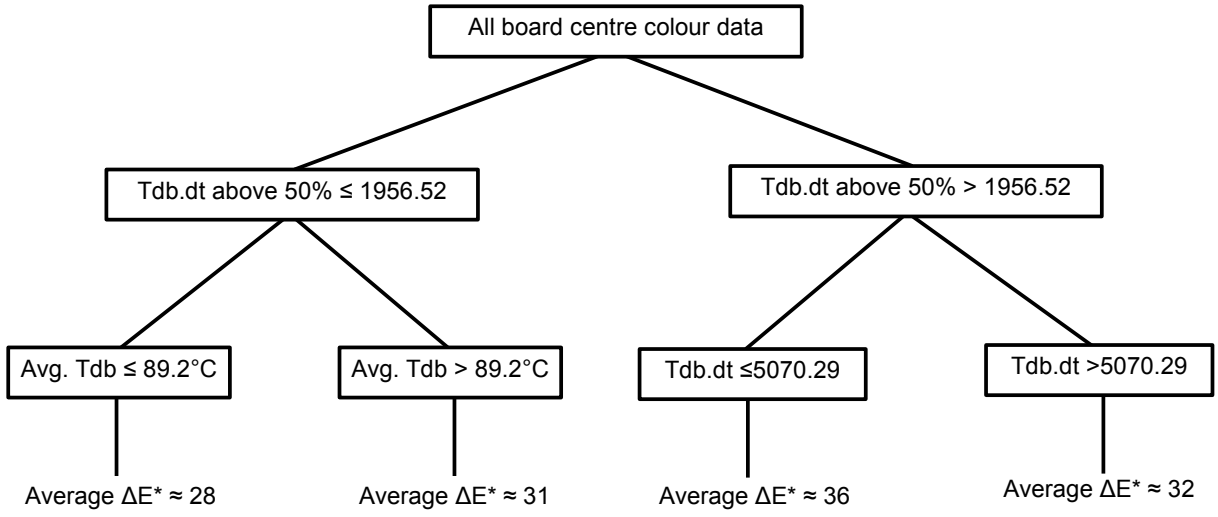

Figure 9: Classification and regression tree of the board centre colour data.

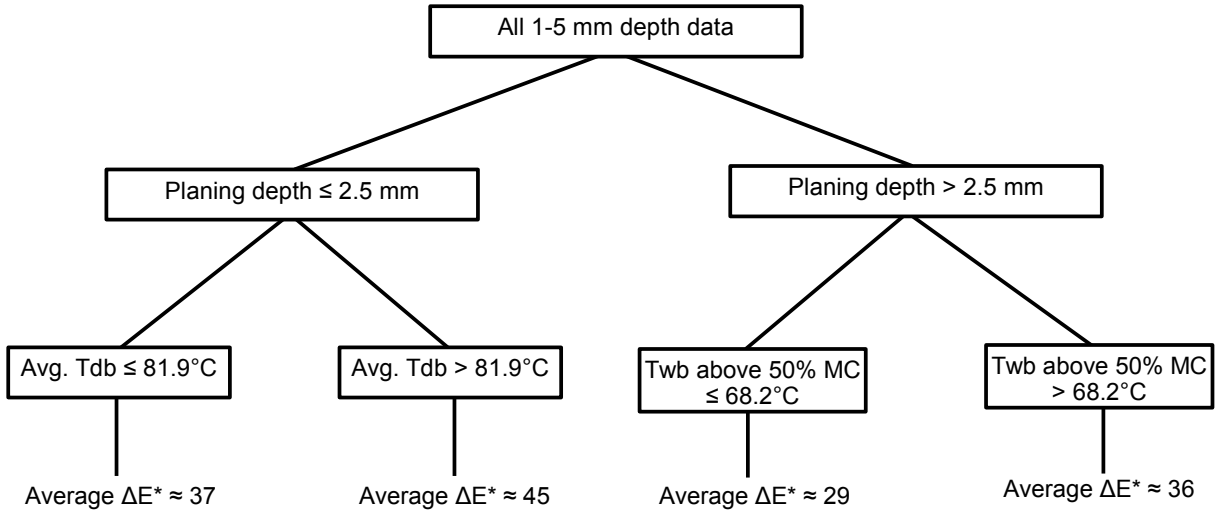

Figure 10: Classification and regression tree of the 1-5 mm depth colour data.

Except for the usefulness of the decision trees for colour control, they also corroborate studies on wood colour of a more academic nature (Boutelje 1990, Kapp *et al*. 2003, Kreber *et al.* 1999, Long 1978,

McDonald *et al.* 2000, Scheepers 2006a, 2006b, 2006c and 2006d, Theander *et al.* 1993, Terziev *et al.* 1993). Specifically, the influence of planing depth and kiln temperatures on surface colour agrees with those studies. Conditions above or below 50% MC also seemed to be important, but it is of course also possible to define an infinite number of variables based on the moisture content that would show up in decision trees.

3.8.5 Conclusion

The use of classification and regression tree analysis to categorise the colour data of kiln dried and planed wood provided decision pathways with predictable results. The method provided results in a decision tree format that were easy to interpret and highly suitable for use in decision making in the industrial lumber production scenario. The results also corroborated other studies on the colour of kiln dried wood. Specifically, the importance of the planing depth and kiln temperatures was reflected by the constructed decision trees.

3.8.6 References

Boutelje, J.B. 1990. Increase in the content of nitrogenous compounds at lumber surfaces during drying and possible biological effects. Wood Science and Technology 24: 191-200.

Breiman, L., J.H. Friedman, R.A. Olshen and C.J. Stone. 1984. Classification and regression trees. Wadsworth & Brooks/Cole Advanced Books & Software, Monterey, CA.

Kapp, S., G.C. Scheepers and T. Rypstra. 2003. Factors influencing the development of yellow stain and kiln brown stain in South African grown Pinus spp. Journal of the Institute of Wood Science 16(2): 113-118.

Kreber, B., A.N. Haslett and A.G. McDonald. 1999. Kiln brown stain in radiata pine: a short review on cause and methods for prevention. Forest Products Journal 49 (4), 66-70.

Long, K.D. 1978. Redistribution of simple sugars during drying of wood. Wood Science 11 (1): 10-12.

McDonald, A.G.; M. Fernandez; B. Kreber and F. Laytner. 2000. The chemical nature of kiln brown stain in radiata pine. Holzforschung 54: 12-22.

Ripley, B.D. 1996. Pattern recognition and neural networks. Cambridge University Press, Cambridge.

Scheepers, G.C. 2006a. Yellow and kiln brown stain in South Africa. In: Liquid water flow and discolouration of wood during kiln drying. PhD thesis by G.C. Scheepers, University of Stellenbosch, Stellenbosch.

Scheepers, G.C. 2006b. Digital image analysis and colorimetric measurement of yellow and brown stained *Pinus elliottii.* In: Liquid water flow and discolouration of wood during kiln drying. PhD thesis by G.C. Scheepers, University of Stellenbosch, Stellenbosch.

Scheepers, G.C. 2006c. The occurrence of discolouration due to kiln drying in South African grown *Pinus elliottii.* In: Liquid water flow and discolouration of wood during kiln drying. PhD thesis by G.C. Scheepers, University of Stellenbosch, Stellenbosch.

Scheepers, G.C. 2006d. The effect of surface tension on liquid water flow and discolouration in softwood. In: Liquid water flow and discolouration of wood during kiln drying. PhD thesis by G.C. Scheepers, University of Stellenbosch, Stellenbosch.

Scheepers, G.C. 2006e. Liquid water flow in *Pinus radiata* during drying. In: Liquid water flow and discolouration of wood during kiln drying. PhD thesis by G.C. Scheepers, University of Stellenbosch, Stellenbosch.

Scheepers, G.C., J. Danvind, T. Morén and T. Rypstra. 2005. An Investigation of Liquid Water Movement in Birch during Drying through Variation of Wood Sap Surface Tension and Initial Average Moisture Content. Proceedings of the 9th International IUFRO Wood Drying Conference, Nanjing, China.

Theander, O., J. Bjurman and J.B. Boutelje. 1993. Increase in the content of low-molecular carbohydrates at lumber surfaces during drying and correlations with nitrogen content, yellowing and mould growth. Wood Science and Technology 27: 381-389.

Terziev, N., J.B. Boutelje and O. Söderström. 1993. The influence of drying schedules on the redistribution of low-molecular weight sugars in *Pinus sylvestris* L. Holzforschung 47, 3-8.

Wiberg, P. and T.J. Morén. 1999: Moisture flux determination in wood during drying above fibre saturation point using CT-scanning and digital image processing. Holz als Roh- und Werkstoff 57: 137-144.

Chapter 4: Final Conclusions

The investigations into the occurrence of yellow stain and kiln brown stain in South Africa showed that the intensity of these types of discolouration was predominantly influenced by geographical origin (and/or climate), tree specie, planing depth of dried lumber, and kiln schedule parameters like temperature and time. The characteristic discolouration pattern of yellow stain and kiln brown stain indicated that this stain type was related to the wetline phenomenon that was found during the liquid water flow phase of drying. Thermal discolouration, on the other hand, occurred homogeneously throughout the volume of lumber and is, therefore, not related to free water flow, but to chemical changes of the macromolecules in wood.

The liquid water flow investigations indicated that the anatomical structure of a wood piece controls:

- fluctuations in the rate of moisture loss from the core during drying above FSP, which are probably due to the existence of distinct cavity size-classes; and
- capillary forces, which could be strong enough to cause temporary and/or permanent cell deformation in *Betula verrucosa* and *Pinus radiata.*

The observed phenomena can be explained by the hypothesis that the largest meniscus in a liquid-filled interconnected capillary network controls the liquid tension in the network. During drying, the largest meniscus will migrate into the capillary network (while the smaller menisci remain stationary) until it is not the largest meniscus anymore, and the new largest meniscus will start migrating. The largest menisci would be able to penetrate deep into the capillary network while smaller menisci, even those at the wood surface, remain stationary. This would give rise to a large free water zone, extending throughout a wood piece, with columns of emptied cavities stretching throughout the piece, and a wetline bordering the free water zone at the wood surface. When a sufficient number of cavities have been emptied of free water, and the interconnection of the capillary network has been compromised, the wetline would have to start receding into the wood piece.

While free water is being transported to and evaporated at the surface, the water-soluble components in the wood sap, or extractives, would be concentrated at the surface. The extractives would react mainly through Maillard reactions, although other reactions could not be excluded due to the complex chemical composition, and produce yellow stain and kiln brown stain. The stain intensity should be the greatest closest to the wood surface where the wetline was when the greatest amount of free water had evaporated. This discolouration pattern was also observed in the results of yellow stain and kiln brown stain characterisation investigations presented in this thesis. It follows that the homogeneous thermal discolouration observed throughout the *P. elliottii* boards has to be related to chemical modification of the water-insoluble macromolecules in wood. The literature review also pointed out that this type of discolouration occurs below fibre saturation point, as in heat treatment processes. In the case of both discolouration types, higher temperatures and longer schedules yielded greater stain intensity.

Classification and regression tree analysis was a useful statistical technique to analyse a large multivariate dataset. The importance of kiln schedule temperatures and planing depth to control yellow stain and kiln brown stain was clearly pointed out by the technique, which can help to simplify process control for colour quality during the industrial processing of wood.